A STUDY OF CONDUCTING ORGANIC CHARGE TRANSFER COMPLEXES AND THEIR INCORPORATION INTO INSULATING POLYMERS

JOHN E. PETER METCALF

A thesis submitted in partial fulfilment of the requirements of the Council for National Academic Awards for the degree of Master of Philosophy.

September 1992

Sheffield City Polytechnic in collaboration with ICI Plc (Electronics Group)

ABSTRACT

A study of conducting organic charge transfer complexes and their incorporation into insulating polymers

John E Peter Metcalf.

Polymers have long been regarded as excellent electrical insulators. Over the past two decades, polymers that have good electrical (and thermal) conductivity have gained considerable interest. They fall into two broad categories, composites of electrically conducting materials with insulating polymers, and polymers that have been chemically treated (doped) rendering them conductive by charge transfer within the polymer structure. Both forms of material possess disadvantages, low percolation thresholds and poor mechanical properties. The early doped polymers tended to be environmentally unstable, while composites tend to have poor mechanical properties.

An extensive review of conducting polymers is presented, covering filled polymers and theories proposed for their electrical conduction. Elastomeric and polymeric ionene polymers, polymer/TCNQ materials, and reticulate doped polymers are reviewed.

The practical study undertaken here concerned the production of conducting polymer composites by reticulately doping insulating polymers with organic, solvent soluble, charge transfer complexes of bis-pyridinium and trimethyl sulphonium iodide, 7,7,8,8-tetracyano-p-quinodimethane (TCNQ) salts.

The TCNQ salts were synthesised and characterised using elemental analysis, uv/vis spectrophotometry, variable magnetic susceptibility, electrical conductivity, and powder X-Ray diffraction. The salts were solvent blended with appropriate insulating polymers and cast to form the conducting reticulate film polymers. A study of the resulting charge transfer complex morphology was made.

CONTENTS

1. INTRODUCTION

From a scientific view the most interesting objectives in the field of conducting polymers are those polymers which conduct as a result of charge transfer within their molecular structure. These are called intrinsically conducting polymers. However, in the search for intrinsically electrically conducting polymers, it is often forgotten that insulating polymers have long been rendered conductive by simply adding electrically conducting fillers. The most common fillers are conductive grades of carbon black (Blythe 1979) followed by carbon fibres, metal powders, flakes and even materials such as nickel coated glass. The resulting composites are readily available commercially (Wilson Fiberfill have a range of 6 conductive phases in 23 different engineering polymers), and are widely used in industry today as anti-static materials and electromagnetic interference (EMI) shields (Gersteisen 1985).

A novel approach to rendering insulating polmers conductive was to incorparate into the polymer a network of conducting, solvent soluble, organic charge transfer complex (Jeszka et al 1981, Ulanski et al 1984a, 1985, Sorm et al 1984). The purpose of this study was to synthesise new and established charge transfer complexes and find suitable solvent and polymer combinations to produce polymer films with a reticulate charge transfer complex to form a basis for understanding these novel conducting polymers.

2. LITERATURE REVIEW

2.1. The Need For Conducting Polymers.

It had long been thought desirable to have a material whose electrical conductivity could be variably controlled and also possess good processability. A successful mouldable conductive material would combine the excellent electrical properties of a metal with the easy processability of a polymer. Such a material could be injection moulded, extruded, or hot formed with the advantage over a metal of superior durability in that it would not corrode. The Polaroid Corporation produced such a polymer (ICO-117 polypyrrole) that may be processed in a torque rheometer (High Performance Plastics 1989).

The first route to this sort of desired material was simple combination of a metal or other conductive material with a polymer. Although there are many examples of such materials to date, they do not preserve the potential conductivity of the conductive phase due to electrical dilution of this phase, and they also lose the desirable mechanical properties of the unfilled polymer due to stiffness and brittleness of the conductive sub-phase. Nonetheless, composite materials of a conductive phase and polymer have found many commercial applications and are very worthy of consideration.

2.2 Replacement of metallic conductors.

It was important to consider the applications for the two types of conductive polymers and to compare the potential of each type. We can first consider whether they will replace metals (eg. copper or aluminium) as a means of transporting electrical power. If we look to the literature for the answer to this question we get conflicting views. Ellis (1986) states that the "necessary qualification" for a polymeric conductor is that the conductivity must approach that of copper (ca. 10^6 Scm^{-1}).

Metal filled polymers have a maximum conductivity of approximately 10 Scm^{-1} (Young (1984)), (see Figure 1). Ellis (1986) cites an intrinsically conducting polymer of conductivity 10 000 Scm^{-1} with a density one third that of aluminium and one eighth that of copper and finding applications in the automobile industry due to the possibility of weight savings. However, he considers this application to be unlikely due to the adoption of fibre-optic technology in the replacement of electrical wires in automobiles. Presumably the fibre trasmits optically encoded signals around the vehicle to the ignition system, stop lights, indicator lights etc..

Ellis (1986) also supports his argument for the continuing search for polymeric conductors by emphasising the advantages of extrudability of these materials.

Mundstedt (1985) does not see the area of power conductors being challenged by polymeric conductors solely due to the

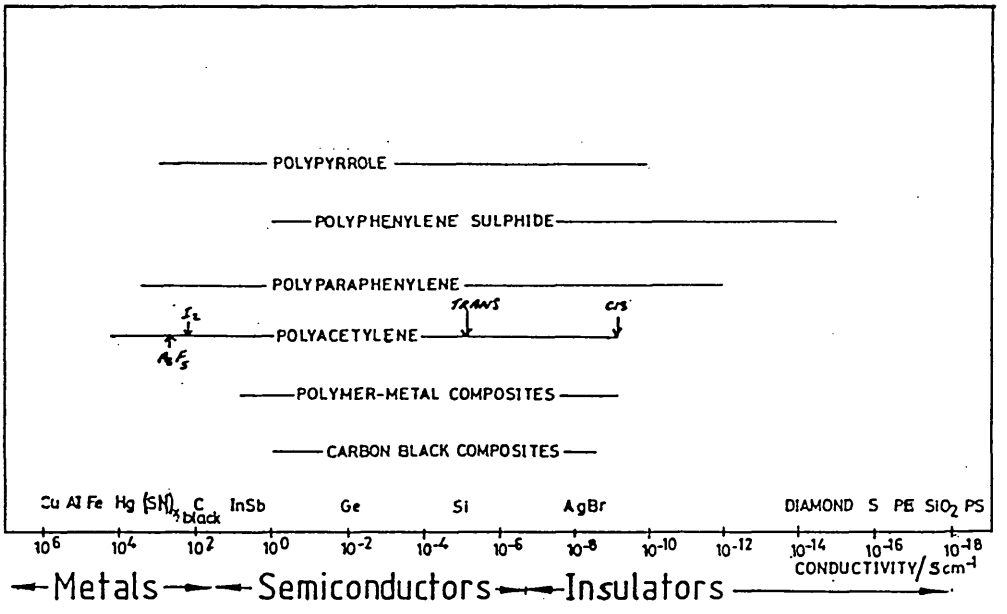

Figure 1.
Comparison between the conductivities of metal filled polymers, carbon black filled polymers, and the conducting polymers.

low conductivity levels so far achieved. To substantiate his argument he compares the ratio of a material's conductivity to its density. Table 1 summarises the specific conductivities of copper, aluminium and a filled polymer. As shown, the specific conductivity of the polymer was lowest. Munstedt (1985) therefore concludes that it was an unrealistic aim to expect polymeric conductors to replace metallic conductors in this type of application. A power cable made of a conducting polymer available today would have to be the diameter of a drainpipe to achieve the desired specific conductivity!

Table 1 Specific conductivities of different materials

	$\sigma(Scm^{-1})$	$D(gcm^{-3})$	$\sigma/D(Scm^{2}g^{-1})$
ALUMINIUM	$3.8*10^{5}$	2.71	$14*10^{4}$.
COPPER	$6.5*10^{5}$	8.92	$7*10^{4}$.
FILLED POLYMERS	100	≃1	100
CONDUCTING POLYMERS	10^{-2}-10^{4}**	≃1	10^{-2}-10^{4}.

** Quoted for polyacetylene.

In summary, it can be shown that filled polymers will not replace metallic power cables because it is unlikely that a suitable composite of a conductive filler and polymer will have both the high conductivity of copper or aluminium and low density of an unfilled engineering polymer.

2.2 Static Electrification and Electromagnetic Interference Shielding Applications

There are other applications for which materials with lower conductivities would have commercial applications. Two main areas for the lower than metallic conduction property band are the discharge to earth of electrostatic charges (ca. 10^{-4} to 10^{-8} Scm^{-1}) and the shielding against electromagnetic interference (> 1 Scm^{-1}) (Techtrends 1987). Electrostatic build up can cause many problems, from the trivial but unpleasant effect of the mild electric shock one receives on discharge after walking across a nylon carpet, to the potentially hazardous situation of explosions due to the ignition of vapours, dust or gases by electrostatic discharge (Sommers, Norman (1970), Gersteisen (1985)). Norman (1970) cites the example of explosions occurring in hospital operating theatres due to static discharge igniting anaesthetic gases. Other areas where static causes problems are described by Gersteisen (1985). They include the build up of charge on photocopier paper pathways, the potential explosive hazard of munition propellants, LPGs and the adverse effect of static which causes micro chip failure of CMOS and microprocessor semiconductor circuits. The importance attached to static damage to the silicon chips may be seen by the amount of anti-static packaging materials manufactured. Ellis (1986) reports that in 1984 an estimated 25 million to 30 million lb. of conductive materials were used for electrostatic discharge purposes in the packaging of electrostatic-sensitive electronic components.

A publication entitled Techtrends (1987) lists conveyer belts, hoses, dust explosions, textile machinery components, tote bins, anti-static wrist straps and matting as other examples where anti-static materials are used.

A full treatment of electrostatic discharge was given by Norman et al (1970). They summarised the generation of static charges, described when static was a nuisance or a hazard and then reviewed methods of reducing static electrification.

In summary, static build-up may be discharged successfully using filled polymers, solely due to the conductivity requirement being between 10^{-4} to 10^{-8} Scm^{-1}, well within the range of commercially available filled polymers.

When a voltage undergoes a rapid change, for example a voltage step from a contact switch opening or closing , or a voltage surge or pulse from a fluorescent light, an electromagnetic (EM) wave or radio frequency (RF) wave of wide frequency content is emitted. This wide frequency EM wave may be shown to be present by performing a Fourier transform on the voltage step, pulse or spike (Chapter 3, Lynn (1972)).

EM and RF waves may interfere with sensitive electronic and digital electronic devices, causing memory loss in computers and disturbances in TV reception (Nangrani 1985). (See Gersteisen (1985) for case histories of interference problems).

Shielding from electromagnetic interference (EMI) and radio frequency interference (RI) is likely to be one of the largest areas of application for conducting polymers (Techtrends 1987) in the future. This area of application was precipitated by the American Federal Communications Commission docket 20780 part 15, subpart J, on the levels of electrical noise emission from electronic equipment (which came into force on the 8th October 1983). It is estimated that EMI shielding effectiveness of 30-40 dB (blocking off 99.90-99.99% of an interference signal) may be achieved by a barrier whose bulk conductivity was 1 Scm^{-1}.

Shielding may be achieved by placing the "electronic device" in an electrically conducting box or what is termed a Faraday cage. Conducting polymer composites, containing metal fillers, can easily satisfy the bulk conductivity requirement and it would be feasible to manufacture cabinets and enclosures using these materials without making significant changes to the present production methods.

An excellent summary of the legislative environment of EMI shielding was given elsewhere (Techtrends 1987). It would appear that in the not too distant future the European Communities will be agreeing a unified standard when an EEC Directive on EMI shielding comes into force. The Directive was based on the recommendations proposed by CISPR Publication No. 22, 1985, "Limits and methods of measurement of RI characteristics of information technology

equipment" (Techtrends 1987) and were similar to those standards already enforced in the USA.

3.1 Conductive Fillers: Carbon Blacks and Metals

The filler was obviously the critical component in terms of controlling the conductivity of filled conducting polymers. Clearly the filler must be conductive while the polymer essentially acts as a matrix binding the conductive phase together (Wnek 1986). However, the orientation and morphology of the filler must be carefully controlled to ensure optimum conductivity.

The conductive materials used for filling insulating polymers are primarily carbon blacks or metals. It was the amount of conductive phase as well as the structure and shape of that phase which determine the ultimate conductivity imparted to polymers. Hence a wide range of conductivities was attainable (Young 1984), typically 10^{-1} to 100 Scm^{-1}.

In the following sections different fillers and the literature covering the associated composites are reviewed. The conduction mechanisms that have been proposed to relate the electrical properties of the composites to their physical structure are also reviewed.

3.1.1 Carbon blacks.

Conductive carbon black is by far the most widely used filler for imparting electrical conductivity to insulating

polymers (Blyth (1979) pp.127). Carbon black is similar to graphite microstructurally and is intrinsically semi-conductive in nature with a conductivity in the range 0.05 to 2 Scm^{-1}.

Carbon black, as opposed to graphite, has been chosen as a conductive filler for polymers because it was said to provide better compatibility (Blyth 1979). The rubber producing industry has long been accustomed to using carbon black as a mechanical reinforcement agent. Blyth (1979) lists the reasons favouring carbon black as follows:

(i). good compatibility, it adheres and mixes well with polymers.

(ii). its similar density to polymers ($\simeq$1 g cm^{-3}) means the composite's density is unchanged.

(iii). carbon blacks are cost effective fillers; they are cheap.

The amount of conductivity a particular type of carbon black imparts to an insulating polymer depends on the physical and chemical properties of that particular grade. The different grades of black are physically distinguished by what is termed their 'structure'; particle size, surface area and porosity.

During their manufacturing process, the carbon black particles, 10 to 100 nm diameter (Techtrends 1987), are permanently fused together into clusters or aggregates (Sichel (1982) Chap 1, Sommers). Aggregates of carbon black

may consist of long chains of carbon black particles. The structure of a carbon black grade is a measure of how many particles of carbon black there are in a chain (Van Beek (1962)). Generally, the higher the structure of a black, the higher the conductivity imparted to a polymer (Bigg(1977), Sichel (1982) Chap 1, Prodst (1984)).

The most preferred manufacturing processes for conductive grades of carbon black have been those that favour the highest structured blacks and those that produce blacks with few defects.

Medalia (1982) outlines the main carbon black manufacturing processes. Most carbon blacks today are produced by the furnace process whereby natural gas and air are burnt in a furnace into which an oil of high polyaromatic content is injected. The oil feedstock cracks forming the carbon black, the structure of which may be controlled by the addition of alkali metal salts. The resulting furnace blacks are either sold in the 'fluffy' form, the form that emerges from the furnace black cleanup process, or in the compressed 'pelleted' form. The density of the blacks are ca. 0.15 gcm^{-3}. The process is continuous and totally enclosed. Other processes include the inefficient channel process, the thermal process and the acetylene gas process.

The channel process is now obsolete. It involved the heating of iron channels over which natural gas was passed. The gas would crack on the hot channel surfaces and the black would then be scraped from the channels.

The thermal process involves a 'heat' and 'make' cycle. A firebrick tower was heated with a natural gas and air mix. The air supply was subsequently cut off and the natural gas cracked on the hot surface of the fire bricks. Thermal blacks have low structure and therefore low conductivity.

An exothermic reaction of acetylene gas will produce acetylene blacks. The high temperature of formation of acetylene blacks gives good defect-free grades. Consequently they are good conductors, as the freedom from defects reduces the probability of conduction electrons being trapped and so unable to contribute to the conduction current (Medalia 1982).

3.1.2 Examples of conductive grades of carbon black.

Suppliers of conductive grades of carbon black are listed by Smoluk (1982). These are Cabot Corps. 'super conductive' grade (presumably Black Pearls 2000 Black) selling at $7.50/lb., Colombian Chemical Corps. Conductex 40-220 at $5/lb. and Noury Chemical Corps. Ketjenblack at $4.59/lb. All the prices quoted are at 1982s levels and are reproduced here as a comparative guide only. Techtrends (1987) gives a more up-to-date pricing for carbon blacks as follows:-

Carbon Black Grade	$/tonne	$/$m^{-3}$
Standard GP black	950	1710
Standard conductive black	1550-2000	2790-3960
Super conductive blacks	9000	17100

As may be seen from the Table, conductive grades of carbon black are approximately ten times the cost of ordinary reinforcing blacks.

Cabot Corporation, the world's largest carbon black producers, manufacture two other oil furnace conductive blacks (Sommers), namely Vulcan XC-72 Black (N472), and Vulcan P Black, the latter having lower conductivity.

The Vulcan XC-72 grade seems to be the favoured black for the production of experimental and development grades of conducting polymer composites (Forster 1971, pp.15 fig 17 Sichel 1982).

Cabot Plastics produce a polymeric conducting composite using carbon black as the filler and polypropylene, polyvinylacetate, polyethylene, polyamide, polystyrene, and polyurethane as the possible base resins (Techtrends 1987).

3.1.3 Carbon black particles, aggregates and structure: classification methods for carbon blacks

Electron microscopy studies of carbon black particles show them to be made up of graphite-like concentric layers of carbon atoms (pp. 98 Norman 1970, pp. 3 Medalia 1982, Jachym 1982), the particles being 10 to 100nm in diameter (Techtrends 1987).

Over small areas the layers are reportedly more or less parallel. However, Van Beek (1962) contradicts this by reporting diffuse X-ray diffraction patterns of carbon black particles as evidence for randomly oriented submicrocrystals of graphite in the carbon black particles.

The layer structure may continue into other spherical particles of carbon black forming permanently fused clusters or aggregates of carbon black. The aggregates of carbon have a tendency to form "pseudo-fibres" or chains termed "structure" (Blyth 1979, Van Beek 1962).

Structure, the surface area of aggregates, any absorbed chemicals on the surface of the carbon black (surface chemistry) and the carbon black particle porosity all characterise different grades of carbon black, be they conductive or reinforcing blacks.

Higher conductivity was synonymous with the higher structured grades of blacks (Sommers, Van Beek 1962). Norman (1970) cites Stubdebaher's (1957) grouping of blacks according to structure; conductivity decreases from (a) to (e) as follows:

(a) Acetylene and super-conducting furnace blacks

(b) Most oil furnace blacks

(c) Gas furnace blacks

(d) Channel blacks

(e) Thermal blacks

As structure was essential for good electrical conductivity it was important to understand why there was a tendency for structure to develop in carbon blacks. Norman and Blyth review possible explanations for this phenomenon. It was postulated that droplets of high molecular weight

hydrocarbons form necklaces at some intermediate stage in the carbon black manufacturing process and this "necklace" structure was maintained when the hydrocarbons cracked. This would seem a reasonable explanation if it were not for the tendency for structures disrupted during shear mixing to re-amalgamate on ageing. There were perhaps thermodynamically driven processes favouring chain reformation which as yet are not fully understood.

The structure of carbon black may be estimated by an oil absorption test as described by Bolt et al (1960). The object is to find " the minimum volume of oil (usually dibutyl phthalate (DBP) measured in cc/100g) which will give, under conditions of controlled mixing, a mix having no voids". A high structured material will have long chains with possibly many side branches and consequently, this form of carbon black will have many voids when the aggregates are packed together. Hence, more oil will be absorbed by these porous blacks, giving an indication of the high structure. The converse of this case may be exemplified by the packing of spheres. Spherical single particles will have a greater packing density leaving less space between spheres. Hence less oil absorption by smaller void space will be indicative of lower structure.

Conductivity was related to structure (Blyth 1979, Van Beek 1962) and for those blacks with higher structure (long chains, many side branches) there will be a greater probability of a continuous conduction conduit path being

formed, i.e. more material being in contact forming a continuous conductivity network.

Surface area measurement characterises the size of the carbon particles and micro-porosity (Sommers). Increasing the number of aggregates per unit weight will generally give increased conductivity. The number of aggregates per unit weight was characterised by the surface area of a carbon black grade. Surface area is measured by absorbed nitrogen gas in units of m^2g^{-1} (Medalia 1982).

An increase in specific surface of a carbon black polymer composite has been shown to decrease the amount of carbon black needed to impart a given conductivity to a polymer (Gilg 1986). Waclawek et al (1987) present conductivities for nine different carbon blacks as a function of specific surface (m^2g^{-1}) and conclude that no "regular dependence" is seen. However, they do report a relationship between conductivity and carbon black grain diameter, showing that an increase in grain size gives a decrease in conductivity.

The surface chemistry, or the nature and structure of the chemicals absorbed on the surface of the carbon black aggregates, can have an important effect on the conduction of a particular grade of black (Waclawek 1987, and their ref. 18). During manufacture "chemisorbed oxygen complexes" are produced on the aggregate surfaces (Sommers). These complexes are insulating materials, therefore they are detrimental to the overall conduction of the carbon black. Absorbed materials may affect the structure of carbon

blacks by breaking the "chains" of carbon black particles on further processing (Medalia 1982, Blyth 1979). The nature of the surface chemistry of a carbon black is characterised by a measure of its volatile content (measured as a percentage), or loss of weight (CO and CO_2) on heating to 950°C (Medalia 1982). The acidic groups on the carbon black surface are estimated by the pH of an aqueous preparation of the black.

Contaminants will dilute the conductivity of a particular grade. The main contaminants present (levels of less than 1%) are grit and ash from the furnace wall linings, and tar from incomplete hydrogenation of the feedstock (Medalia 1982).

In summary, carbon blacks with higher structure, low volatile content and high surface area are those that have a favourable profile for good electrical conductivity.

3.2 Metal filled polymers

Filling electrically insulating polymers with metals has been a well established way of increasing their conductivity. All forms of metals and all types of metal morphology (powders, spheres, flakes, fibres) have been utilised, however it has become apparent that the different types and morphologies play an important role in the eventual conductivity of the composite. Filled polymers also tend to become stiff and brittle.

Copper and aluminium fillers would at first inspection be ideal fillers as they both have excellent conductivities.

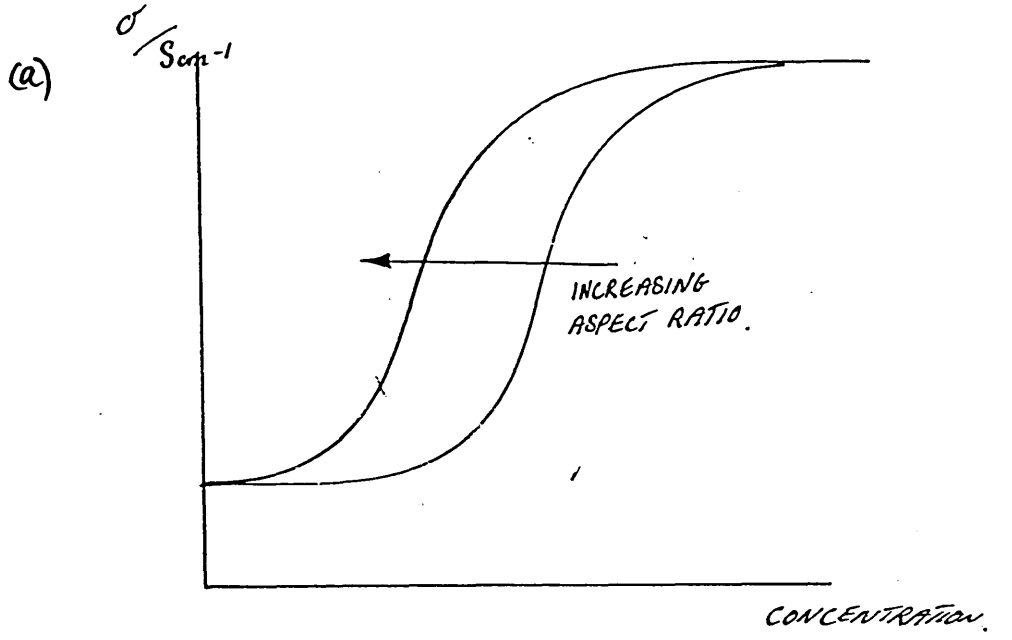

CONDUCTIVE SPHERES IN AN INSULATING POLYMER

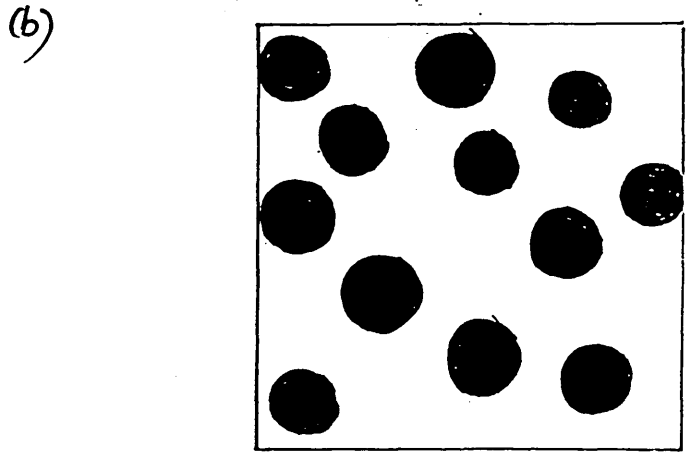

CONDUCTING FIBRES IN AN INSULATING POLYMER

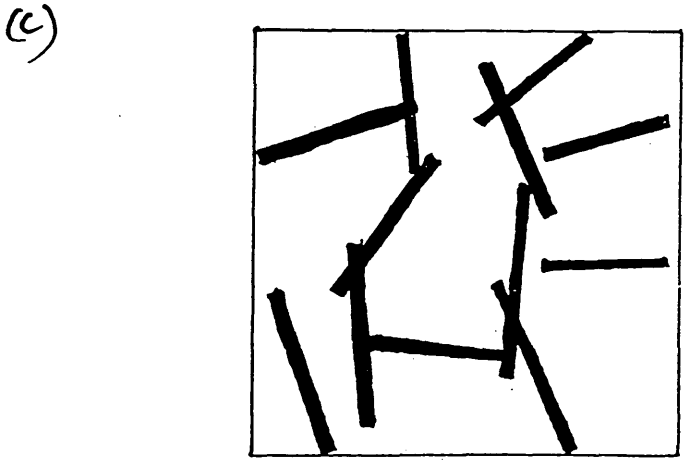

HIGH ASPECT RATIO L/D

Figure 2.
Aspect ratio effect on the percolation threshold (a). aspect ratio increase pushes the conductivity against concentration curve to the left, (b). conducting spheres in an insulating polymer (c). conducting fibers in an insulating polymer.

HONEYCOMBE NETWORK OF CONDUCTING PARTICLES

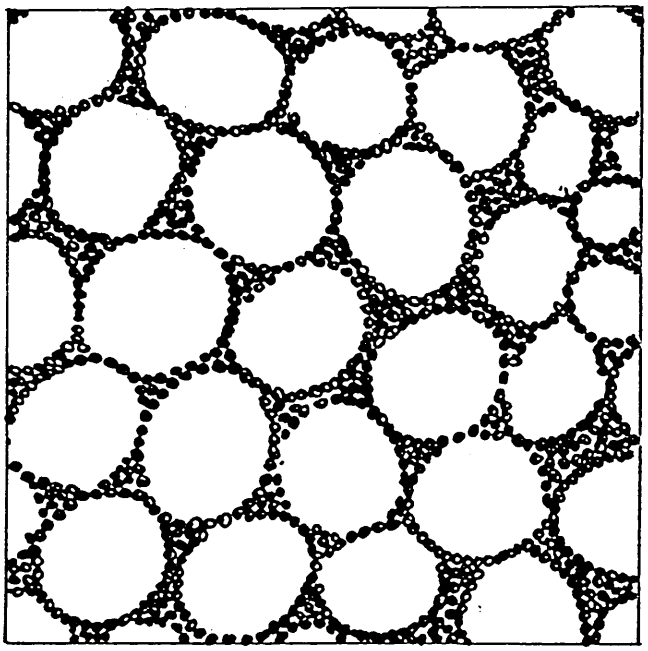

CONDUCTING PARTICLES DIAMETER MUCH
SMALLER THAN POLYMER PARTICLES

Figure 3.
Segregation of a conducting metal phase in polymer resin.

Unfortunately, they both produce non-conducting oxide coatings. Hence stainless steel is a preferred filler as no corrosion products hinder the inter-particle (stainless steel) conductivity.

High aspect ratios of particles increase the probability of network formation within the polymer (see figure 2c) (Bigg 1977,81,86, Davenport 1981). The percolation threshold was decreased to 7% by the use of fibres (Gersteisen 1985/6) (see figure 2a).

Segregation of the conductive phase into a honeycomb structure (figure 3) also lowers the percolation threshold down to 7% (Malliaris and Turner 1971). However, this method would only be suited to polymer processes that do not involve shear, for example rotational moulding.

The density of the composite may be kept low if metal coated fibres (graphite and glass) (Bigg 1983, Janeczek and Driscoll 1985, Luxton 1986) or coated spheres (Heinze and Ritter 1976) are used.

The main reasons that metal filled polymers are produced are their potential EMI shielding capabilities (Gersteisen, Bradish 1976, Smoluk 1982, Bigg 1983,1986, Gerbig 1985, Chung and Leung 1987, Techtrends 1987) and their thermal conducting properties (Nielsen 1974, Hansen and Tomkiewicz 1975, Kusy and Carneliessen 1975, Bigg and Bradbury 1981, Agari and Uno 1986). Good agreement between theory and thermal conductivity has been observed (Agari

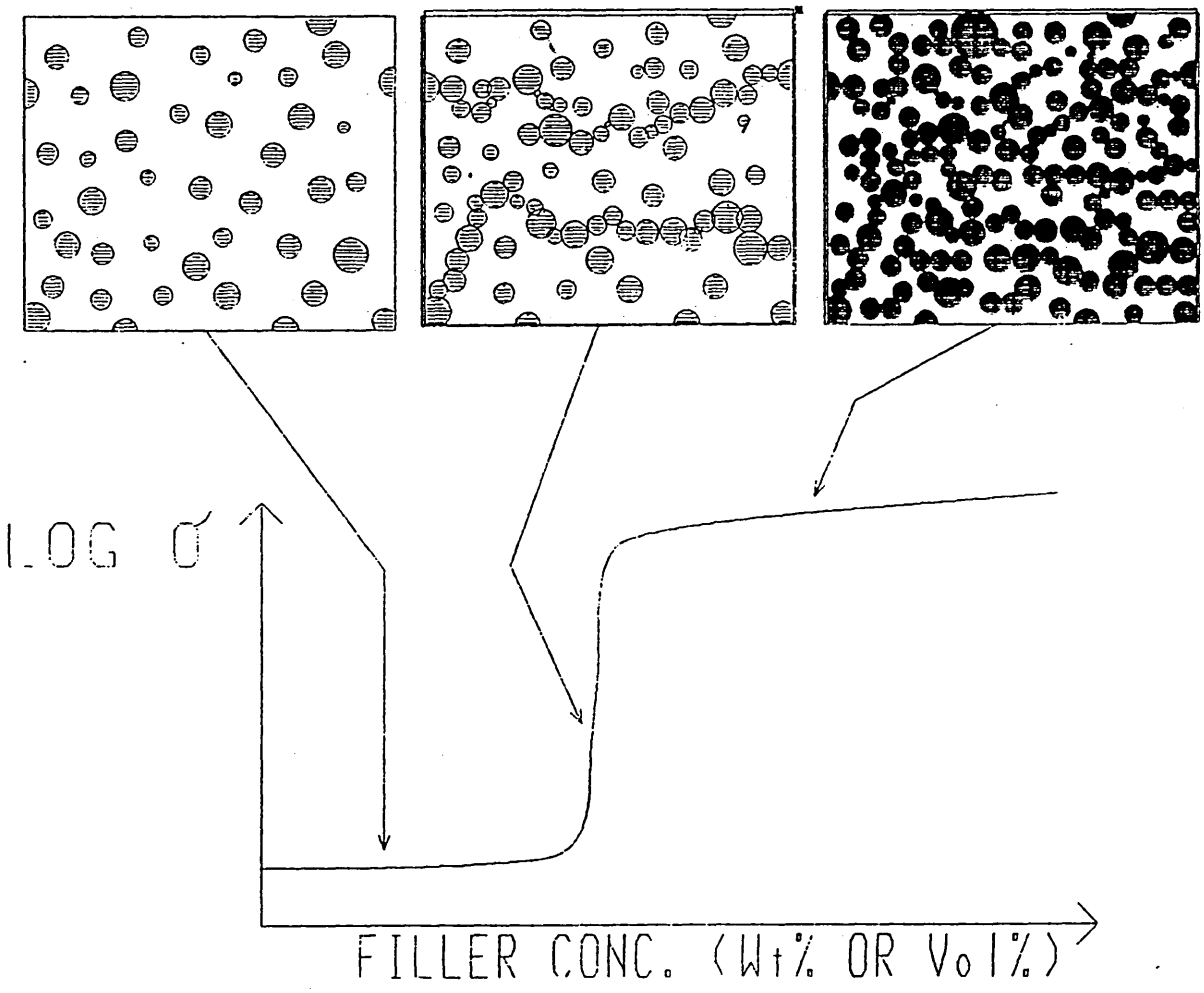

Figure 4.
A filled polymer composite showing the percolation threshold.

and Uno 1986). However, no predictive theory has been fully developed to explain the electrical conductivity of composites of this type.

3.3 Conduction mechanisms of filled polymer composites.

The loading of polymers with a conductive phase gives rise to a sharp rise in conductivity at some critical volume fraction of conductive phase. This transition point is termed percolation. The point of percolation will depend on many factors such as the shape of the conductive phase (Bigg 1977), the wettability of the filler by the polymer matrix (Miyasaka 1982), and the specific surface of filler (Gilg 1986).

Typically percolation thresholds occur between 20 to 40 volume percent for a randomly dispersed conductive phase in an insulating matrix phase (Young 1984, Bigg 1977, Sichel 1982, Gurland 1962,1966, Duke 1982).

The point of percolation may be thought of as the point where the conduction phase and the insulating phase just come into contact with each other forming a conduit path throughout the composite that will allow an electrical current to pass from one side of the sample to the other (see figure 4). However, Sichel (1982) has shown via electron microscopy that it is not necessary for particle to particle contact to occur in order for percolation to take place. (Waclakew, 1987, has also noted that it is not necessary for a conducting network to be formed in the

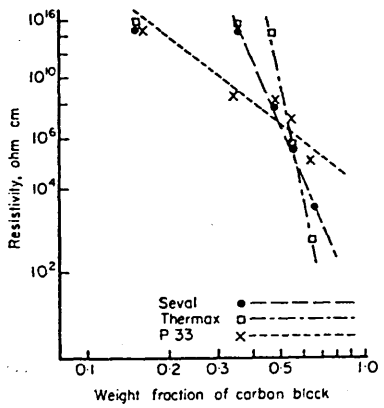

Effect of carbon black concentration on resistivity: Bulgin formula test plots: Thermal blacks.

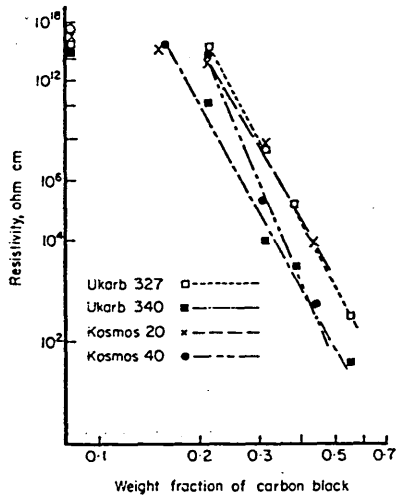

Effect of carbon black concentration on resistivity: Bulgin formula test plots: Gas base furnace blacks.

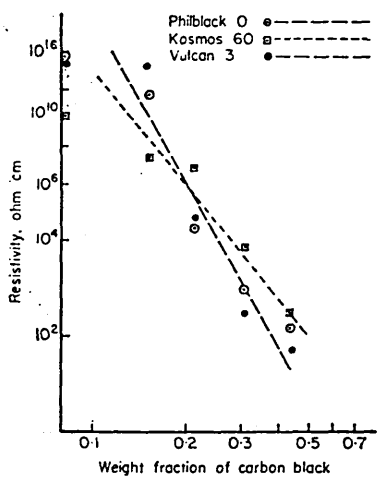

Effect of carbon black concentration on resistivity: Bulgin formula test plots: Oil base furnace blacks.

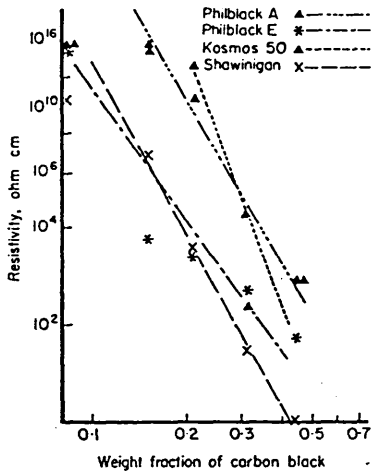

Effect of carbon black concentration on resistivity: Bulgin formula test plots: Oil base furnace blacks and acetylene black.

Figure 5.
Plots of resistivity verses concentration of carbon black replotted using the Bulgin equation.

whole volume of the sample to give this transition in conductivity). Small gaps of a few nanometers between the conducting phases were observed which has lead to the proposal that charge carriers (electrons) tunnel across this gap through the insulating polymer (Sichel 1982, Bahder 1971).

Clearly, the mechanism for conductivity in composites is more complicated to explain than those for single phase homogeneous materials.

Some of the theories, presented in the literature, which address the relationship between conductivity and filler loading, and those which try to relate the morphologies and physical properties of the conductive phase to the electrical properties of composites are now reviewed.

An empirical equation relating the conductivity of a carbon composite to carbon black concentration was formulated by Bulgin (Norman 1970) and has the form:

$$\ln\sigma = (A/f_w)^{-p}$$

where σ = conductivity

A and p are constants which have different values for different grades of carbon black.

f_w = the weight fraction.

(See Norman (1970), Figures 3.11 to 3.16 for a composite showing this relationship (reproduced here as figure 5)).

Blyth (1979) has reviewed the conductivity model proposed

by Voet et al. (1965). The model is based on an electron tunnelling effect whereby the conduction through the composite is controlled by the emission current of electrons crossing narrow gaps of insulating polymer separating the conductive phases. An emission current has the form :

$$j = AV^n \exp(-B/V)$$

where:

- j is the emission current.
- n and B are constants.
- A is a function of the tunnel frequency i.e. the number of jumps per second.
- $\exp(-B/V)$ is the transition probability through the energy barrier of the gap.
- n takes a value from 1 to 3
- V is the applied voltage.

At any one applied voltage, it may be shown that the natural logarithm of conductivity is inversely proportional to the average interparticle separation l_{av}, i.e. the tunnelling distance:

$$\ln\sigma \propto 1/l_{av}$$

This equation was modified to relate the conductivity to the cube root volume fraction (f_v) of the second phase:

$$\ln\sigma \propto f_v^{-n}$$

where n = 0.33

Blyth(1979) concluded that this model was inadequate in

describing the conductivity of a composite since the value of n for this model was 1/3 in contrast to that from the Bulgin empirical model where n is in the range 0.6 to 5.0. However, the Voet model based on electron tunnelling would appear a reasonable starting point, since tunnelling was thought to play a roll in the conduction mechanism as mentioned earlier.

Forster (1971) and Bahder (1971) have each attempted to explain conduction in carbon black composites. Foster qualitatively describes the conduction properties in carbon black composites as being a mixture of two classical models. He concludes his paper by saying that conduction in the conductive phase may be described by a band model, and interparticle conduction is controlled by a 'hopping' model. He suggests that the 'hopping' model dominates the conduction mechanism at room temperature. At other temperatures, thermally induced dimension changes affect the conductivity of the composite. A rubber filled polymer showed no temperature dependence while a cross linked polyethylene (XLPE) showed a decreasing conductivity with increasing temperature. The rubber samples' dependence was explained by the contraction of the matrix and expansion of the filler maintaining the same interparticle separations, whereas the behaviour of the XLPE sample was explained by an increase of filler separation with increasing temperature giving decreased conductivity. No modelling of the results were presented in this paper.

Bahder (1971) derived empirical models for the conduction mechanism of carbon black/polyethylene (PE) and XLPE composites using an a.c. bridge analogy. The model was developed to relate the electrical parameters to the structure of the carbon black chains in the materials. These polyethylene based materials were intended for use as semi-conductive shields in high tension electrical cables for power transmission. The use of such materials as an outer layer prevents corona discharge in the main insulation of the cables (see also Reboul 1982). The Voet model was rejected as a basis for a theoretical model as it predicted a conductivity over 50 orders of magnitude different from the observed value. The model adopted treated a carbon composite as a parallel resistor/capacitor network as show diagramatically below.

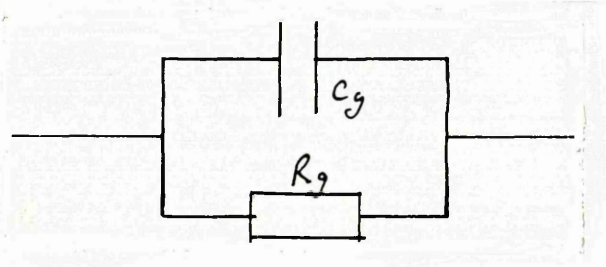

The current flow in the gaps was attributed to a tunnelling effect. Field emission effects were rejected as the apparent resistivity for field emission is too low compared with the observed values and the filler interparticle separation is too small for thermionic phenomena to occur.

The equation presented has the following form:

$$R_g = (2BCg/AD) \exp(BG)$$

where:

A = $9.45*10^{-6}$ $S\text{Å}^{-1}$ and is constant for carbon blacks.

G = the separation of conductive filler (Å).

D = the diameter of the conductive filler particles (Å).

B = 2.05 Å^{-1}.

Cg = capacitance of gap.

Rg = resistance of gap.

The equation was derived from the tunnel current density between two parallel metal electrodes separated by a very thin dielectric. It shows that as the separation gap increases the conductivity decreases, as would be expected.

Bahder modified the equation to relate the conductivity to the shape of the carbon black aggregates and the separation of carbon chains:

$$\sigma \propto (LD/G).e^{-2.05G}$$

where:

L = length of the carbon black chains.

G = the separation of conductive filler (Å).

D = the diameter of the conductive filler particles (Å).

Consequently the requirements for a conductive composite are that the carbon is in the form of long continuous (high structure) chains with small gaps separating them, as borne out in practice. Since the equation was derived for

touching spheres of carbon black, it would be reasonable to suggest that the model underestimates the conductivity as electron microscopy shows that carbon black particles merge into each other rather than just merely touch.

The Bueche (1972) approach to explaining the conductivity/concentration curves is to use an analogy with the theory proposed by Flory for gel formation during the polymerisation of small molecules each of which is multifunctional. Each molecule can form direct chemical bonds with more than one additional molecule. Bueche (1972) considered a parallel conductive network in a sample and derived the equation for the conductivity of the composite given by :

$$\sigma = V_m\sigma_m - V_p W_g \sigma_p$$

where:

σ_m = conductivity of the matrix (polymer).

σ_p = conductivity of the particles (filler).

V_p = volume fraction of particles.

W_g = gel fraction or the fraction of conductive phase forming the conductive network.

and $W_g = 1-(1-\alpha)^2 y/(1-y)^2 . \alpha$

α = the branching probability

y = the smallest root of the equation:

$\alpha(1-\alpha)^{f-2} = y(1-y)^{f-2}$

where:

f = the functionality of the particles or the number of "bonds" made with other particles (packing factor).

Bueche showed that critical concentration always occurs when a is equal to 1/f-1, and a transition occurs at $V_p=0.74/(f-1)$ for a close-packed system of spheres. However, he states that there was poor agreement between this theoretical equation and practice due to "poor particle dispersion and variable particle packing structure" in real systems.

Jackym (1982) also uses a Flory type analogy with the gelation during polymerisation of polyfunctional monomers. He describes a carbon black polyester composite produced by the addition of carbon black to the liquid resin which was cured by radical polymerisation. The outcome of their method was to produce a 'combined' composite with some of the carbon black being chemically bonded to the polymer chain.

This type of composite has a lower loading requirement to achieve the same conductivity as would otherwise be produced by the conventional mixing of the two phases. The conductivity ratio of the composites to the base polymer was given by:

$$\sigma/\sigma_p = 1-(1+Kf/2)V_c + (\sigma_{pc}/\sigma_p).W_g.(1+Kf/2).V_c$$

where:

σ/σ_p = the conductivity ratio of the composite to base polymer.

K = V_p/V_c the ratio of volume fraction of polymer to carbon.

f = the functionality of the particles or the number of "bonds" made with other

particles (packing factor).

V_c = volume fraction of carbon black in the composite.

σ_{pc} = conductivity of polymer bonded with carbon black.

W_g = volume fraction of carbon black that forms infinitely long conductive chains.

Good agreement with the observed conductivity was obtained when $\sigma_{pc} = 10^{-2}$ Scm^{-1} was used, although no explanation was given for this choice of value.

The authors claim that the relationship shows conductivity to be dependent on polymer chain length and size of the carbon black particles. A decrease in polymer chain length or increase in carbon black particle size predicts an increase in the critical concentration. Therefore the conductivity versus carbon black concentration curve was pushed to the right, which is detrimental to producing conducting polymers with low filler loadings.

Gurland (1962) and Aharoni (1972) considered the average number of contacts between conducting particles to be a governing factor in the conduction of filled polymers. Gurland defined a "parameter of continuity" as the probability of infinitely long chains of particles coming into contact. The necessary condition for a chain of infinite length is:

$$m > 2.\{1-f(0)\}.$$

where:

m = number of contacts/particle.

$f(0)$ = fraction of particles with no contacts.

Gurland showed experimentally using a silver and Bakelite composite that the abrupt transition from insulator to conductor on the conductivity/concentration curve almost coincided with a step on the plot of chain contact probability versus concentration.

Aharoni (1972) assumed that the conductivity was directly dependent on the surface area of the conductive phase and therefore on the 2/3 power of the volume over the transition region of the conductivity versus concentration curve.

Aharoni (1972) proposes a parameter, m, ("the average number of contacts of a particle of the conductive phase with continuous particles of the same phase"). He argues that for $m_1 = 1.0$ the probability of an infinite conductive chain becomes non zero and the composites' conductivity begins to increase. At $m_2 = 2$, nearly all the particles are connected in infinite chains.

This approach showed good agreement with iron particles dispersed in poly(imide-co-amide) amide. He also reports good agreement for other workers experimental results (see table 2).

Table 2. Conducting composites and their average number of contacts/particle for the onset and finish of transition between insulator and conductor.

SAMPLE	m_1	m_2	REFERENCED AUTHOR
Fe/Poly(imide-co-amide)	1.00	2.00	Aharoni (1972).
Ag/Bakelite	1.00	1.59	Gurland (1962).
Ni/PVC	----	2.01,1.59 1.75,2.17	Malliaris & Turner (1971).
Carbon black/Rubber	1.00	1.95	Gul & Zhuravlev (1978).

In a later publication by Gurland (1966), "percolation" theory was employed to explain the observed transition for the silver/Bakelite composite.

3.4 Percolation: The insulator to conductor transition for filled polymers

The transition from insulator to conductor for a composite material composed of conductive and insulator phases has been explained elsewhere using bond percolation theory (Stephen 1978, Clarke 1978). The probability that a particle in an 'array' was part of a network of connected particles of infinite size was called the percolation probability. The critical probability above which the probability was nonzero was the point at which contact between conducting particles in the insulating matrix occurs. This critical probability has been estimated for several 3-D lattices by Monte Carlo calculations (Frish 1962), and exact series expansion methods (Sykes 1964). It has been suggested, for the case of randomly dispersed conductive phases in insulating matrices, that it was "unnecessary to specify a particular 3-D lattice geometry"

for the type of conductive composite studied (Clarke 1978 or Lagues 1980). Consequently, percolation theory may be generalised as a description of the conductivity of a two phase system and it may be said that the system follows a universal scaling law of the form :-

$$\sigma \propto (X-Xc)^{s} \qquad Xc > X$$

where:

σ = conductivity.

X = concentration.

Xc = critical concentration.

s = 1.7

Theoretical studies on percolation have been carried out by Kirkpatrick (1973) and Stephen (1978). A survey of experimental results on electrical conductivity in 3-D percolation systems has been reported by Clarke et al. (1978) (many of the systems are not polymer composites). The reported values of Xc ranged from 0.07 to 0.75 and the value of s to range from 1.38 to 2.0.

Benguigui et al. (1987) studied the dielectric properties of carbon black/cross linked polyethylene composites and used a percolation model to explain their behaviour. Experimental results showed good agreement with percolation theory, the ratio of the complex dielectric constants of composite and conductor phases having the relationship:

$$\epsilon^{*}/\epsilon c^{*} = [X-Xc]^{t} F\{(\epsilon i^{*}/\epsilon c^{*})/[X-X]^{t-s}\}$$

where:

ϵi^*, ϵi^* are the complex dielectric constants of conductor and insulator phases respectively.

t and s ca. 1.3 in 2-D

t ca. 1.9 and s ca. 0.75 in 3-dimensions.

Above the percolation threshold, the conductivity followed the relationship:

$$\sigma \propto [X-X]^t$$

At a given frequency, the dielectric constant and relaxation frequency also followed a percolation type equation :

$$\epsilon \propto [X-Xc]^{-(2s+t)}$$

(2s+t) was found experimentally to have the value 2.8+/-0.5 whereas theory predicts 4.75, for s=2 and t=0.75.

The relaxation coefficient W_r followed the relationship:

$$W_r \propto [X-Xc]^{(s+t)}$$

with an experimental value of (t+s) found to be 2.6+/-0.2 whereas theory predicts 2.8.

Janzen (1975) proposed that the critical concentration threshold for a carbon black composite may be estimated from the density and the specific void space for a "randomly dense packed bed of filler" (powder). The relationship proposed was:

$$Xc = (1+4dv)^{-1}.$$

where:

Xc = critical volume fraction

d = density of filler in g cm^{-3}

v = specific void space cm^3 g^{-1}

(as measured by DBP ml/100g sample ASTM D3493-76)

The equation relates the physical properties of carbon black directly to the critical volume fraction, implying that high structure blacks (ie large v) give the lowest critical concentrations as is observed in real materials. Probst (1984) states that the predominant factor in lowering Xc values is the structure of carbon blacks. To take advantage of conductive grades of carbon black and mechanical strengthening of reinforcing blacks he suggests the use of both grades of black and proposes a modified Janzen equation for two carbon black fillers, vis:

$$Xc = [1+4d(v_a x + v_b(1-x)]^{-1}$$

where:

v_a = DBP of compressed sample of carbon black a.

v_b = DBP of compressed sample of carbon black b.

x = the weight fraction of black a.

Probst also presents a table of threshold concentrations for Phillblack XE-2 in 14 different polymers. The values of

Xc range between 1.0 to 4.4 wt% as opposed to a single value 3.3 wt% predicted by the Janzen equation. This spread in Xc values was attributed to differing thermodynamic and physical properties such as melt flow index, vinyl acetate concentration (in the EVA polymers), extent of cross-linking or thermoplastic state. Clearly specific void space and density of filler cannot solely predict the critical threshold value which is also dependent on the matrix material.

Bigg (1977, 1983) has shown that the aspect ratio of the conductive filler has a pronounced effect on the value of Xc. Experimental results show that an increase in conductivity was achieved for a given loading of filler by increasing its aspect ratio of the conductive filler. Fibrous fillers improved conductivity more significantly than spheres, flakes or irregular particles. No correlation between practice and theory for electrical conductivity was observed using a model proposed by Nielsen (1974). However, good agreement was observed when comparing thermal conductivity results with this model. This disparity was thought to be due to the differences in the conduction mechanisms of the two types of phenomena.

The aspect ratio effect was attributed to the increased probability of particle-to-particle contact which increased the probability of an infinite chain being formed in the matrix.

Rewriting the percolation equation to include a constant of

proportionality we obtain :

$$\sigma = \sigma_o \ (X-Xc)^s$$

It has been said that the critical concentration of a system will be dependent on "the dimensionality of the system, arrangement of particles and their degree of dispersal" (Wegner 1981). The application of percolation theory to a system should therefore be viewed in terms of the shape factors being the controlling terms in (X-Xc), and the conduction mechanisms in the σ_o term.

The models reviewed have been concerned with the role of geometrical factors, e.g. length of carbon black chains (structure) and separation of the conductive particles in controlling the critical transition from insulator to conductor. Miyasaka (1982) offers the opinion that too much emphasis was placed on these factors and that the thermodynamic effects have virtually been ignored.

We examined how Jansen's equation predicted a single value for the critical volume fraction of one type of carbon black in all polymers, but in practice a range of values has been observed. Miyasaka (1982) proposed that the excess interfacial energy introduced by carbon particles into a polymer matrix reaches a "universal value", wg^*, when the carbon black particles begin to coagulate forming a conductive network. They found that the larger the surface tension of the polymer and the larger the adhesion strength between carbon and polymer (both a measure of affinity

between the two phases) the greater is the required filler loading to reach the critical concentration value.

For spherical particles of diameter R, the equation derived for the critical volume concentration was:

$$Xc = [\ \{1+3(\phi_c^{\frac{1}{2}}-\phi_p^{\frac{1}{2}})^2\}/\delta g^*.R]^{-1}$$

where:

Xc = critical volume fraction.

ϕ_c = surface tension of carbon black particles.

ϕ_p = surface tension of polymer.

R = diameter of carbon black particles.

δg^* = interfacial excess energy.

$= KN^*S_o$

S_o = surface area of carbon particles.

K = the interfacial energy per unit area of the interface

$= \phi_c + \phi_p - 2(\phi_c \cdot \phi_p)^{\frac{1}{2}}$

N^* = number of conducting particles at the critical concentration.

The equation was in good agreement with the experimentally observed critical volume fraction versus surface tension plots.

The model also explains the rapid transition from insulator to conductor since δg^* was assumed to remain constant after the critical volume fraction was exceeded. Also δg^* was the upper limit of the interfacial energy which all the

polymers can have in common, i.e.:

$$\text{For } N < N^* \quad \delta g = K.P.N.S_o \quad \text{and } P = 1$$

$$\text{therefore} \quad \delta g = K.N.S_o$$

$$\text{as } \delta g \text{ reaches } \delta g^* \text{ and for } N > N^* \text{ , } P = N^*/N$$

$$\delta g^* = K.N^*.S_o$$

Wnek interprets the results of Miyasaka (1982) in terms of the wettability of the filler by the polymer matrix. The larger the difference in surface tension between polymer and carbon black, the greater the tendency for "chaining" of the carbon black to occur. If the difference is small, the tendency was for the filler to be homogeneously distributed in the matrix. It is the longer fibre structured fillers which increase the number of interparticle contacts and hence reduce the number of large tunnelling gaps.

4.1 Polymer Blends with Charge Transfer Complexes (CTC)

The blending of polymers with carbon black or metals provides one strategy for a conducting composite. A new method is the blending of insulating polymers with so called "organic-metals" or charge transfer complexes. Not only do these composites have interesting electrical properties (high dielectric materials, anti-static materials, EMI shielding, anisotropic conductivity) but they are potentially good candidates for materials with novel optoelectrical and optical effects. Non-linear-optical (e.g. frequency doublers), photochromic, photoconductive and photovoltaic behaviour are some potential properties. Such materials may find application in photocopiers, solar cells, light weight batteries, gas/light/pressure sensors, display devices, lithography and xerographic reproduction. These are but a few practical applications such materials may provide in the future. They may even find use in the future development of optical computers if they are found to have the ability to act as fast optical switches.

4.2 Charge transfer complexes: one dimensional organic conductors.

There are many examples of organic charge transfer molecules that are electrically conductive (Bryce 1984). These substances are usually precipitated as small fine, needle shaped crystals and are characteristically brittle. A charge transfer complex is produced by the partial transfer of an electron from a donating molecule of low

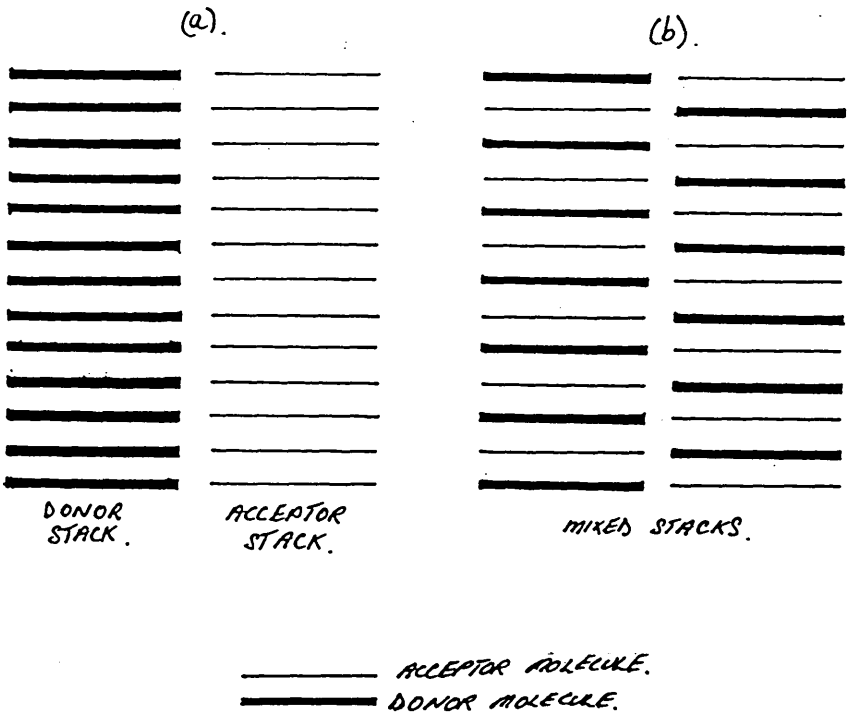

Figure 6.
Stacking of charge transfer complexes (a). Segregated stacking, (b). mixed stacking.

ionisation potential to an electron accepting molecule of high electron affinity (Blyth 1979). It must be stressed that it is only non stoichiometric electron transfer that gives rise to relatively highly conducting solids.

After partial transfer of charge, the subsequent consideration for a conductive charge transfer complex is crystal structure. High conductivity is associated with a crystal structure where the donor molecules stack one on top of another. Adjacent to this stack, the acceptor molecules stack in a similar way (figure 6a). This is the so called segregated stacking arrangement. No conclusive reason has been postulated as to why segregated stacking should arise, but it is generally accepted that segregation yields higher conductive complexes than charge transfer complexes of mixed stacks with alternating donor and acceptor molecules (figure 6b) (Blyth 1979, Bloor 1983, Bryce 1984,1985). Stacking may not be direct but can involve e.g. tilting, displacement etc.

The final requirement for conduction is the existence of a conduction path within the molecular crystal. Such a path would occur if the molecules formulating the stacks possess delocalised pi-orbital electrons over their carbon skeletons which can overlap pi-orbitals of adjacent molecules in the stack leading to long range overlap through the stack. Consequently, anisotropic conductivity occurs along these delocalised electron orbitals giving rise to the term quasi-one-dimensional organic conductors.

In summary, the prerequisites for high conductivity in a charge transfer complex are:

i). partial charge-transfer from the donor to acceptor stacks.

ii). segregated stacks of donor and acceptor molecules.

iii). delocalisation of pi-electron orbitals along the stacks.

Other factors that may contribute to increased conductivity are:

i). lack of solvent inclusion in the CTC crystals.

ii). donor and acceptor of a similar symmetry and size.

iii). uniform intermolecular spacing, regular overlap.

iv). planar molecules.

Electrical conduction can therefore occur by the transfer of an electron from the donor to the acceptor stack, once in the acceptor stack conduction proceeds up through the stack in a one-dimensional direction via the delocalised pi-electron orbital path of adjacent acceptor molecules. Alternatively conduction via holes can be envisaged in the donor stack.

4.3 Simple and complex salts of 7,7 ,8,8-tetracyano-p-quinodimethane (TCNQ)

The most widely used acceptor molecule was first synthesised at Du Pont in 1962. This is TCNQ which has two pairs of cyano groups at each end of the molecule, which make for a powerful electron acceptor. There are many

(a).

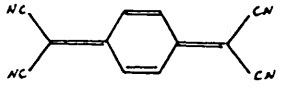

7,8,8 TETRACYANOQUINODIMETHANE (TCNQ).

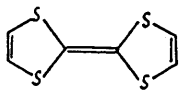

TETRATHIOFULVALENE

(b).

RING OVER BOND STACKING

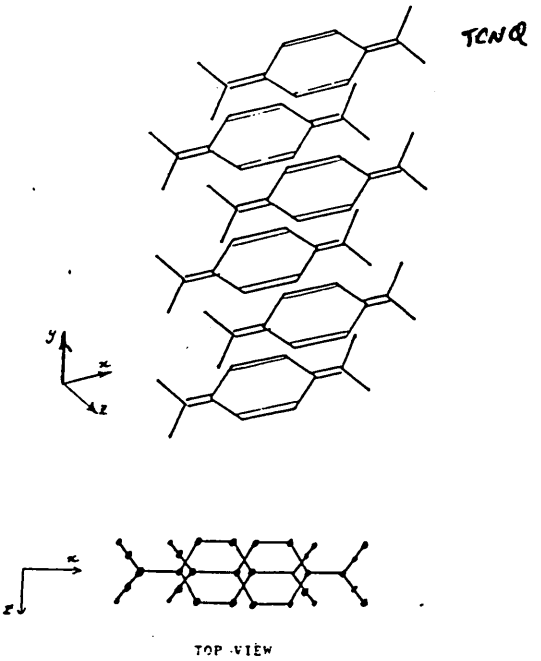

Figure 7.
(a). The 7,7,8,8 Tetracyanoquinodimethane (TCNQ) acceptor molecule and Tetrathiofulvalene (TTF) donor molecule (b). Ring over double bond overlap of the TCNQ charge transfer complex moiety (an example of displacement).

examples of TCNQ salts synthesised to date (Bryce 1984) with electrical conductivity ranging from 10^{-14} to $10^{2}Scm^{-1}$.

Figure 7b shows how the TCNQ molecules stack in one conductive complex; note the 'ring-over-bond' stacking.

Simple salts of TCNQ were made more conductive by incorporation of neutral TCNQ molecules ($TCNQ^{o}$) within the acceptor stack. Coulombic repulsion makes it unfavourable for an already occupied TCNQ site ($TCNQ^{-}$) to accept another electron (i.e. making the doubly charged dianion $TCNQ^{2-}$). However, if a neutral TCNQ molecule is adjacent to this charged TCNQ molecule, the electron may "hop" to the $TCNQ^{o}$ site, thus allowing another electron to reside on the originally charged TCNQ molecule. Charge transfer complexes with additional neutral TCNQ molecules in the acceptor stack are referred to as complex salts and are generally more conductive than the simple salts.

As yet charge transfer complexes have found little use in practical applications. It was the possibility of synthesising a high temperature superconducting material that drove many researches on in the search for new organic conducting materials. For this reason, many of the published charge transfer complex papers concentrate on the electrical characteristics of the charge transfer complexes. Although some charge transfer complexes undergo a superconducting transition at low temperature by the application of pressure (Bryce 1984) many complexes undergo a metal-to-insulator transition attributed to Peierls

distortion (Peierls 1955, Epstein 1971).

In 1987 the wind was taken from the sails of the organic chemists' hunt for a high temperature superconductor by the ceramic scientists discovery of the so called 1-2-3 compound, $YaBa_2Cu_3O_{7-x}$, a high temperature (93 Kelvin) superconducting material (Wu 1987). However, this does not mean that interest in charge transfer complexes will abate, since scientists are now looking at properties of charge transfer complexes other than their electrical conductivity, e.g. optical properties.

Research into potential properties of charge transfer complexes was hindered by the morphology of the materials, which consist of small, fragile, needle shaped crystals. Any potential application would probably have to exploit the properties of the charge transfer complexes in a compacted polycrystalline form. A more favourable and practically exploitable form of charge transfer complex would result if they were produced as flexible films or processable bulk materials.

4.4 Polymeric/elastomeric ionene anion radical salts of TCNQ

TCNQ may form a charge transfer complex directly with an appropriately prepared polymer. Polymers with positive sites in the polymer backbone will couple with TCNQ. The spacing of the these sites and possibly the rigidity of the polymer chains will influence the stacking of the TCNQ and therefore affect the overall conductivity of the polymer.

As with simple charge transfer complex compounds, polymer charge transfer complexes with TCNQ as the counter ion may form simple or complex salts (Bloor 1983). The conductivity can greatly increased by the incorporation of neutral TCNQ between the anion radical $TCNQ^-$ molecules (Ferraro and Williams 1987).

The charge transfer complex polymers reviewed in this section are all film forming semi-conductors in character, with conductivities in the region of 10^{-8} Scm^{-1} for the simple salts and 10^{-3} Scm^{-1} for the complex salts. The exact level of conductivity of the neutral TCNQ doped polymer depends on the dopant concentration.

It is unlikely that these levels of conductivity will be exploited for the purpose of EMI shielding, but they do fall into the range required for anti-static materials. Some of the polymers show interesting variable conductivity as a function of applied stress (strain gauge); another shows instability on exposure to oxygen.

Herman (1968,1972) produced a series of semiconducting

rubbery polymer CTCs with TCNQ as the counter ion. Polypropylene glycols (PPG) and solithane TCNQ simple salts were reported along with a polymer estane (polyurethane) TCNQ:lithium (LiTCNQ) blend. The two latter polymers were film forming, the PPG polymers' morphology was not reported.

For the elastomeric ionene of PPG reacted with LiTCNQ to give the PPG.TCNQ complexes, a series of differing molecular weight polymers was studied (150 000 to 4000 000). A PPG of known molecular weight was reacted with tolylene diisocyanate. Chain extension was achieved by the action of dimethylaminoethanol and a dihalide, thus forming elastomeric series of ionenes with variable cation sites on the quaternary nitrogen atoms. These ionenes were then complexed with LiTCNQ to give the TCNQ-ionene complexes. D.C. measurements showed an Arrhenius relationship for temperature variations, with breaks in the plots attributed to the glass transition temperature (Tg) of the PPG. Good stability was observed using time-lapse UV spectrophotometry.

Direct correlation was observed between the separation of the positive sites on the polymer backbone and the conductivity of the material by altering the molecular weight of the PPG. The highest conductivity was observed for the lowest molecular weight polymer (see Table 3).

Table 3. Conductivity of various molecular weights of PPG.

Sample molecular weight/1000	Conductivity/Scm-1
150	$3.6*10^{-11}$.
450	$6.7*10^{-12}$.
1000	$2.5*10^{-12}$.
2000	$1.4*10^{-15}$.
4000	$2.5*10^{-15}$.

A solithane TCNQ complex was formed by swelling a solithane film reacted with dibromohexane. The swelling solution consisted of a THF/methanol mixture with 10% by weight of LiTCNQ. The TCNQ replaced the Br^- anion to form the complex.

Torsion measurements determined the modulus of rigidity ($2*10^{-9}$ dynes/cm^2) to have an inflection at Tg (ca. 30°C) of the solithane TCNQ complex.

Dielectric measurements showed the real part of the dielectric constant to be in the range of 23 to 42 at 23°C.

A rubbery solithane ammonium TCNQ complex (5 wt% of TCNQ) film was subjected to mechanical stress and the conductivity variation observed. A thin sample showed no appreciable change in conductivity as a function of stress, but a thick sample showed a marked increase in the conductivity upon stressing in all mutually perpendicular directions. This was contrary to previously observed carbon filled rubbers which show a rapid decrease (two orders of magnitude @ 80% elongation) in conductivity with elongation. The polymer/TCNQ samples remained either

constant or increased by 50% at 80% elongation. The difference was attributed to stress induced orientation or an increase in the molecular mobility of electrons with increasing stress i.e. electron hopping or tunnelling between molecules is more probable with increased stress. Whatever the reason for the increased conductivity, this phenomenon may find use in pressure sensors or as strain gauges.

Nakatani (1975) reports the electronic spectra and electrical conductivity of simple and complex anion radical salts of TCNQ with poly(1-methyl-4-vinylpyridium). The simple salt may be abbreviated to $P4VP^{+}TCNQ^{-}$ and the complex salt to $P4VP^{+}TCNQ^{-}TCNQ_{x}^{o}$ (0</=x</=1.5).

On the addition of increasing amounts of neutral TCNQ to the simple salt, a new electronic absorption band appears at 3500 cm^{-1} as shown by a mirror reflection IR spectrophotometric method. The charge transfer band between the anion radicals $TCNQ^{-}$ (ca. 1100nm) disappears.

The new band was attributed to a charge resonance between the $TCNQ^{-}$ anion radical and the neutral $TCNQ^{o}$ as observed from the dependence of absorption intensity on the amount of added $TCNQ^{o}$.

Green, homogeneous films were produced with a conductivity of $7*10^{-8}Scm^{-1}$ to $8*10^{-3}Scm^{-1}$ for the simple and complex salts respectively. The maximum conductivity was observed in the complex salts at a mole fraction for the $TCNQ^{-}$ to

$TCNQ^{o}$ of 0.5. The variation of conductivity with temperature obeys an Arrhenius behaviour with an activation energy a minimum of 0.07eV at the same 0.5 mole ratio.

Nakatani gives four classifications for their polymer-TCNQ salts:-

(i). For P4VP+TCNQ-, the conduction occurs by charge transfer between the anion radical TCNQ- molecules, forming the dianion $TCNQ^{2-}$ and neutral $TCNQ^{o}$ moities ($TCNQ^{o}....TCNQ^{2-}$).

(ii). For a salt with small amounts of $TCNQ^{o}$ which will act as an electron accepting impurity (the given analogy is an impurity doped semi-conductor).

(iii). For $P4VP^{+}TCNQ^{-}TCNQ_{x}^{o}$ ($0.25<x<1.0$) the conductivity state due to charge resonance between $TCNQ^{-}$ and $TCNQ^{o}$

(iv). For $P4VP^{+}TCNQ^{-}TCNQ_{x}^{o}$ ($x>1.0$), large concentrations of $TCNQ^{o}$ diminish the conduction by trapping electrons.

In a later publication, Nakatani (1975b) reports the oxidation of the $P4VP^{+}TCNQ^{-}$ polymer films, finding $TCNQ^{o}$ and α,α-dicyano-p-toluylcyanide as the degradation products. The appearance of the films changes from green to a brown colour accompanied by a loss in conductivity.

An orange product was extracted from the oxidised films, and was identified as the α,α-dicyano-p-

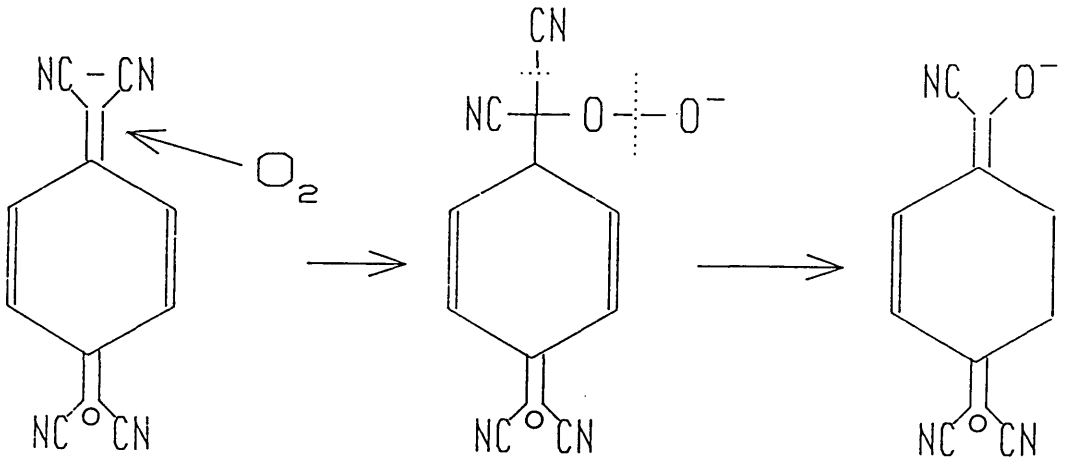

Figure 8.
Oxidation of TCNQ to α,α,-dicyano-p-toluoylcyanide.

toluylcyanide by the comparison of electronic spectra and thin layer chromatography R_f values for sodium α,α-dicyano-p-toluylcyanide. A suggested mechanism was proposed and is reproduced in figure 8.

It was further noted that Li^+TCNQ^- in solution also produced α,α-dicyano-p-toluylcyanide on exposure to UV light as compared to the $P4VP^+TCNQ^-$ and $P4VP^+TCNQ^-TCNQ_x^o$ reactions with oxygen in the dark to produce the same degradation product.

Ikeno (1977,1978) studied both the electrical conductivity and dielectric properties of polymeric and elastomeric TCNQ complexes.

Poly(N,N,N',N,'-tetramethylhexamethyleneparaxylene diammonium)TCNQ salts exhibit high dielectric constants (70-7000 at 30kHz-1MHz @ R.T.). The conductivity of the simple salt was reported as $3.7*10^{-8}Scm^{-1}$, increasing to $1.6*10^{-4}Scm^{-1}$ after doping with neutral TCNQ. The dielectric constant also increased on doping. The conductivity temperature dependence was Arrhenius, the activation energies decreasing with doping. The activation energy of polarisation agreed with the value for the conductivity, suggesting that the mechanisms for both polarisation and conduction are one and the same. The polarisation was explained by a microscale Maxwell-Wagner mechanism, and the conduction by a Flory type polymer gelation theory.

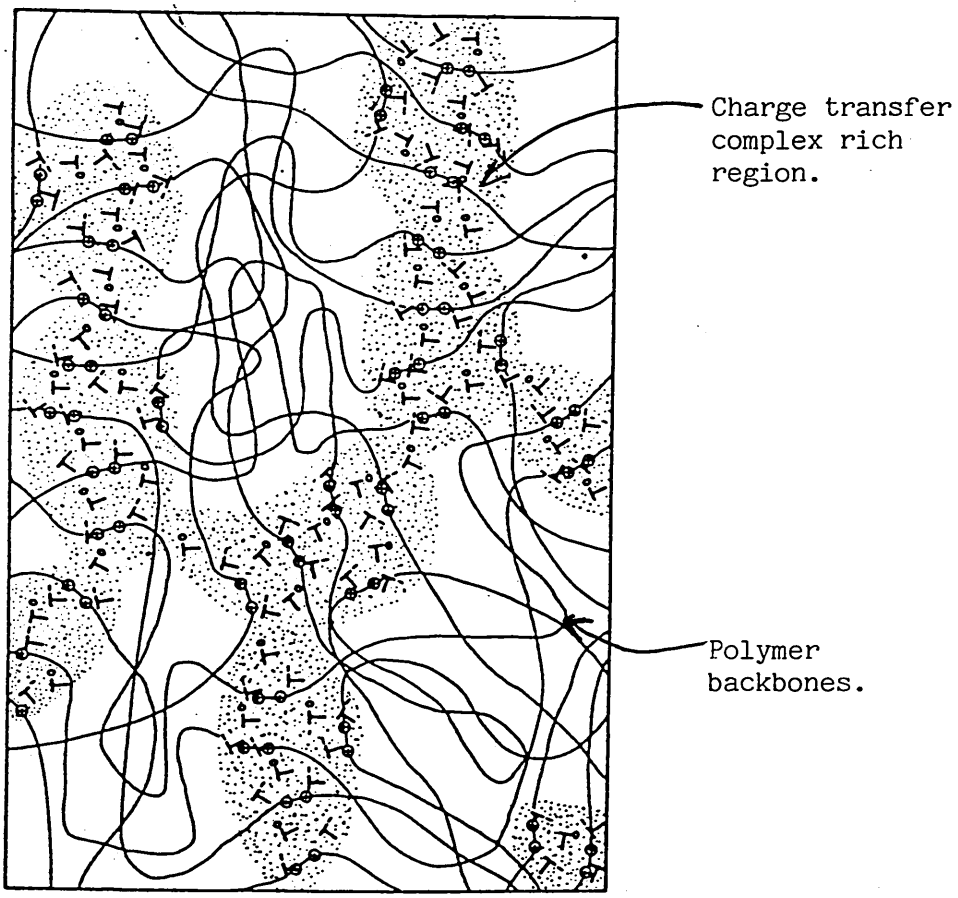

Figure 9.
Model proposed by Ikeno et al. (1979) showing the effect of doping with $TCNQ^{o}$,$TCNQ^{-}$ rich regions are represented by continuous dotted areas.

The structural models first proposed assumed a structure as shown below :-

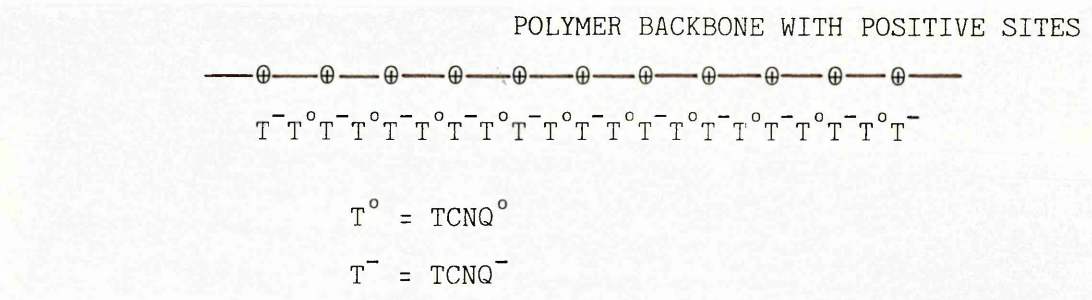

Ikeno proposed a different model, where the TCNQ molecules locate themselves in positions determined by complicated eletrostatic fields within the polymer, it being "impossible to identify the polycation polymer to which TCNQ molecule was coupled" (see figure 9). Conduction was assumed to involve either charge transfer or resonance. It was also suggested that it may be possible for conduction to occur between side-by-side stacks of TCNQ thus creating a "polyfunctional" system.

Summarising, the dielectric polarisation properties and conductive properties depended on two factors; the fraction of continuous and isolated conducting pathways, and the nature of the conduction path. Electron transfer in continuous paths gives electrical conductivity whereas electron transfer in isolated paths gives polarisation.

Ikeno (1978) also produced films of simple anion radical salts of TCNQ with an elastomeric ionene polymer containing poly(tetramethylene oxide) chains. Again the complex salts showed increased conductivity and decreased activation energy over the simple salt. The stiffness of the polymer

was observed to increase on doping with $TCNQ^{o}$, it being suggested that dopant may act as a crosslinking agent between positive sites on the elastomer backbone. However the film remained flexible, but lost its lustrous appearance.

Doping levels ranged from 12 to 33 wt% of TCNQ as opposed to 60 to 67 wt% for the work with polymeric salts (see Ikeno 1977).

The same structural model, involving phase separation of the ionic from the nonionic elastic units was assumed. Thus regions rich in TCNQ give a possible conduction pathway through the bulk of the material.

The final example of a polymer anion radical TCNQ salt is one prepared by Oshima (1987) who demonstrated the "usage of rigid and ordered polymer chains for obtaining good polymeric TCNQ salts". Oshima used poly(l-histidinium) (PLH) (15/4 helix structure monomer repeat unit of 3.00Å) to act as a rigid "pillar" to control the alignment of the $TCNQ^{-}$ molecules. A fine, dark blue precipitate of PLH as the counter polycation of TCNQ salts (stoichiometry of 1:1) was synthesised. The D.C. electrical conductivity temperature gives a non linear Arrhenius plot, the non linearity being explained by a variable range hopping conduction mechanism.

The conductivity at 300K was found to be $5*10^{-5}$ Scm^{-1} and independent of PLH molecular weight. The activation energy at 300K was measured to be 0.18eV. The stacking separation

of the TCNQ molecules was tentatively assigned 3.23Å which is close to the repeat monomer separation of 3.00Å.

4.5 Polymer/Charge transfer complex blends

Imparting electrical conductivity to polymers by the addition of TCNQ is not a new idea. In 1964 General Electric took out a British Patent (B.S. 1,067,260) for a nitrogen containing polymer TCNQ complex. In later years more work was carried out with the blending of already formed charge transfer complexes (organic conductors) with insulating polymers.

Ikeno (1978b, 1979) studied a series of monomeric-TCNQ salts blended with insulating polymers in the desire to produce high dielectric constant (ϵ_r) and low dielectric loss ($\tan\delta$) materials for the manufacture of film type capacitors. One of the blends studied had N-n-butylquinolinium-TCNQ (BQ-TCNQ) dispersed in polystyrene (PS) or polysulphone (PSul).

The polymer films were prepared simply by dissolving weighed amounts of complex and polymer in a mutual solvent, in this case dimethylformamide (DMF). This solution was cast onto a glass plate and vacuum evaporation was used to remove the solvent, leaving a thin polymer film on the substrate.

Ikeno et. al. (1979) have reproduced micrographs of blend polymers of BQ-TCNQ in PS, n-methylquinolinium-TCNQ (MQ-TCNQ) complex salt in PSul, and quinolinium-TCNQ complex

salt in PS prepared as above. The micrographs showed how the conductive phases are dispersed in the polymers as "very fine needle to thread-like crystals".

In having a dispersed conductive phase in an insulating polymer, it was envisaged that high dielectric constant materials would be produced by a polarisation process rather than an orientation polarisation effect, as seen in other conventional polymeric dielectric materials.

Table 4 summarises the electrical properties of these materials. Note that increased neutral TCNQ doping increases conductivity, as already observed for most charge transfer complexes and polymeric charge transfer complexes. The room temperature conductivities are not significantly large (maximum value obtained was for the MQ(C)-TCNQ(9.3wt%)/PS blend of $10^{-5}Scm^{-1}$). It is the dielectric constants and loss tangents that are of interest for these materials. Relatively high values of $\simeq$100 for ϵ_r and a low value of 3% for tanδ have been attained over the commercial frequency range. The BQ(C)-TCNQ blends show poorer linearity for dielectric constant versus frequency plots than do the MQ(C)-TCNQ and HQ(C)-TCNQ blends over similar frequency ranges (30Hz to 1MHz). This was attributed to the higher conductivity of the latter charge transfer complexes.

Table 4. Conductivities of blend polymers after Ikeno et al. (1979)

Polymer Base Resin	Complex salt* content(wt%)	Conductivity Scm-1
None	100 simple salt	$1.7*10^{9}$.
None	100 complex salt	$1.1*10^{-4}$.
PS	2.5	10^{-11}.
PS	5.0	10^{-11}.
PS	10.0	10^{-8}.
PSul.	5.0	10^{-13}.
PSul.	10.0	10^{-8}.
PSul.	20.0	10^{-6}.

PS = Polystyrene : PSul. = Polysulfone

* n-Butylquinolinium-TCNQ complex salt

The matrix resin also has an effect on the values of ϵ_r observed. Polysulphone was reported as a more compatible polymer with the complexes, giving a "homogeneous solution" of complex and polymer. The compatibility was thought to be due to the polar nature of the polysulphone, which destroys or deforms the charge transfer complex structure and consequently gives a lower conducting phase in the polymer. The non polar nature of polystyrene would not destroy or deform the complex structure, therefore poor compatibility leads to distinctive phase separation of the complex and consequently the conductivity of the complex in the matrix is higher. A highly conductive, separately dispersed phase gives an overall higher dielectric material. Therefore, to obtain a high dielectric constant and low loss tangent material you require certain prerequisites:-

(i). High conductivity phase for dispersal.

(ii). Low compatibility between conductive phase and polymer matrix to maintain the distinct conductive phase.

(iii). Ability of the complex to maintain its conductivity on blending with a polymer.

(iv). No continuous conductivity path throughout the matrix.

5.1 Photoconductivity of Charge Transfer Complex/Polymer Blends

The addition of a charge transfer complex to a polymer may enhance the photoconductivity of a polymer (Ulanski 1981). A photoconducting material is an electrical insulator in the dark and a semi-conductor in the light. The most common application for photoconductive materials at present involves their use as "drum" coatings in reprographic photo-copiers (e.g. polyvinycarbazole PVK). The effect is often referred to as the Xerographic effect.

Wojciechowski et al. (1981) and Rahman et al. (1985) both studied polymers doped with charge transfer complexes as a means of increasing the base polymer's photoconductivity.

Wojciechowski et al.'s material was produced by solution casting polycarbonate and trans-stilbene-tetracyanoethylene with methylene chloride as the mutual solvent. The material was shown to have the dopant homogeneously dispersed in the polycarbonate matrix.

The paper concentrates on the theoretical considerations of

a photodischarge parameter, showing the mode of photodischarge to be dependent on charge transfer complex donor to acceptor ratio, and the space charge distribution in the material. Charge carriers were generated in the material by the action of a phonon impinging on the material. The efficiency of phonon conversion to charge carriers, or the quantum efficiency, was found to be dependent on the square of the applied electric field.

Rahman et al. (1985) studied the sensitivity (ratio of photocurrent to dark current) as a function of the dopant acceptor concentration. The material was solvent cast and consisted of anthracene as the donor and TCNQ as the acceptor in a polystyrene matrix. The strategy is based on two methods, the Damber and Xerographic techniques. The material under investigation had one face in electrical contact with a graphite and copper electrode. The polymer and electrode were "sandwiched" between water, the water in this case acts as transparent electrodes. An electric field was applied across the material via the water electrodes by charging with an external circuit. The decaying charge on the material was then monitored twice at the same applied voltage. Once when no light fell on the samples surface and again when illuminated with a light source. Plots of the photocurrent versus decay time were obtained, from which the photocurrent intensity was said to be proportional to tanß-tanα, the intercepts on the decay time axis of the light and dark curves respectively. The sensitivity was found to have a maximum value for the material with an

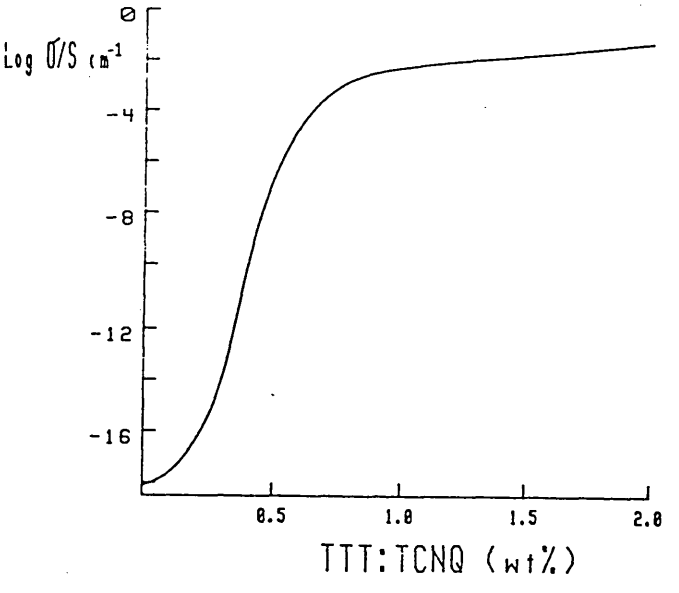

Figure 10.
Conductivity of polycarbonate reticulately doped with TTT:TCNQ.

anthracene to TCNQ ratio of 1:10, at an applied voltage of 0.25 Volts. The technique was shown to be a simple and reliable one, and it was envisaged that it would be used to study other polymer doped systems in the hope of finding one that may be used as a solar cell material.

5.2 Reticulate (network) Doped Polymers.

In this section a review of reticulately doped polymers is given. Reticulate doping involves the formation of a network of a conducting charge transfer complex phase penetrating the bulk of the insulating polymer. Reticulate doping reduces the percolation threshold to a remarkably low level of 0.3wt%, as opposed to levels of 20-40% associated with conventionally filled polymers. The mechanical properties of reticulate doped polymers are said to be unchanged by the addition of a charge transfer complex.

Kryszewski, Ulanski, Jeszka and Tracz form a group of workers at the Polish Academy of Science, Lódz, who have extensively studied polymers doped with charge transfer complexes. In some systems, they have managed to reduce the amount of dopant for percolation down to 0.3 wt% additive (see figure 10).

Such a low concentration of additive was achieved by growing micro-crystals of charge transfer complex while the polymer matrix was solidifying from solution. The first such material was reported by Jeszka et al. (1981). It

consisted of a polycarbonate matrix doped with tetrathiotetracene(TTT):TCNQ. Separate solutions of polycarbonate/TTT, and polycarbonate/TCNQ, dissolved in O-dichlorobenzene, were first prepared. The two solutions were mixed and cast onto hot glass at a temperature of 117°C. The TTT and TCNQ combined to form the charge transfer complex with a crystalline morphology. The conditions for micro-crystallite growth and densification of the polymer matrix were controlled by solvent evaporation. Methods of controlling solvent evaporation were not reported in this paper.

Within a certain temperature range the crystals of charge transfer complex grow from nucleation sites in the polymer matrix forming a dendritic type morphology which penetrated the bulk of the polymer base resin. At some optimum casting temperature the dendrites all grow so that they just touch their nearest neighbour, thus creating a network of conducting phase within the insulating polymer. Hence these materials have been termed reticulately doped polymer since reticulate means network.

Typical electrical properties of reticulately doped polymer film with 1 wt% of TTT.TCNQ in polycarbonate include a room temperature film conductivity of $3*10^{-2}$ Scm^{-1}. The charge carriers are electrons with a mobility of $9*10^{-2}$ $cm^2V^{-1}s^{-1}$, and the density of charge carriers is 10^8 cm^{-3}. Mobility, is a measure of how easily the charged species will move through the material under the influence of an applied electric field. Comparing the mobility of the reticulate

doped polymer with that of copper ($46cm^2V^{-1}s^{-1}$) we see that the reticulate polymers mobility was low.

The material's network of charge transfer complex was reported to be stable up to 177°C. Above this temperature the network was irreversibly destroyed and consequently the conductivity was lost. However, the conductivity of the film was stable at ordinary temperatures. One film did not lose its conductivity after several years at ambient conditions (Ulanski 1985a,b). The conductivity was not stable at elevated temperatures. A reticulate doped film of TTF.TCNQ in a polypropylene matrix had poor conductivity stability at raised temperatures. An initial conductivity of $1.9*10^{-2}$ Scm^{-1} was reduced by half after exposure to air of 50% relative humidity at 80°C in a time period of 240 hours (Munstedt 1988).

(N.B. Polypropylene was reported to be the matrix material in Munstedt's (1988) paper. This may have been mis-reported and probably should have been polycarbonate, since the Lödz group have never reported polypropylene systems as they would have encountered great difficulty producing such systems via solution casting).

In later papers the Polish workers consider the factors of casting temperature, solvent evaporation rates and viscosity of solutions on the morphology of the micro-crystals growth in the polymer matrix and their subsequent effect on the electrical properties of the material. The monitoring and control of such factors has led to some

interesting anisotropic conducting materials as well as the low level percolation materials already mentioned.

In Ulanski (1984a,1985) the Polish workers attempt to explain the effects that the controlling factors have on the morphology of the materials. Casting temperature, the solvents used and the choice of polymer matrix all have an effect on the morphology of the charge transfer crystallites formed in the matrix and consequently affect the overall conductivity of the composite material. To study these different effects Ulanski et al. (1984) studied TTT.TCNQ and TTF.TCNQ in Poly(bisphenol-A) carbonate (PC), polyoxyphenylene (PPO), polystyrene (PS), poly(p-chlorostyrene) (PchS), poly-N-vinylcarbazole (PVK), copolymers of PS and PchS and some mixtures of the above. The solvents used where p-dichlorobenzene, chlorobenzene and 1,2-dichloroethane.

For each system of charge transfer complex/polymer/solvent there was an optimum temperature that would produce the best conductive network to attain the maximum conductivity. At too high a temperature the complex either remained homogeneously dissolved in the polymer resin or the dendrites stopped short of touching their next nearest neighbour, both resulting in low conductivity materials. Too low a temperature and the forming charge transfer crystals did not have a dendrite morphology but formed needle-like crystals; the crystals may have different stoichiometry, hence the different morphology. The lower

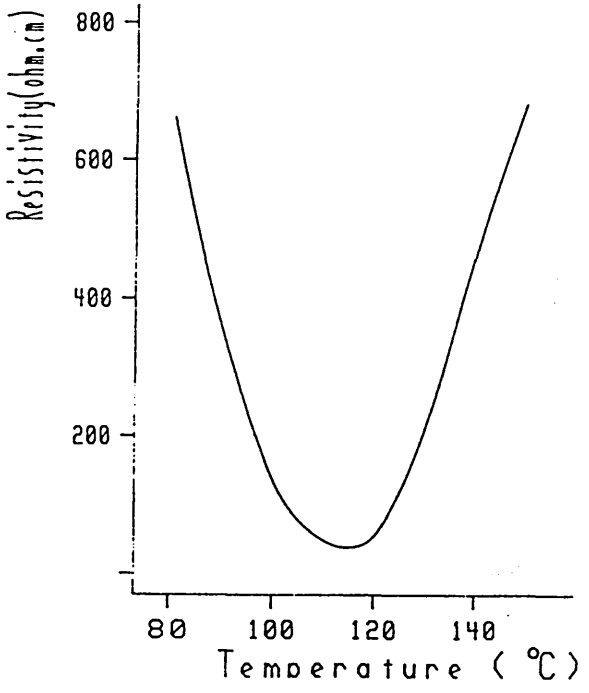

igure 11.
he casting temperature dependancy of a polycarbonate
1wt% TTT:TCNQ reticulate polymer cast from
ichlorobenzene.

than optimum temperature materials also had low conductivity. Formation of the needle-like crystals was attributed to the rapid precipitation of the complex when the solutions were less viscous.

Figure 11 shows a plot of conductivity versus casting temperature for a polycarbonate (PC) plus 1wt% TTT.TCNQ blend cast from o-dichlorobenzene.

If the solubility of the complex in the solvent was too high, it was found that the complex would not precipitate at any temperature. This was exemplified by PC+1wt% TTT.TCNQ and o-dichlorobenzene. Only small numbers of crystallites formed since TTT.TCNQ was very soluble in this solvent.

The crystallite morphology was reported to be affected by the solvents used, but this did not necessarily give lower conductivity composites. Using chlorobenzene instead of o-dichlorobenzene with a PC+1wt% TTT.TCNQ system, a fine needle-type morphology was produced. The maximum conductivity was similar but the optimum casting temperature was slightly reduced (see table 5).

Table 5. Optimum cast temperatures and conductivities of polycarbonate films cast from chlorobenzene with different contents of TTT-TCNQ charge transfer complex (CTC) after Ulanski 1985a.

CTC Content (wt%)	Optimum cast Temperature (°C)	Specific Conductivity Scm^{-1}.
1	110	$2*10^{-2}$.
0.7	95	$2.5*10^{-2}$.
0.5	90	$1*10^{-2}$.
0.4	80	$6.6*10^{-3}$.
0.3	77	$1.3*10^{-3}$.

The final effect on the morphology of the crystals formed was that due to the base polymer. By fixing the charge transfer complex and solvent used, a study of the effect of differing polymer matrices was investigated. The polymers were ranked in order of their merit as good matrix materials, as follows: PC, PPO and PS, PS-chS, PchS and PVK (Ulanski 1984a, 1985).

For some polymers(PVK, PchS), a charge transfer complex is formed between the TCNQ moiety and the donor-like polymer sites in a similar way as to those charge transfer polymers already discussed in an earlier section. For other polymers (e.g. PS and PPO) different charge transfer complex morphologies were obtained and it was generally concluded that the polymer had a significant effect on the crystallisation of the complex and consequently the resulting end conductivity of the materials (Ulanski 1984a).

In Ulanski et al. (1985) the viscosity of solutions and solvent evaporation rates are other morphological

controlling factors considered. In this paper a method was described whereby the electrical current flowing in the cast solution was monitored as a function of evaporation time. The solution thickening and network formation were observed to find the conditions for the maximum conductivity at the optimum concentration of charge transfer complex. In this way, as little as 0.3% by weight addition of charge transfer complex was found to give a conducting composite.

In this publication (Ulanski et al. 1985), they describe how dissolved charge transfer complexes start to crystallise as the complex concentration reaches a critical value due to solvent evaporation. Increasing concentration was accompanied with increasing solution viscosity, which may limit the rate at which the charge transfer complex diffuses through the polymer to a growing crystal front. Hence areas of supersaturation of charge transfer complex in the polymer matrix may be formed if the viscosity of the solution is too high. It was also said that the value of supersaturation, rate of nucleation and crystallisation lead to different morphologies of the charge transfer complex in the polymer and it was these parameters that were studied.

The charge transfer complex-polymer-solvent systems chosen for this work were TTT.TCNQ/PC/o-dichlorobenzene or chlorobenzene.

Monitoring of the charge transfer complex crystallisation

was performed by measuring the current flowing through the solution as a function of time. Two steel wires on a glass substrate were used as electrodes, and the applied voltage was kept small (1Vcm-1) to minimise the ionic transfer of material to the electrodes. Observations using an optical microscope gave information on the thickening of the solutions and network formation. The solvent evaporation was not forced.

For a system of 4wt% PC + 0.04wt% TTT.TCNQ in o-dichlorobenzene three temperatures, above, below and at the optimum casting temperature were considered. At the optimum temperature (120^{o}C) the charge transfer complex reaches the critical concentration for crystallisation at high viscosity. Spontaneous rapid crystallisation of the complex occurs as the dendritic form accompanied with a sudden increase in the current flow through the solution. The current steadily grows as a network forms until the viscosity of the solution reaches a value that hinders diffusion of any more charge transfer complex to growing crystal fronts. At this point the current remains constant with time.

Above the optimum temperature, dendritic crystals form but fail to produce the desired network as the critical viscosity is reached before the growing dendrites can connect with their nearest neighbour, thus the solution current increases then tails off at a much lower level than for the optimum temperature situation.

Below the optimum temperature, the solubility is lower and the charge transfer complex crystals form earlier. The solutions are less viscous and evaporation is slow leading to more stable crystallisation conditions. Morphologically the crystals are large, poorly branched and needle-like.

An interesting explanation for the low levels of additive to give a conductive material was considered. It was stated that the best morphology for a conductive material was one where dendritic charge transfer complexes were formed. Conduction occurred relatively easily along the branches of the dendrites. What was not clear was the mechanism by which the charge carriers move from one dendrite to the next. It was considered that the carriers maybe "injected" through thin polymer layers between dendrites from very sharp crystal ends around the dendrites' outer edges.

It was also suggested that micro-crystals, not easily seen, may be forced along channels formed between solidified polymer aggregates at the moment of final polymer solidification. If a channel was present, it was envisaged that the connection with other micro-crystals growing in the opposite direction along the same channel could occur. Therefore increased connectivity and "injection current" gave effective conductivity between dendrites.

Using the above method, a system of TTT.TCNQ/PC/dichlorobenzene was studied. The optimum cast temperatures versus resistivity from their paper is reproduced here as figure 11.

Percolation at 0.3wt% additive was obtained giving a conductive material ($1.3*10^{-1}Scm^{-1}$). The temperature dependence was weak as for the TTT.TCNQ/PC/O-dichlorobenzene material (Jeszka 1981). If the temperature exceeded the glass transition temperature of PC (ca. 135^{o}C) the network was destroyed by the expansion of the matrix.

The low percolation level of the reticulately doped polymers was considered in more detail in a paper on the effectiveness of doping by Ulanski et al. (1984b). Statistical models (percolation theory) could not satisfactorily explain why such low levels of dopant in these materials could produce a conductive composite. Ulanski et al. (1984b) applied a percolation model to their materials and compared the theoretical (calculated) value of conductivity with that observed for the real material. Assuming the material may be represented by a 2-D bond percolation system, and taking into consideration the geometry and conductivity of the charge transfer complex dendrites, they derived an equation for the theoretical value of the material's conductivity as:

$$\sigma_m = \sigma_{ct}[(2p-1/9p).x^2$$

where:

σ_m = conductivity of material.

σ_{ct} = conductivity of charge transfer complex.

p = number of contacts per cube wall; assume all dendrites are in contact with each neighbour by a single contact.

= 1

x = volume fraction of charge transfer complex.

Using this equation for PC+1wt% TTT.TCNQ with σ_{ct}=10Scm^{-1} 1.1*10^{-4}Scm^{-1}. This was found to be two orders of magnitude smaller than the experimentally measured value of σ_m = 5*10^{-2}Scm^{-1}.

To explain this difference, a mechanisms was proposed for effective transport of charge carriers between dendrites and the forced channelling of crystal growth. The charge transport through the polymer matrix gaps between dendrites was thought effective enough to give the higher conductivity observed, despite any lack of contacts similar to that observed in carbon black composites. Therefore, charge was injected (or field assisted tunnelling) across the polymer interface from the ultra sharp crystal spikes (Ulanski 1985c). The second explanation for the observed high conductivity was more speculative and involved the forced growth of the charge transfer complex crystals along channels between solidified polymers giving an increased probability of contact between crystals of neighbouring dendrites.

Dendritic or needle-shaped morphology of the charge transfer complex crystals does not effect the a.c. conductivity of the material (Ulanski 1985c). For several different charge transfer complex/polymer/solvent systems the a.c. conductivity was almost linear (not exceeding 5%) for all systems over the frequency range of 0.1kHz to

1000kHz. It was therefore concluded that conductivity was not limited by crystal contact.

The systems of reticulate doped polymers reviewed so far have been thin films with conductivity throughout the bulk of the material. In a Patent Application (Kryszewski 1984) methods for producing surface conducting materials are described. The method is a variant on the bulk conducting films. A polymeric material has either the donor or acceptor, or both, added to the base resin. This polymer could then be melt processed into components in the usual way by e.g. extrusion or injection moulding. The component may then have a surface treatment with a solvent or solution of donor or acceptor by vapour blowing exposure, damping, wetting or spraying. The solvent may penetrate the surface layer of the polymer and the donor or acceptor materials would come together to form a conducting network of charge transfer complex. Excess solvent would be removed by evaporation leaving the finished component with a conductive surface. Applications examples are given as anti-static or EMI shielding materials. Masking with templates could produce conductive pathways on the surface of objects (Ulanski 1985b). One sided conducting films could be used for capacitors, solar cells, electrochemical cells and as semi-conductive components.

Three examples of the production of surface conducting materials are given in the patent with conductivities ranging from $2.5*10^{-3}cm^{-1}$ $3.3*10^{-5}cm^{-1}$. One of the examples

is summarised below:

100 parts by weight of polycarbonate was dissolved in 4000 parts by weight chlorobenzene to which 2 parts by weight TCNQ was added. The solution was cast onto polyester film at 97°C. A yellow, non conducting film (10μm) adhering well to the polyester was obtained. This was wetted for five minutes with a 0.2 wt% TTF in chlorobenzene/n-heptane mixture (1:3) and then dried with hot air. The charge transfer complex crystallites had formed and the material's surface conductivity had risen too $3.3*10^{-5}Scm^{-1}$, adequate for the dissipation of static charge.

Polymer composites, where both the donor and acceptor materials are added first, are made conductive by the action of a solvent on the surface. The solvent increases the mobility of the donor and acceptors in the surface layers therefore allowing them to diffuse together to form the conductive network.

It was claimed that such materials are highly resistant to weathering agents and light. No diffusion of the complex from the polymer was apparent.

To investigate whether charge carriers are effectively injected from a charge transfer complex through a polymer material, Jeszka et al. (1984) studied the properties of polymer films with one electrode being a reticulate doped polymer. Comparisons were made with metal/polymer/metal electrodes.

The experimental material was PC doped with 0.3wt% TTT.TCNQ cast from O-dichlorobenzene @ 130°C (film thickness 30 μm). Gold electrodes were evaporated onto one side only or both sides of the materials.

Three experiments were performed:

1). Absorption/resorption currents.
2). Steady state d.c. conductivity.
3). Photoconductivity/photoinjection

The absorption/resorption test showed greater current intensity after a fixed time for the reticulate doped material than for the metal electrode sample. A difference was noted for the absorption and resorption of the negatively biased reticulate electrode material as compared to the metal electrode material. Steady state conductivity measurements revealed asymmetry between the biased electrodes of the reticulate electrodes, and a non linear Arrhenius temperature dependency for both positive and negative bias. No strong photoinjection from the reticulate electrodes was observed.

The observed differences of the absorption/resorption currents were attributed to field injection of charge carriers from the sharp "spikes" of the charge transfer complex into the adjacent polymer.

5.3 Anisotropic conductivity of reticulate doped polymers

Ulanski et al. (1984a) present a polymeric material showing anisotropic conductivity for a charge transfer complex doped polymer. The method involved the solidification of a charge transfer complex/polymer/solvent system by controlling the direction of evaporation of the solution. By this method of "zone solidification" a material with PC+1wt% TTT.TCNQ in o-dichlorobenzene showed a preferred orientation of crystal growth in the direction of the evaporation gradient. The conductivity along the direction of growth was ca. $10^{-3}Scm^{-1}$ with little temperature dependency (activation energy (Ea) ca. 0.015eV). Perpendicular to the preferred orientation the conductivity ranged between $10^{-8}Scm^{-1}$ and $10^{-13}Scm^{-1}$ giving a ratio of parallel to perpendicular conductivity of 10^5 and 10^{10}. The perpendicular conductivity was shown to have a greater temperature dependency with an activation energy of ca. 0.18eV. The difference in temperature dependency was attributed to the polymeric material separation of the "Crystal columns" by polymeric material, limiting conduction in this direction.

Sorm et al. (1984) studied polymer blends of 1-methyl-3-alkylimidazolium-7 (IM) and TCNQ simple ($IM^+.TCNQ^-$) and complex ($IM^+.TCNQ^-.TCNQ^o_x$) salts in PMMA, PVCa and PAN. The materials were made by mixing and then casting (glass substrate at 110°C) the solutions, for example; 4wt% PMMA in o-dichlorobenzene and $IM^+.TCNQ^-.TCNQ^o_x$ in DMF. A typical conductivity for a system of PMMA + 3wt% $IM^+.TCNQ^-.TCNQ^o_x$, was ca. $5*10^{-4}Scm^{-1}$. They found conductivity and

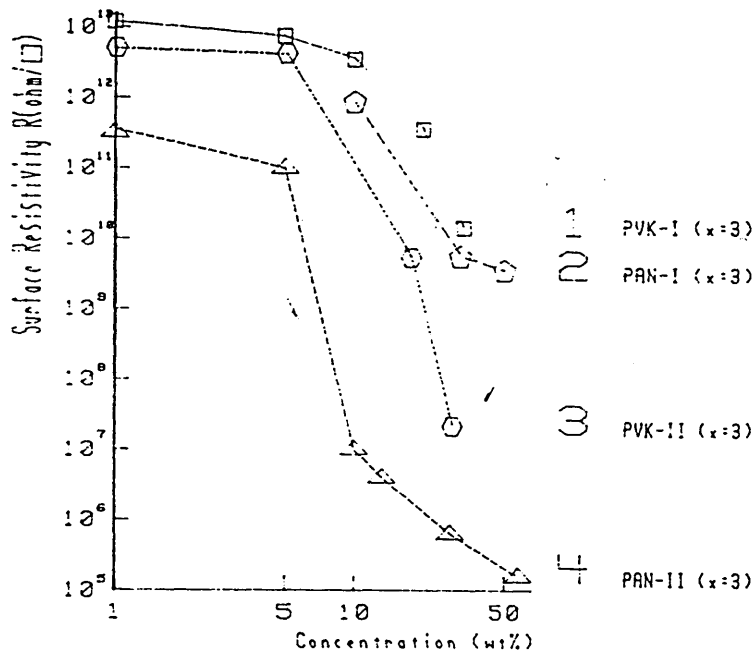

PVK = POLYVINYL-CARBAZOLE

PAN = POLYACRYLONITRILE

I = simple salt of 1-methyl-3-alkylimidazolium-TCNQ

II = complex salt of 1-methyl-3-alkylimidazolium-TCNQ

x = number of methylene groups in the donor

Figure 12.
Surface resistivity verses concentration of polyvinyl-carbazole and polyacrylonitrile polymers doped with simple and complex salts of 1-methyl-3-alkimidazolium-TCNQ.

morphology had a dependency on the number of methylene groups in the donor moiety of the charge transfer complexes. The maximum conductivity was ca. $10^{-3}Scm^{-1}$ for a PMMA + 7wt% $IM^{+}.TCNQ^{-}.TCNQ^{\circ}_{x}$ system with 2 methylene groups.

It was noted that complex salts are less soluble than the simple salts and they also attain a percolation threshold (ca. 5wt% of TCNQ salt) sooner than the simple salts (see figure 12). The polymers with phase separation were also more stable than homogeneous polymers. It was observed that the films with dissolved TCNQ salts turn green to brown after several days in air, indicating oxidation similar to that observed by Kakatani (1975a) whereby TCNQ and oxygen undergo a reaction forming α,α-dicyano-p-toluylcyanide (figure 8).

The effect of charge transfer complex addition on a polymer's mechanical properties was discussed by Kryszewski (1984). Little effect was observed for low additions. However, the conductivity is reduced by a few percent, irreversible by an elongation of 2 to 6%. At greater deformations, conductivity falls abruptly. The effect of mechanical deformation on the conductivity was attributed to the breaking of the contacts between crystallite phases.

6. EXPERIMENTAL PROCEDURES

6.1 Synthesis of Charge Transfer Complexes.

All glassware was cleaned with distilled water, methanol and the preparation solvent prior to any synthesis. The apparatus required for synthesis consisted of a 250ml reflux flask and associated condenser, heating mantle, Buchner flask and filter. The starting materials (Aldrich) were dried before use, in a vacuum oven, and weighed using a four point balance. Solvents (usually acetonitrile) were measured using a calibrated measuring cylinder. The acetonitrile was dried by storing over molecular sieves.

Due to the toxic nature of acetonitrile, all preparations were performed in a fume cupboard. Protective clothing was worn as routine.

The synthesis was performed as stated in the results section, the product being removed from the reaction liquor by filtering. The products were dried, weighed and stored in sealed sample bottles.

6.2 Charge Transfer Complex Characterisation Procedures

6.2.1 Elemental analysis

Elemental analysis was performed 'out-of-house' by The City University, London. The theoretical quantities of carbon, hydrogen and nitrogen present in the samples were calculated as follows:

For example, the calculation for the the expected formula of the product $DHPE^{2+}(TCNQ)^{-}{}_2TCNQ^{o}$ (or $C_{48}H_{24}N_{14}$)

Carbon	48 * 12.011	=	576.528
Hydrogen	24 * 1.008	=	24.192
Nitrogen	14 * 14.007	=	196.098
Total		=	796.818

% C = 576.528/796.818 = 72.35%
% H = 24.192/796.818 = 3.04%
% N = 196.098/796.818 = 24.61%

These values were compared with the analysis, the closeness or percentage difference being an indication whether or not the pure product had been synthesised. A difference of 1% or less was considered an adequate synthesis of the material.

6.2.2 Thermogravimetric Analysis

These studies were performed to determine the decomposition temperature of the complexes. The apparatus used was a Mettler TA3000 system. This apparatus sweeps through a set temperature range and records any mass loss of sample.

Approximately 5mg of sample was placed in an aluminium pan of known weight. The pan had been previously heated to red/white heat over a bunsen flame to ensure that any residual chemicals were burnt off. The sample was covered with an aluminium lid and placed in the furnace stage of the apparatus. The run parameters were entered into the processor, as instructed by the apparatus manual, and a run was commenced. The analyser automatically sweeps the desired temperature range, recording both the temperature and any sample weight loss due to any loss of solvent or

decomposition products.

6.2.3 UV/Visible spectra

To investigate the electronic absorption spectra of the complexes in solution or in their solid state, UV/Visible spectrophotometry was employed. The apparatus was a Perkin-Elmer 550S UV-VIS spectrophotometer .

The relative amounts of neutral and anionic TCNQ in the sample lattice were calculated using the Beer Lambert law (pp2 Williams 1980) and a measure of the heights of the neutral TCNQ absorption peak (395nm) and the $TCNQ^-$ anion (845nm) peak. The Beer Lambert law is as follows;

$$A = ELC$$

where:

A = absorption
E = molar extinction coefficient ($m^2 mol^{-1}$)
L = sample path length (m)
C = concentration (mol l^{-1}).

The molar extinction coefficients for the two TCNQ species are as follows:

for $TCNQ^-$ $E_{842} = 3750\ m^2 mol^{-1}$.
$TCNQ^o$ $E_{385} = 2200\ m^2 mol^{-1}$.
TCNQ $E_{385} = 6150\ m^2 mol^{-1}$.

The equation used to calculate these ratios was given by:

$$\frac{Abs(395nm)}{Abs(842nm)} = \frac{(y.2200)+(x.6150)}{(y.3750)} = R \qquad (6.2.3)$$

where:

R = absorption at 395nm/absorption at 842nm as taken from the UV/Visible spectra.

y = number of molecules of $TCNQ^-$.

x = unknown number of neutral TCNQ molecules.

A). Solution Studies:

For solution studies, spectrophotometric grade (Aldrich gold label) solvents were used. Quartz cuvettes were used throughout all the studies.

The solutions were prepared by adding a few grains of the material to the solvent in a volumetric flask. The grains were dissolved and the solution transferred to the cuvettes using a clean pipette. The spectrophotometer base line was recorded by placing a cuvette containing the solvent only in the rear arm and no cuvette in the near arm of the spectrophotometer. A spectrum was obtained when the cuvette with the charge transfer complex solution was placed in the apparatus. A wavelength scan from 900nm down to 250nm were performed.

B). Solid State Studies

Solid state spectra were performed on samples of the charge transfer complexes suspended in potassium bromide (KBr) discs. The discs were prepared as follows:

A few grains of the sample were ground up with dry KBr for 5-10 minutes using an agate pestle and mortar. The finely ground powder was then pressed into a disc using an evacuable 13mm die and a hydraulic ram capable of exerting a pressure of $752Nm^{-2}$ on the sample. The pressure was maintained for 10 minutes. A transparent disc was obtained if care was taken over this procedure. The clarity of the

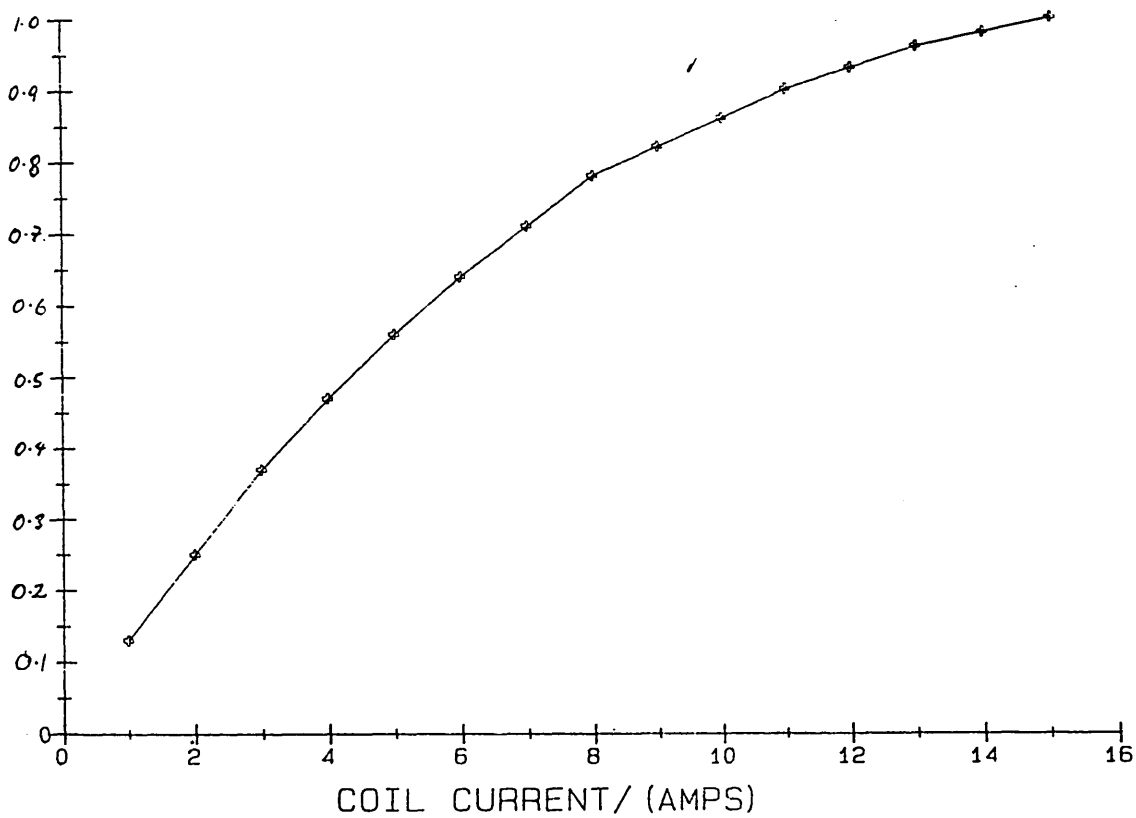

Figure 13.
Magnetic field as a function of magnetic coil current for the Faraday balance.

disc was maintained if contact with excess moisture was avoided. It was noted that after several hours the discs became opaque and consequently not suitable for measurement.

The spectrophotometer was zeroed with a blank disc (KBr only) in the appropriate arm of the apparatus, and a spectrum of the charge transfer complex in the KBr was obtained in the same manner as for the solution studies.

6.2.4 Magnetic Susceptibility Measurements

The magnetic susceptibility measurements were performed on a Faraday balance equipped with an Air Products Displex refrigerator and APD temperature controller. The temperature range attainable was between 300K and 20K. There was some doubt as to the position of the temperature sensing probe. Ideally, this should be as close as possible to the sample. Helium gas was introduced into the sample chamber to act as a heat exchange medium between the cold head and sample. It was assumed that the probe and sample were at the same temperature after holding at the required temperature setting for five minutes. A typical experimental run would take two days.

The magnetic field as a function of magnet coil current is shown in figure 13. The field was measured using a flux meter and matched search coil. The calibration of the flux meter was checked using two permanent magnets of known fields. This experiment revealed that during a typical

experimental run, a sample would sit in a fixed field of approximately 0.86T, given by an electromagnet coil current of 10 amps.

A sample was placed in a PTFE holder, generally referred to as the sample bucket. This was suspended from one arm of the balance. The sample and bucket resided between the pole pieces of an electromagnet. The sample chamber was evacuated to a pressure of less than 10^{-4} torr. Helium gas was slowly introduced into the chamber replacing the vacuum. The balance was zeroed with no field, and the field would then be applied (0.86T). The temperature was recorded. The balance reading produced by the field acting on the sample was recorded as a weight change from zero. The temperature controller was reset to a new value. The field was reduced to zero and the balance tared out once again. The procedure was repeated down to 20K in steps of 5K.

The calculation of the molar magnetic susceptibility $\chi_m(JT^{-2}mol^{-1})$ from the observed weight change on the Faraday balance was performed as follows:

$$\chi_m = \frac{(\Delta WTsample - B).C.RMM}{\text{Sample wt}} - \text{Diamag. Corr.}$$

where:

χ_m = molar susceptibility of sample $(JT^{-2}mol^{-1})$.

$\Delta WTsample$ = the weight change observed when the field was raised from zero to the working field (mg).

B = the sample bucket constant given by the

weight change observed for the empty bucket when the field was raised from zero to the working field (mg).

RMM = the relative molecular mass of the sample.

Diamag. Corr. = diamagnetic correction as calculated from the elemental constituents of the sample molecular formula ($JT^{-2}mol^{-1}$).

C = the calibration constant given by:

$$\frac{\chi_m \text{calibrant.weight of calibrant(mg)}}{\Delta WT_{cal} - B}$$

where:

ΔWT_{cal} = weight change on balance for the calibrant when the field was raised from zero to the working field (mg).

$\chi_m$calibrant = magnetic susceptibility of calibrant
= 101.65 $10^{-3}JT^{-2}mol^{-1}$ at 293K.

Notes:

1). All the atoms of the charge transfer complexes had a fixed diamagnetic susceptibility, generally much smaller than the paramagnetic susceptibility of the complex. Due allowance was made for this diamagnetic effect since this would reduce any paramagnetic pull on the sample. A correction factor was applied to the magnetic susceptibility value by subtraction of the appropriate constants (the corr. value). The correction factors were obtained from any good science data literature (e.g. C.R.C. Handbook of Physics and Chemistry).

2). The calibrant used was cobalt mercury thiocyanate ($HgCo(SCN)_4$) (Figgis 1958) of mass susceptibility (at room temperature) 206.67 $10^{-9}JT^{-2}kg^{-1}$, or a molar susceptibility

of 101.65 $10^{-3}JT^{-2}mol^{-1}$ since the relative molecular mass of $HgCo(SCN)_4$ is 491.851.

6.2.5 Paramagnetism

According to Crangle (1977), when a magnetic field is applied to a paramagnetic material, it becomes magnetised. The magnetisation depends linearly on the field and always disappears when the field is removed. The rate of change of magnetisation with field is called the paramagnetic susceptibility, when referred to one mole it is the molar susceptibility (χ_m). When the atoms or molecules of a material each have a magnetic moment and a field is applied, the magnetic potential energy of the system is reduced if the elementary magnets turn towards the direction of the applied field, thus producing a component of magnetisation in the field direction. The thermal motion of the particles, however, will tend to keep the magnetic axes in disorder. The equilibrium condition in a magnetic field depends on the relative values of the magnetic potential energy and the thermal energy.

Paramagnetic materials have a temperature dependant positive susceptibility. The paramagnetism outweighs the diamagnetic component present in all materials.

6.2.6 The Curie-Weiss law

Many materials show a linear relationship between the reciprocal of the susceptibility and temperature, with an

intercept on the positive temperature axis at the paramagnetic Curie temperature ϕ. The dependence of the molar susceptibility on temperature has the form:-

$$\chi_m = C_m/(T-\theta)$$

where:

χ_m = molar susceptibility ($JT^{-2}mol^{-1}$)
C_m = molar Curie constant ($JKT^{-2}mol^{-1}$)
θ = Curie temperature(K)

This is known as the Curie-Weiss law (Crangle 1977). C_m and θ_p are constants and are related to the fundamental properties of the atoms or ions of the material (pp10 Crangle 1977). If the intercept was at 0K, the material was said to obey a Curie law:

$$\chi_m = C_m T^{-1} \quad .$$

According to Crangle (pp29 Crangle 1977), for the molar Curie constant of a material obeying the Curie law it may be shown that the effective paramagnetic Bohr magnetons per ion was given by:

$$p_{eff}^2 = (3k/N_v u_B^2)/C_m = 0.8C_m$$

where:

p_{eff} = the effective Bohr magneton number (Bohr magnetons per ion).

N_v = Avogadro constant = $6.02217\ 10^{23}\ mol^{-1}$.

k = Boltzman constant = $1.38062\ 10^{-23} JK^{-1}$.

u_b = Bohr magneton = $9.2732\ 10^{-24}\ JT^{-1}$.

Hence from the gradient ($1/C_m(T^{-2}mol^{-1}JK)$) of a plot of reciprocal molar susceptibility against T we may find the

experimentally determined effective Bohr magneton number, p_{eff}(bohr magnetons/ion). This value could then be compared with the theoretical value given by:

$$u_{eff} = g[J(J+1)]^{\frac{1}{2}}$$

or $u_{eff} = 2\{s(s+1)\}^{-\frac{1}{2}}$ for a orbital quenched system.

where:

s = the spin quantum number (pp33 Crangle 1977)).
J = a quantum number derived from the interaction of the spin and orbital quantum numbers L and S.
g = Lande factor.

Note: see pp20 Crangle 1977 for full derivation of g and J.

For compounds containing unpaired electrons, both the spin angular momentum and the orbital momentum of the electrons can contribute to the observed paramagnetism. However, for complexes of transition metal ions the orbital contribution is largely quenched by the field due to the surrounding ligands. In this case, the simple "spin only" formula applies:

$$u_{eff} = [n(n+2)]^{\frac{1}{2}} \text{ Bohr magnetons,}$$

where:

n is the number of unpaired electrons. Values of u_{eff} as a function of n are:

n	u_{eff}
1	1.73
2	2.83
3	3.87
4	4.90
5	5.92
6	6.93

This approach has been shown to be valid for rare earth and

transition metal ions (pp31 and 34 Crangle 1977). However, it is uncertain whether it is valid for TCNQ charge transfer complexes, and there appears to be no theoretical basis to indicate that it is. However some workers have used this approach in the absent of more appropriate theories (Ashwell 1983b, 1984b).

6.2.7 Ferromagnetic impurities in a paramagnetic material

To test for the presence of a ferromagnetic impurity on the measurement of paramagnetic susceptibility, Crangle (1977) suggests measuring the apparent susceptibility at different field strengths. In a pure paramagnetic the susceptibility is independent of the field.

If the apparent susceptibility ($\chi_{m\ app}$) is plotted against inverse field ($1/B_o$), a straight line graph will indicate that a ferromagnetic impurity is present in a paramagnetic material (pp 163 Crangle 1977).

From Crangle $$\chi_{m\ app} = \frac{x.\theta}{B_o} + (1-x)_m$$

where:

$\chi_{m\ app}$ = apparent molar susceptibility.

χ_m = true molar susceptibility.

x = fraction of ferromagnetic impurity.

θ = magnetisation per unit mass ($JT^{-1}kg^{-1}$).

B_o = induction in free space (field) (T).

Therefore the true susceptibility would be indicated by the intercept at $1/B_o = 0$ since $(1-x)$ can be assumed to be

equal to unity (i.e. x is very small).

The experimental procedure to test for ferromagnetic impurities was adopted as follows:

The bucket constant, B, was determined for each magnetic field that the sample would be subjected too. A known weight of calibrant was placed in the sample holder and the calibration constant, C, determined at each of the fields. The sample under investigation was then placed in the sample holder alone, and a temperature run was commenced. The magnetic susceptibility at each field and temperature was calculated and plotted against the inverse field.

6.2.8 X-Ray Powder Diffraction Measurements.

X-ray powder diffraction studies were performed on a Phillips diffractometer with a cobalt (1.7902nm) X-Ray source. The samples were ground and mounted in the appropriate sample holder.

The calibration of the diffractometer was checked by obtaining a diffraction plot using a high purity Johnson Matthey copper powder sample. The d-spacings were calculated from the diffraction peaks (at the 20 values) and compared with the d-spacings as given by the ASTM standard.

The d-spacings were calculated using the Bragg equation:

$$n\lambda = 2d\sin\theta$$

rearranging $d = \frac{n\lambda}{2\sin\theta}$

where:

d = interplanar spacing of the lattice.

n = an integer = 1.

λ = the X-ray wavelength = 1.7902 nm.

θ = the diffraction angle.

The comparison of the d spacings obtained from the diffractometer and the spacings given on the ASTM index card for copper are shown below:

d spacings as obtained from the diffractometer (Angstron)	d spacings for Cu according to ASTM (Angstron)	percent difference
2.0960	2.088	-0.38
1.8131	1.808	-0.28
1.2692	1.278	+0.69
1.0914	1.0900	-0.13
1.0454	1.0436	-0.17

The percentage differences were very small and it was concluded that the diffractometer was suitably calibrated correctly.

6.2.9 Electrical measurements of the charge transfer complexes and the reticulate doped polymers.

6.2.9.1 Apparatus and Sample preparation.

Electrical conductivity measurements were performed on compacted pellets of charge transfer complexes or thin films of polymer/charge transfer complex blends. The apparatus used consisted of a Keithly 172A multimeter, a APD temperature controller, a vacuum sample chamber and associated vacuum rotary pump.

Compacted pellets of charge transfer complexes were made by grinding the complex in an agate pestle and mortar and compacting the powder in a standard KBr 13mm die for 5 minutes at a die pressure in excess of 150 Nm^{-2}. Electrical contacts with the samples were made with silver paint and gold electrodes as shown below:

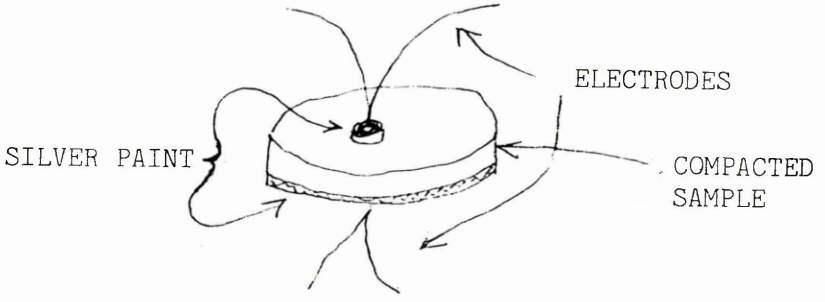

The 4-wire terminal arrangement was used to negate the resistance of the electrodes, contact resistance and terminal wires. One face of the disk sample was completely

silvered, the other side had a small silver 'dot' as the second contact.

To ensure that the samples were 'outgassed' the sample chamber containing the sample was evacuated overnight down to a pressure of (0.05±0.01) torr before any measurements were made.

The electrical resistance of each sample was recorded at various temperatures. The current/voltage characteristic of the sample was also observed.

The conductivity of the sample was calculated using the recorded sample resistance, thickness and top electrode diameter using the equation :-

$$\sigma = 4d/R.\pi.D^2 \quad .$$

where:

σ = the conductivity of the sample (Scm-1).

d = distance between the electrodes,
ie. the thickness of the sample (m).

R = resistance measurement (ohm).

D = diameter of small electrode (m).

The error in the conductivity ($\Delta\sigma$) calculation was given by:-

$$\Delta\sigma = \sigma.(\Delta d/d + \Delta R/R + 2\Delta D/D)$$

where Δd, ΔR, ΔD were the errors in d, R, and D respectively.

A typical error value for σ was ± 0.02 Scm^{-1}. The initial

percentage error contribution from the measurements of sample thickness, resistance and electrode diameter were approximately 20%, 3% and 20% respectively. The combined error was unacceptable (43%) due to the high contributions from the dimension measurements. These arose due to the sample thickness and electrode diameter being measured initially to within ±0.1mm using a micrometer. These errors were reduced by employing an optical microscope calibrated with a 0.01mm division graticule. Hence, errors in the dimension measurements were brought down to, typically 3%.

6.2.9.2 Compaction pressure and conductivity of compressed charge transfer complex samples.

Various sample compaction pressure are reported in the literature, 152 MNm^{-2} by Ferraris (1987), 29 MNm^{-2} by Ikeno (1977), and 1.4 MNm^{-2} by Kommandeur (1961). To test whether the compaction pressure of the polycrystalline samples affected the conductivity measurements, an experiment was devised. Five compactions were made from the same batch of $DHPE^{+}(TCNQ)^{-2}TCNQ^{o}$ each compacted at a different die pressure. The ram force on the press was calibrated using a force transducer and converted to the pressure on the 13mm die head. The following die pressures were used:-

Ram force/kN	Die pressure/Nm^{-2} .
20	150
40	300
60	450
80	602
100	752

60mg of material was used each time with a compaction time

of 5 minutes. Disks of approximately 0.3 to 0.4mm thick, 13mm in diameter were produced. The disk conductivities were measured under vacuum (0.05±0.01 torr) at room temperature. The conductivity versus pellet compaction pressure were plotted for the 5 samples. Any trend in the plots was observed.

6.3 Solubility Studies/blending charge transfer complexes with polymers

The solubilities of the charge transfer complexes were determined by immersion in a range of solvents of known solubility parameters as discussed by Brydson (1975). The bis-pyridinium TCNQ salts were soluble in acetonitrile (CH_3CN), solubility parameter of 23.6$(MJ^{-3})^{\frac{1}{2}}$ (as calculated by the Heat of Vaporisation method (Brydson 1975)). Since two materials are said to be mutually soluble if their solubility parameters are within 2 $(MJm^{-3})^{\frac{1}{2}}$ of each other, polymers between a solubility parameter of 22-26 $(MJm^{-3})^{\frac{1}{2}}$ were considered.

The solubility parameter of the trimethylsulphonium TCNQ iodide salt was determined to be approximately 23$(MJm^{-3})^{\frac{1}{2}}$.

6.4 Polymer/charge transfer complex blending.

Four methods of blending the polymers with the charge transfer complexes were performed:

i). A known weight of polymer and charge transfer complex were added to a measured quantity of solvent in a reflux flask.The mixture was vigorously shaken to dissolve the additives. If complete dissolution was not attained with prolonged shaking, the solution was gently warmed until dissolution was attained.

ii). Known weights of charge transfer complexes were added to pre-dissolved polymer/solvent solutions.

iii). Separate solutions of the polymer and charge transfer complex were made up and then mixed together.

iv). Separate solutions of polymer, solvent and one component of the charge transfer complex were mixed, the other component of the charge transfer complex was mixed with another polymer, solvent solution. Then both the solutions were mixed, the charge transfer complex formed on mixing.

6.5 Methods of film casting

Three methods of film casting were tried:

i). The solutions were cast onto distilled water or mercury.

ii). The solutions were cast onto glass microscope slides at room temperature.

iii). The films were formed by spin coating the solutions onto a rotating disc. A centrifuge was adapted to take a polished aluminium disc. The power to the centrifuge and hence the

rotation speed, was controlled by a mains variac. The revolutions per second of the disc were monitored via an infra-red emitting L.E.D. and phototransistor sensor (R.S. 307-913) using an oscilloscope. Spin speeds of 128 to 156 revolutions per second were achievable.

The disc was rotated at a set speed and a solution of the polymer and charge transfer complex was poured onto the disc. The disc was allowed to rotate for a further 5 seconds. The solvent was allowed to evaporate from the film leaving the disc coated with the film. The film was removed from the disc. Removal was aided by first coating the disc with a releasing agent (soap solution) prior to spinning with the blend solutions.

Spin coating was only performed with acetone based solutions and not with acetonitrile due to safety considerations (toxicity).

6.6 Film morphology

The morphology of the films were studied optically using an optical microscope fitted with crossed polaroids and a camera.

An attempt was made to study some films using a scanning and transmission electron microscope.

7. EXPERIMENTAL RESULTS AND DISCUSSION OF RESULTS

7.1 Synthesis of the charge transfer complexes and characterisation

Three new charge transfer complexes based on bis-pyridinium TCNQ salts, and one from the literature, were synthesised. The products consisted of small black, brittle fine needles typical of charge transfer complexes. Single crystal work (oscillatory X-Ray diffraction; Wiessenberg diffraction) was ruled out as attempts to produce (or grow) large single crystals of the complexes were unsuccessful. Consequently the full crystallographic structures of the materials were not determined. However, an attempt to characterise the products was made in terms of elemental analysis, thermal analysis, UV/VIS spectrophotometry, magnetic susceptibility, X-ray powder diffraction, electrical properties, and solubility in a range of polymers for subsequent blending.

7.1.1 Synthesis of Bis-pyridinium TCNQ salts.

These charge transfer complexes were based on variations of trans-1,2-bis(4-pyridyl)ethylene (DPE) as donor and TCNQ as acceptor. The preparations of the charge transfer complex salts were as follows:

7.1.1.1 Synthesis of $DHPE^{2+}(TCNQ)^{-}_{2}TCNQ^{o}$

Stage 1:

2g of DPE was dissolved in acetonitrile (CH_3CN), and concentrated hydrochloric acid was added dropwise. The

white precipitate of 1,2-Bis(4-pyridinium)ethylene dichloride ($DHPECl_2$) was filtered and dried (yield 55%).

Stage 2: Synthesis of LiTCNQ

3g of TCNQ was dissolved in 120 ml CH_3CN and 8g of lithium iodide was added. The solution was refluxed for one hour to produce LiTCNQ and iodine. The purple reaction product (yield 61%) was filtered and washed in toluene to remove the iodine and unreacted TCNQ.

Stage 3:

0.4g of LiTCNQ and 0.2g of TCNQ were dissolved in hot CH_3CN (200ml). The solution was refluxed for five minutes.

Stage 4:

0.26g of $DHPECl_2$ in 10ml of water were added to the refluxed solution from stage 3. The liquor was left overnight wrapped in paper towels for slow cooling to aid large crystal growth.

The product was a black, crystalline powder (yield 36%), giving a green solution in CH_3CN.

The yield of this product was poor and the method involves the use of large quantities (when compared to the quantities of starting products) of toxic acetonitrile. No elemental analysis was carried out on the products of stages 1,2.

(a). TCNQ -----> LiTCNQ

$$Li^+ + I^- + TCNQ \longrightarrow Li^+ + TCNQ^- + \tfrac{1}{2}I_2$$

$$I^- \longrightarrow \tfrac{1}{2}I_2 + e^-$$

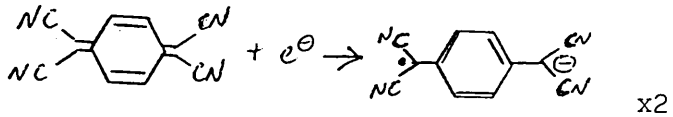

x2

(b).

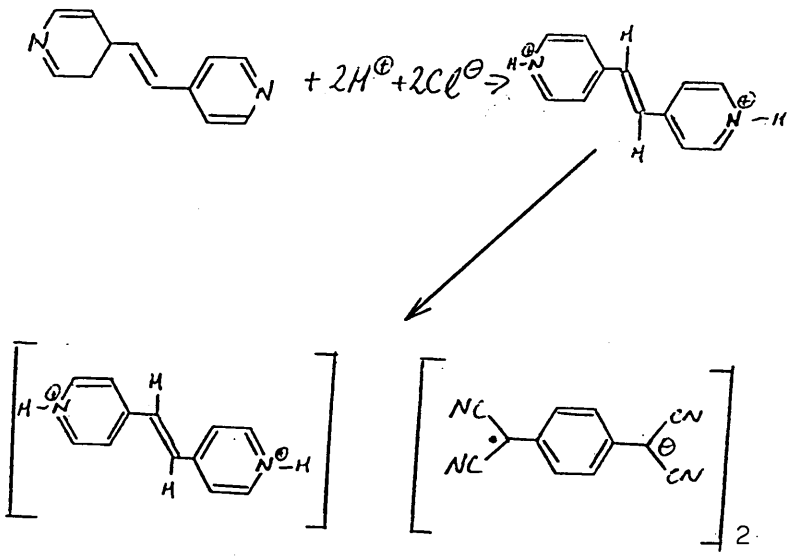

7.1.1.2 Synthesis of $DHPE^{2+}(TCNQ)^{-}_{2}$

0.4g of LiTCNQ was dissolved in hot CH_3CN (200ml). To this, 0.26g of $DHPECl_2$ (in 10ml of water) was added (mole ratio of 2:1).

The solution was left overnight to cool wrapped in towels. The product was a fine black powder (yield 45%) with a dispersion of whitish grains (soluble in water) which were suspected to be lithium chloride. It was confirmed at a later date by a Lassaigne test that chlorine was indeed present in this sample.

All other attempts to prepare this complex led to the presence of LiCl. Washing the product in water to dissolve the highly water soluble LiCl resulted in the product of interest changing colour. It was suspected that the water was decomposing the product, so that washing out the impurity was ruled out.

7.1.1.3 Synthesis of $DPE(TCNQ)_3$

A solution in CH_3CN of 0.18g of DPE and 0.61g of TCNQ (mole ratio of 1:3) was refluxed for one hour. The solution was left overnight wrapped in towels. The product was olive green (yield 23%) or orange (yield 64%) depending on the suspected mole ratio (1:3 or 1:2 respectively) of the final product. It was the green 1:3 product that was required. However the reaction proved unreliable and many attempts to produce the green phase were unsuccessful. The synthesis inevitably produced an orange phase contaminated with

unreacted TCNQ.

An attempt to find a consistent method of synthesising the olive green phase was made. 0.612g of TCNQ was dissolved in 100ml of CH_3CN and 0.182g of DPE was dissolved in 50ml of CH_3CN separately. The solutions were mixed and refluxed for over one hour, after which the solution colour had changed from a clear yellow/orange to a dark green colour. The solution was then left to cool slowly overnight. The yield was low (13%), and contained some unreacted TCNQ plus some of the orange phase.

A more reliable method of producing the olive green phase was found when methanol was used instead of the CH_3CN. This synthetic route was being tried by another worker and, as yet, no quantitative results have been obtained.

7.1.2 Synthesis of trimethylsulphonium TCNQ iodide ($Me_3S^+(TCNQ.I)^-$)

The synthesis of $Me_3S^+(TCNQ.I)^-$ was reported by Lequan et al (1985), and the adopted preparation was as follows:

A hot solution of 206mg of $Me_3S^+I^-$ ($1*10^{-3}$ mole) in 7 cm^3 of CH_3CN was added to a solution of 102mg of TCNQ ($0.5*10^{-3}$ mole) in 5 cm^3 of CH_3CN. The solution was left to cool overnight in the freezer. The product comprised long black crystals (yield 19%), with a green supersaturated liquor.

Again the product yield was low. However, the ease of synthesis and the morphology of the product made it a good candidate for incorporation into insulating polymers.

7.2 Elemental analysis of the charge transfer complexes

The elemental analyses are compared with the theoretical values as calculated by the method given in the experimental details section.

7.2.1 $DHPE^{2+}(TCNQ)^{-}_{2}TCNQ^{o}$ ($C_{48}H_{24}N_{14}$)

	THEORY	FOUND	DIFFERENCE
%C	72.35	72.31	-0.04
%H	3.04	3.09	-0.05
%N	24.61	24.01	-0.60

The analysis suggests that the desired product had been successfully synthesised.

7.2.2 $DHPE^{2+}(TCNQ)^{-}_{2}$ ($C_{36}H_{20}N_{10}$)

	THEORY	FOUND	DIFFERENCE
first batch			
%C	72.96	57.22	-15.74
%H	3.40	3.32	-0.08
%N	23.63	17.22	-6.41

Clearly the synthesis had not been successful so a second attempt was made to produce the desired product.

second batch

	THEORY	FOUND	DIFFERENCE
%C	72.96	59.01	-13.95
%H	3.40	3.45	+0.05
%N	23.63	17.16	-6.47

The analysis again suggests that the desired product was

not synthesised or contained major impurities. A Lassaigne test was performed on the product to test for the presence of Cl^- ions in the product. The test was positive and would suggest that the white flecks (soluble in water) present in the product could by lithium chloride (LiCl) from the reaction of Li from the LiTCNQ and the chloride from the $DHPECl_2$. LiCl is very soluble in water.

If theoretical elemental calculations were performed for $DHPE^{2+}(TCNQ)^-_2$:2ClLi ($C_{36}H_{20}N_{10}Cl_2Li_2$) the following results for the two batches were obtained:-

	THEORY	FOUND	DIFFERENCE
first batch			
%C	63.83	57.22	-6.61
%H	2.98	3.32	+0.34
%N	20.68	17.22	-3.46
%Cl	11.47	-----	-----
%Li	2.05	-----	-----

second batch

	THEORY	FOUND	DIFFERENCE
%C	63.83	59.01	-4.82
%H	2.98	3.45	+0.47
%N	20.68	17.16	-3.52
%Cl	11.47	-----	-----
%Li	2.05	-----	-----

The analysis gave a closer fit to the theoretical values, however, the differences were still significant andit seems that non-stoichiometric quantities of contaminants were present.

For a trial formula $C_{36}H_{20}N_{10}Li_1Cl_2$
the result was as follows:-

	THEORY	FOUND	DIFFERENCE
first batch			
%C	64.49	57.22	-7.27
%H	3.01	3.32	+0.31
%N	20.89	17.22	-3.67
%Cl	10.58	-----	-----
%Li	1.03	-----	-----

second batch

	THEORY	FOUND	DIFFERENCE
%C	64.49	59.01	-5.48
%H	3.01	3.45	+0.44
%N	20.89	17.16	-3.73
%Cl	10.58	-----	-----
%Li	1.03	-----	-----

Again the fit was unsatisfactory, and it was concluded that the desired product was not synthesised. Analysis for Li and Cl would need to be undertaken to confirm the suspected presence of these two elements.

7.2.3 DPE(TCNQ)$_3$ ($C_{48}H_{22}N_{14}$) (Olive green phase)

First batch

	THEORY	FOUND	DIFFERENCE
%C	72.54	70.76	-1.78
%H	2.79	2.33	-0.46
%N	24.67	26.06	1.39

Due to the high percentage difference in the carbon fit, a second batch of the product was synthesised. The elemental analysis is shown below:-

Second batch

	THEORY	FOUND	DIFFERENCE
%C	72.54	71.54	-1.00
%H	2.79	2.73	-0.06
%N	24.67	24.49	-0.18

The product was assumed to be synthesised. However, the percentage difference for the carbon does appear again to be on the high side but within the 1% limit set.

7.2.4 $Me_3S^+(TCNQ\text{-}I)^-$ ($C_{15}H_{13}N_4SI$)

	THEORY	FOUND	DIFFERENCE
%C	44.13	44.74	0.61
%H	3.20	3.04	-0.16
%N	13.72	13.79	0.07

The product was assumed to be synthesised.

7.2.5 Discussion of synthetic work

The synthetic work took up the majority of the practical work. Synthesis was hindered by the precautions necessary for handling toxic solvents and chemicals.

Product yields were low, and the confirmation of the synthesis by chemical analysis was time consuming. However progress was made and the characterisation of the prepared products was performed.

At this stage of the work, it was decided to concentrate only on one charge transfer complex for blending with insulating polymers. The choice was $Me_3S^+(TCNQ\text{-}I)^-$ due to its comparative ease of synthesis compared with the other charge transfer complexes coupled with its purity/yield

and its morphology.

7.3 Thermogravimetric Analysis (TGA) and Melting Point

The thermogravimetric analysis was performed on a Mettler TA3000 system. The melting points were determined on a micro melting point apparatus.

(i). $DHPE^{2+}TCNQ^{-}{}_{2}TCNQ^{o}$.

The complex was stable up to (240-280)°C, no weight loss of product occurring until this temperature.

The complex decomposed at (150-250)°C as determined by melting point apparatus.

(ii). $DHPE^{2+}TCNQ^{-}{}_{2}$.

The complex was stable up to (220-260)°C, and decomposed at (200-300)°C.

(iii). $DPE(TCNQ)_3$ (olive green phase).

The complex was stable up to (260+/-20)°C, and decomposed at (250-350)°C.

(iv). $Me_3S^{+}I^{-}$.

Trimethylsulphonium iodide was stable up to (150+/-10)°C, as determined by TGA. No melting point determination was carried out.

These results show that the charge transfer complexes and $Me_3S^{+}I^{-}$ are stable up to a minimum temperature of 200°C.

Therefore the blending and casting temperatures were kept below this value to ensure no thermal decomposition of the complex.

7.4 Ultra violet/visible (UV/VIS) studies

The calculations of the unknown number of neutral TCNQ molecules, x (using equation 6.2.3, page 84), are shown below along with the peaks present on the UV/VIS spectra.

(i). TCNQ and DPE.

Acetonitrile as solvent:

Compound	Peak at (nm)
a). TCNQ (only)	395
b). DPE (only)	295

These two results are in agreement with Rembaum et al (1969)

In KBr (solid state):

Compound	Peak at (nm)
a). TCNQ (2nd sample)	335,395,430
b). DPE	255

(ii). $DHPE^{2+}TCNQ^{-}_{2}TCNQ^{o}$.

Acetonitrile as solvent:

Run Number	Abs.(395nm)/Abs.(842nm)	x
1	2.90	1.4
2	3.60	1.8
3	2.79	1.33

These results show that there are 1.5±0.2 neutral TCNQ molecules present in the lattice.

(iii).$DHPE^{+}TCNQ^{-}_{2}$.

Acetonitrile as solvent:

Run Number	Abs.(395nm)/Abs.(842nm)	x
1	1.99	0.8
2	2.00	0.8
3	1.35	0.45

Run 3 was inconsistent with the first two runs showing only 0.45 neutral TCNQ molecules in the lattice compared to 0.8 molecules for the first and second runs.

(iv). $DPE(TCNQ)_3/DPE(TCNQ)_2$ (olive green and orange phase).

Acetonitrile as solvent:

Run Number	Abs.(395nm)/Abs.(842nm)	x
green phase (1:3)	2.90	1.4
green phase (1:3)	10.7	6.2
green phase (1:3)	13.7	8.0
orange phase(1:2)	5.8	3.2
orange phase(1:2)	No 842nm peak	---
orange phase(1:2)	No 842nm peak	---
orange phase(1:2)	10.3	5.9
red phase (1:1)	No 395/842nm peaks	---

These results are inconsistent with each other and require further study before any conclusion may be drawn. The inconsistency was assumed to be due to the presence of unreacted TCNQ and to partial decomposition of the product.

Toluene as solvent:

A peak was observed at 395nm, but none at 842nm. This result confirms that no charged TCNQ molecules were present in the non-polar solvent.

In KBr (Solid State):

TCNQ complex	Peaks at (nm)
green phase	340,380,430
green phase	340,380,430
green phase	305,395
orange phase	300,315,410,435
orange phase	340,405
orange phase	335
orange phase	335
orange phase	408,440
red phase*	408,440

Note; green phase (1:3 molar ratio): orange phase (1:2 molar ratio): red phase (1:1 molar ratio).

* The red phase was previously synthesised by another worker.

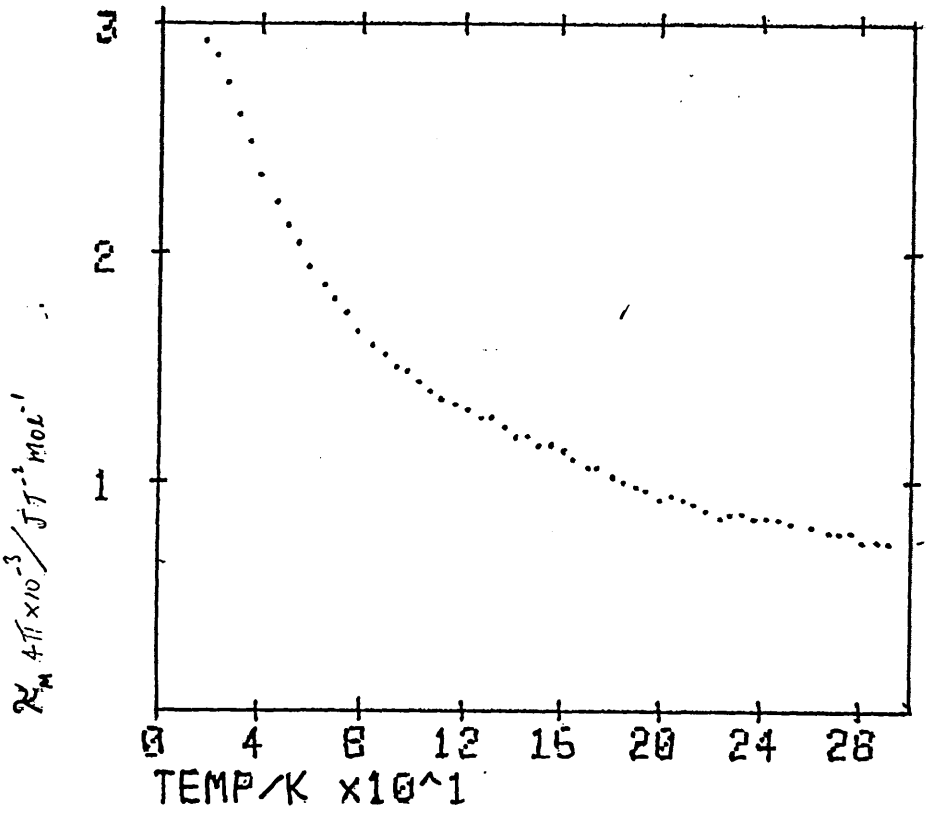

igure 14.
agnetic susceptibility against temperature with core iamagnetism correction for $DHPE^{+}(TCNQ)^{-}_{2}(TCNQ)^{o}$.

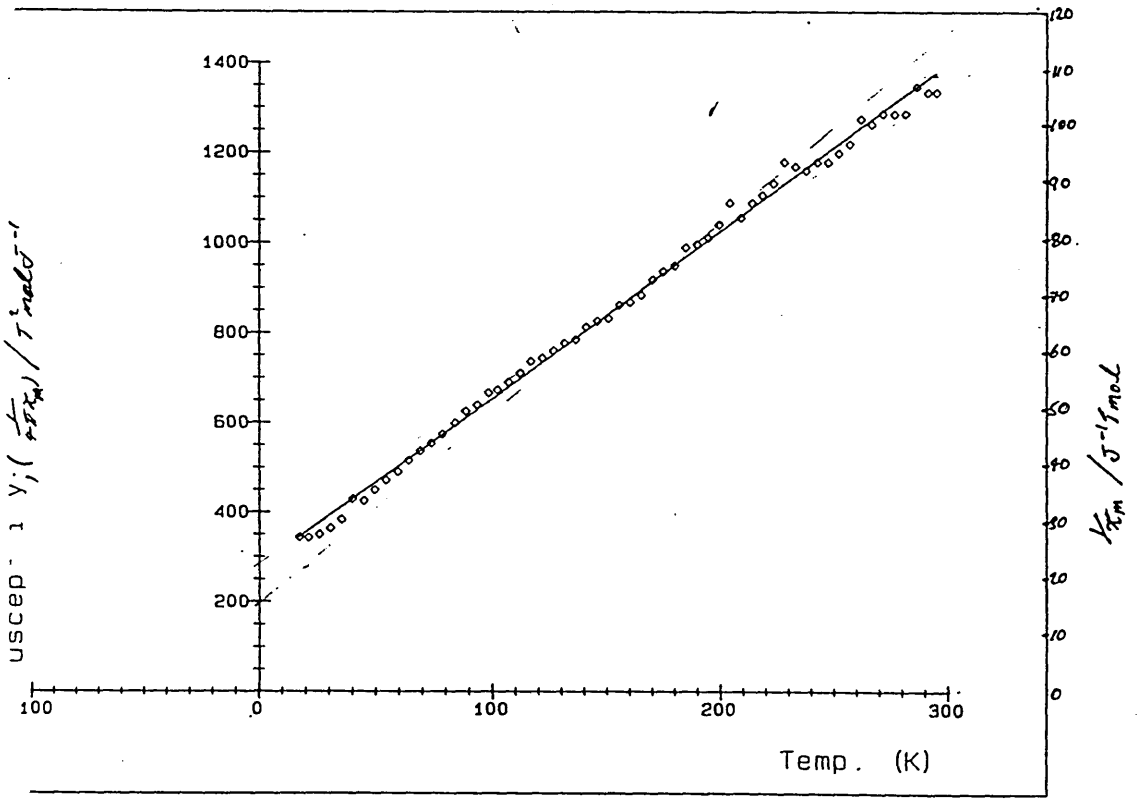

igure 15.
nverse magnetic susceptibility against temperature
ith core diamagnetism correction for $DHPE^{2+}(TCNQ)^{-}_{2}(TCNQ)^{0}$.

7.5 Magnetic Susceptibility Results

i). $DHPE^{2+}(TCNQ)^{-}_{2}TCNQ^{o}$

The molar magnetic susceptibility and inverse magnetic susceptibility versus temperature plots are shown in Figures 14 and 15. The material has a room temperature molar magnetic susceptibility (χ_m) of $(9\pm1)*10^{-3}JT^{-2}mol^{-1}$. It showed Curie-Weiss type behaviour with the molar magnetic susceptibility following the formula:

$$\chi_m = \chi_{Cm}/(T-\theta) \quad (JT^{-2}mol^{-1})$$

where:

χ_{Cm} = Molar Curie Constant = (0.3 ± 0.3) $JKT^{-2}mol^{-1}$.

θ = Curie temperature = -87K.

The molar Curie constant gives a value for the number of Bohr magnetons per ion, μ_{eff}, as (1.65 ± 0.07) μ_b/ion. If we assume that a simple "spin only" formula applies, and compare this value with 1.73 μ_b/ion given by theory, $\mu_{eff}=[n(n+2)]^{\frac{1}{2}}$ where n=1, the difference in the values is -4%. Thus good agreement was shown and it may be assumed that one unpaired electron was present in the material (only if the spin-only formula applies). However, note that the μ_{eff} value derived from the molar Curie constant is subject to an experimental error of 100% (as given by the error gradients), and unlike many materials with a Curie-Weiss paramagnetic behaviour (pp.8 Crangle 1977), the temperature intercept was negative. Materials with negative intercepts are more synonymous with antiferromagnetic materials (pp64 Crangle 1977).

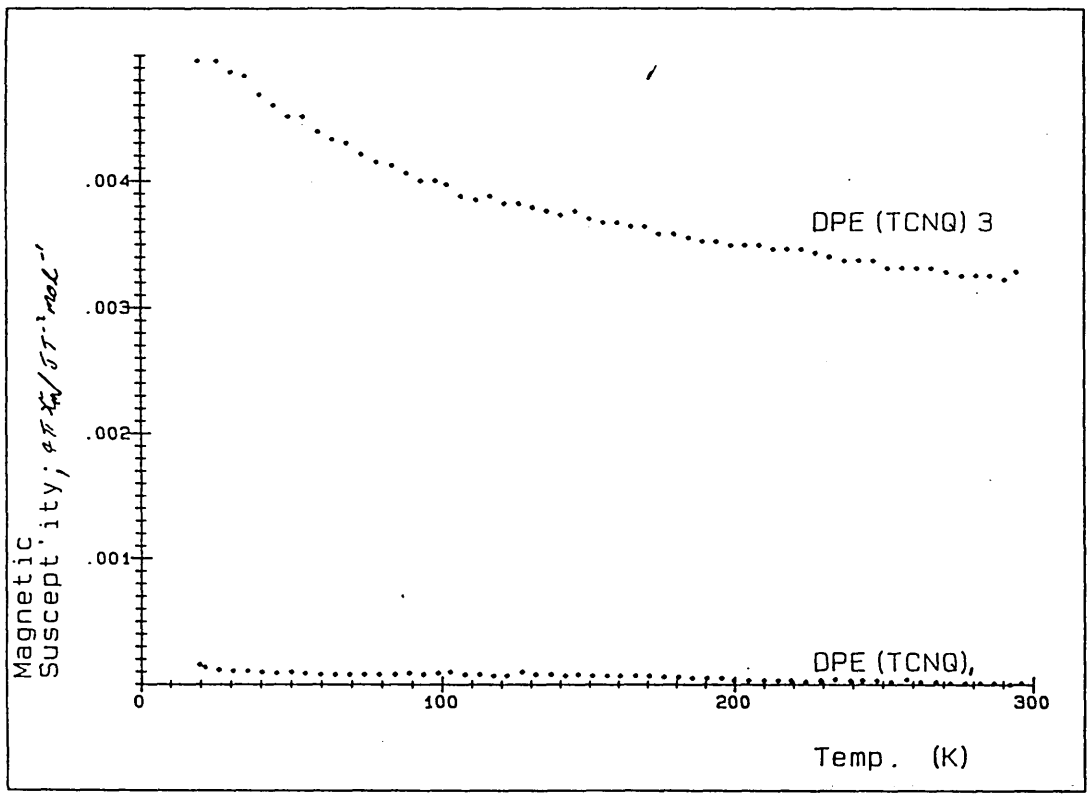

Figure 16.
Magnetic susceptibility against temperature with core diamagnetism correction for $DPE(TCNQ)_3$ (green 1:3 phase) and DPE:TCNQ (red 1:1 phase).

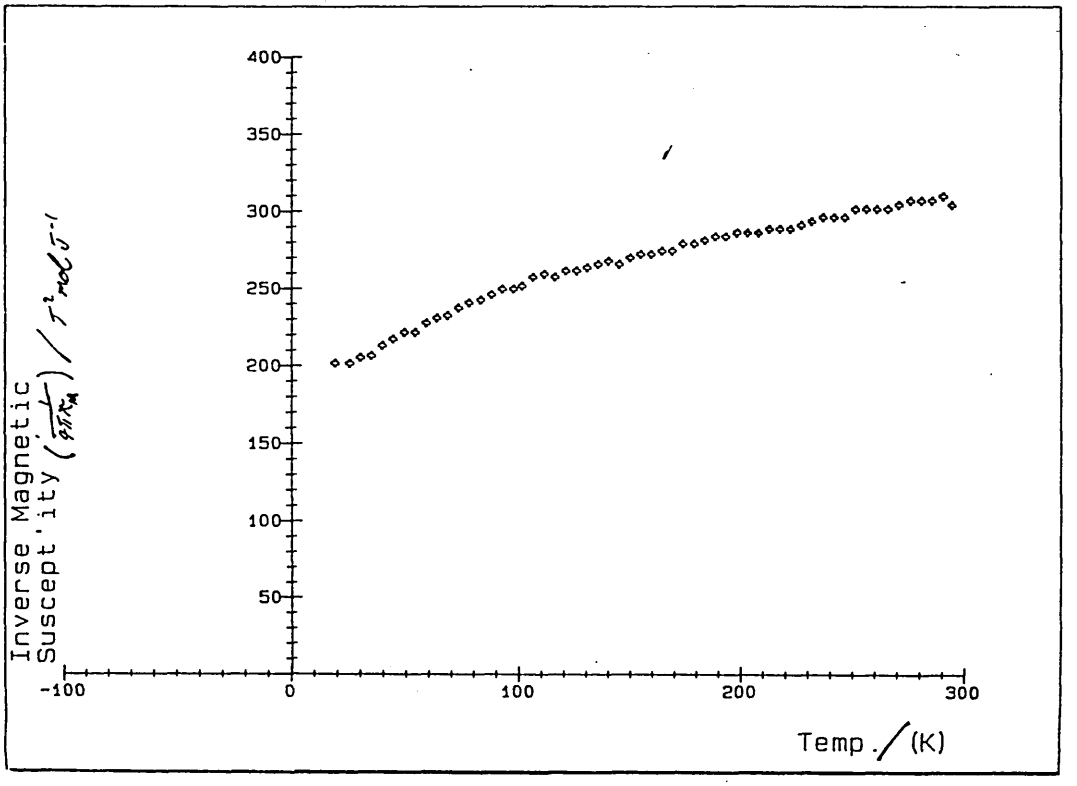

Figure 17.
Inverse magnetic susceptibility against temperature with core diamagnetism correction for $DPE(TCNQ)_3$ (green phase) at 0.86T induction field.

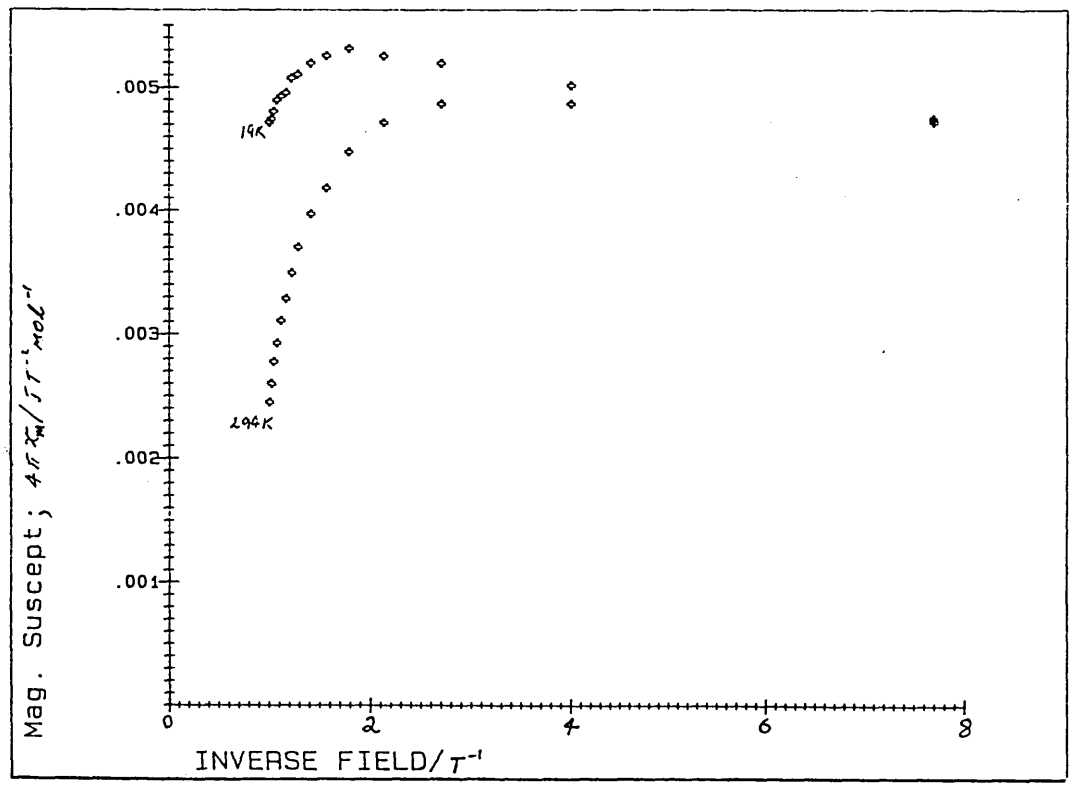

Figure 18.
Magnetic susceptibility against inverse magnetic field for $DPE(TCNQ)_3$ (green 1:3 phase).

ii). $DPE(TCNQ)_3$

The molar susceptibility and inverse susceptibility versus temperature plots are shown in Figures 16 and 17. The inverse susceptibility versus temperature did not show a linear plot as would have been expected for a Curie-Wiess type material.

The room temperature magnetic susceptibility was $(4.4\pm0.2)\ 10^{-2}JT^{-2}mol^{-1}$.

The pull on the material in the balance was field dependent which would suggest that it may be acting as a ferromagnetic material. To test for the presence of a ferromagnetic impurity, the apparent molar susceptibility was plotted against inverse field as suggested by Crangle (pp 163 Crangle 1977). A straight line plot with an intercept on the susceptibility axis would be indicative of a ferromagnetic impurity. No such plot was observed (figure 18), therefore no evidence of a ferromagnetic impurity could be deduced from the results. Further work was performed on this material to investigate the field dependent phenomena.

Attempts to synthesise further batches of green phase material were made so that the magnetic properties could be investigated. Even so, no conclusive results were found and time restraints required the investigation into the suspected ferro-magnetic behaviour of this material to be abandoned.

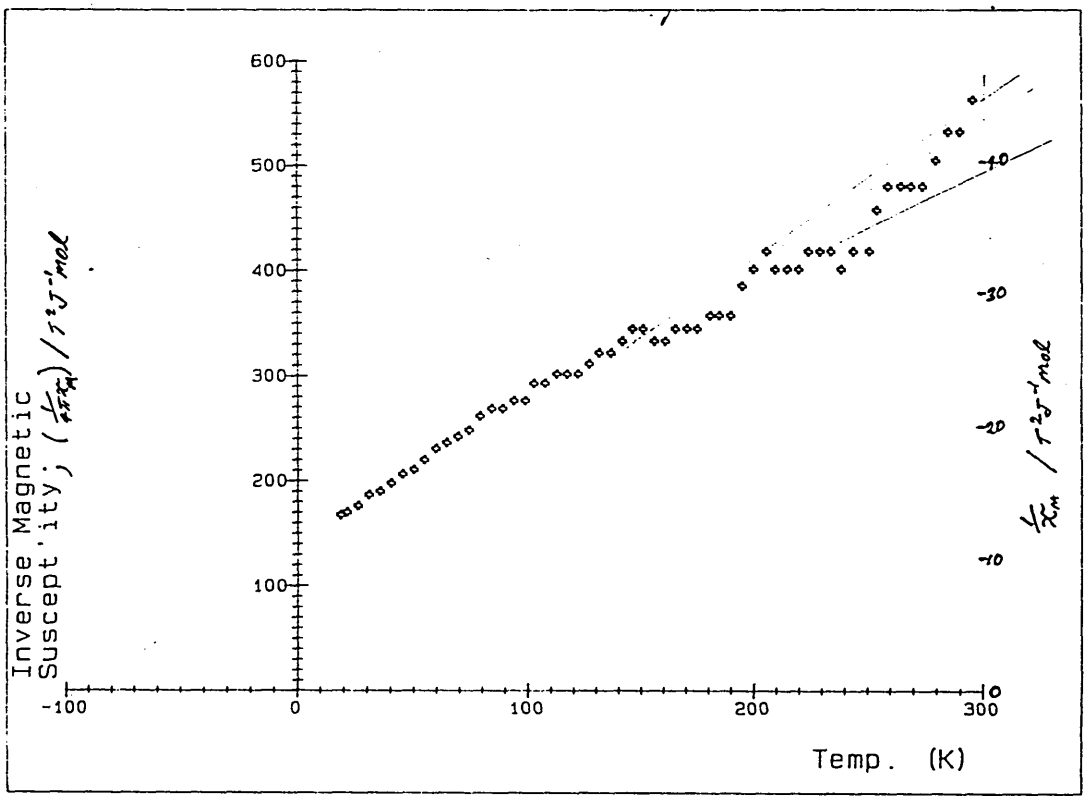

Figure 19.
Inverse magnetic susceptibility against temperature with core diamagnetism correction for $DPE(TCNQ)_2$.

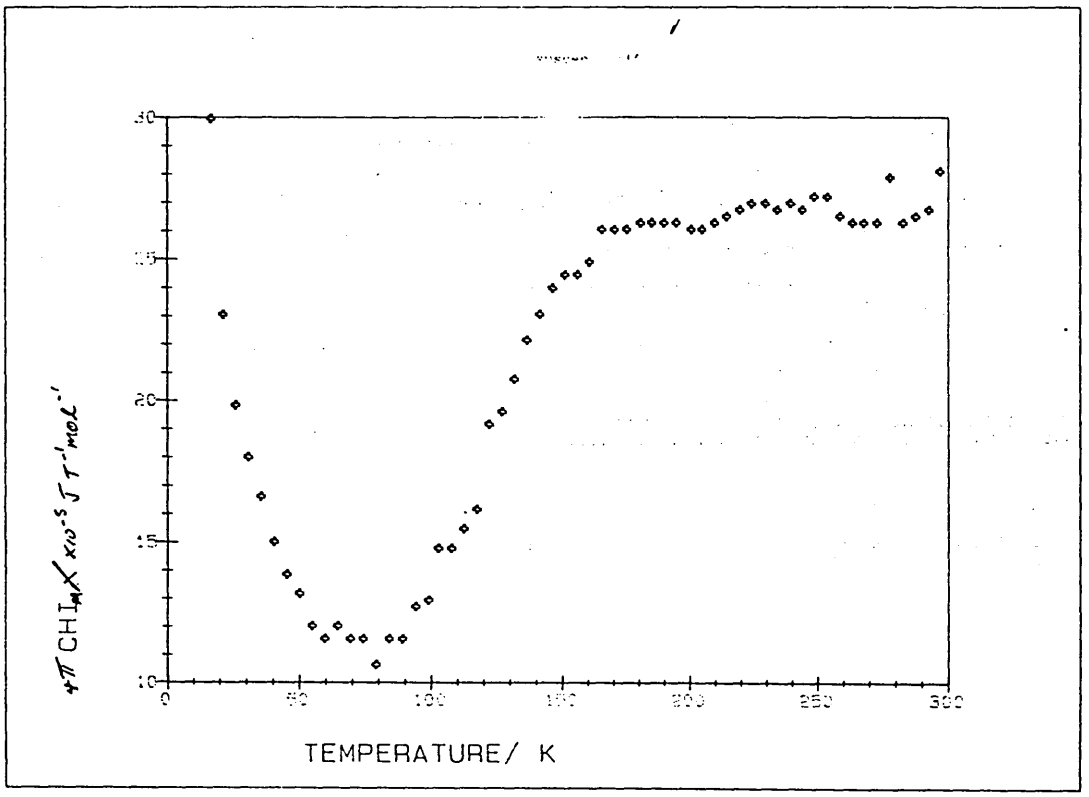

Figure 20.
Magnetic susceptibility against temperature with core diamagnetism correction for $Me_3S(TCNQ)^-$.

It was concluded that the material was not ferromagnetic due to the low room temperature susceptibility. Also, the elemental analysis was not satisfactory which would affect the susceptibility calculations as a knowledge of the sample's relative molecular weight was required.

ii). $DPE(TCNQ)_2$

The room temperature molar magnetic susceptibility was $(2.2\pm0.2)JT^{-2}mol^{-1}$.

The orange phase produced in the synthesis of $DPE(TCNQ)_3$ gave a straight line plot for the inverse molar susceptibility versus temperature plot (figure 19). The data was very scattered, but a molar Curie constant of (8±2) $JKT^{-2}mol^{-1}$ was obtained giving a μ_{eff} value of (2.6+/-0.2) μ_b/ion. This would indicate that two unpaired electrons are present in the lattice if we assume that a simple "spin only" formula applies.

iv). $Me_3S^+(TCNQ)^-$

The molar susceptibility versus temperature of the complex is shown in figure 20. The plot was non-linear and no predictive theory describes the behaviour shown. However, it was noted that the susceptibility ($3.3\pm0.2JT^{-2}mol^{-1}$) was approximately linear from 300K to 165K. Then it fell to a minimum at 80K ($1.5\pm0.2JKT^{-2}mol^{-1}$) before increasing once again.

7.6 Calculation of the experimentally determined molar magnetic susceptibility values

It was noted that the calculations of the molar magnetic susceptibility was subject to two errors.

The Faraday method was a relative one, the apparatus being calibrated in terms of a substance of known magnetic susceptibility, the calibrant, in this case $HgCo(CNS)_4$.

The room temperature susceptibility was used to calculate the calibration constant, C. However, the calibrant was a paramagnetic material and its molar susceptibility changes with temperature, according to the formula:

$$\chi_m = 30.8/20+T \quad (JT^{-2}mol^{-1}).$$

where:

T = temperature (K)

This would give a room temperature molar magnetic susceptibility of 101 $JT^{-2}mol^{-1}$ and 1 $JT^{-2}mol^{-1}$ at 19K, a difference of two orders of magnitude over this temperature range. No correction was made to the results for the change in the calibrant's susceptibility over the temperature range. Consequently non of the magnetic susceptibility results presented includes any correction for this error.

The value of the calibrant susceptibility used in the susceptibility calculations was in terms of mass susceptibility. It may have better expressed in terms of the molar mass susceptibility.

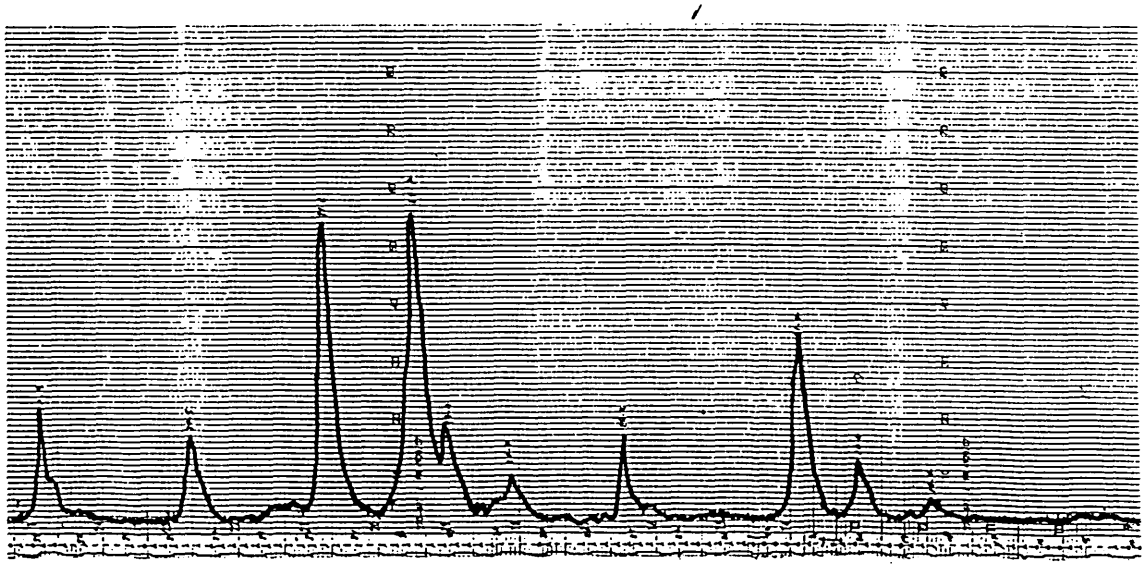

Figure 21.
Powder X-ray difraction for TCNQ.

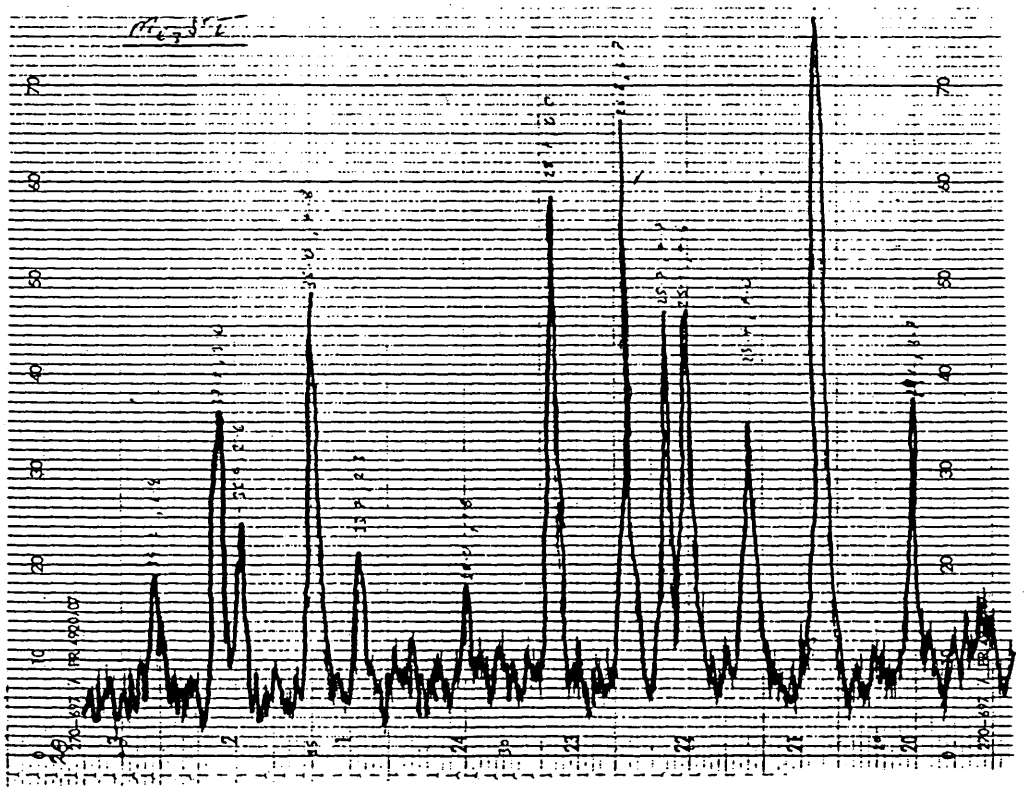

Figure 22.
Powder X-ray diffraction for Me_3SI.

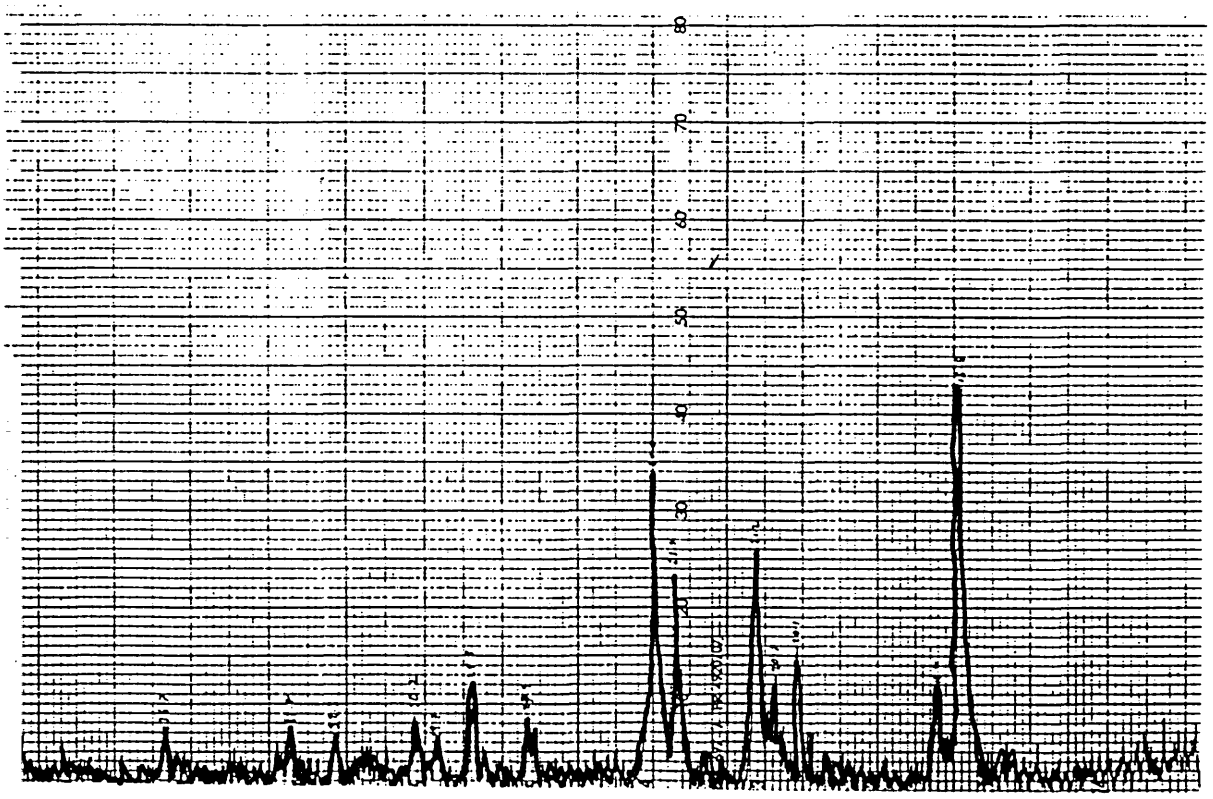

Figure 23.
Powder X-ray diffraction for $Me_3S^+(TCNQ\text{-}I)^-$.

The calibration constant calculation involves a term for the weight change for the calibrant. This was only determined at room temperature.

The experimental procedure should therefore in future be changed to find the calibrant weight change over all the temperature range of interest. The molar magnetic susceptibility of the calibrant at each of the measuring temperatures should be incorporated into the sample molar susceptibility calculations.

Note also that the 'bucket' constant was not determined at each temperature. This was not considered significant, as the bucket material was PTFE, a diamagnetic material and its magnetic susceptibility would be independent of temperature. Therefore, the pull exerted by the bucket should be constant over the temperature range.

Unfortunately the Faraday balance is no longer available and these magnetic studies cannot be amended. The calculation of the magnetic susceptibility was performed by computer. It was recommended that the changes to the programme be performed.

7.7 X-Ray Powder Diffraction results for $Me_3S^{\pm}(TCNQ.I)^{=}$ salt.

The diffraction patterns for TCNQ, Me_3SI and $Me_3S^{+}(TCNQ)^{-}$ are shown in Figures 21 to 23. The d-spacings obtained from the plot are shown below:

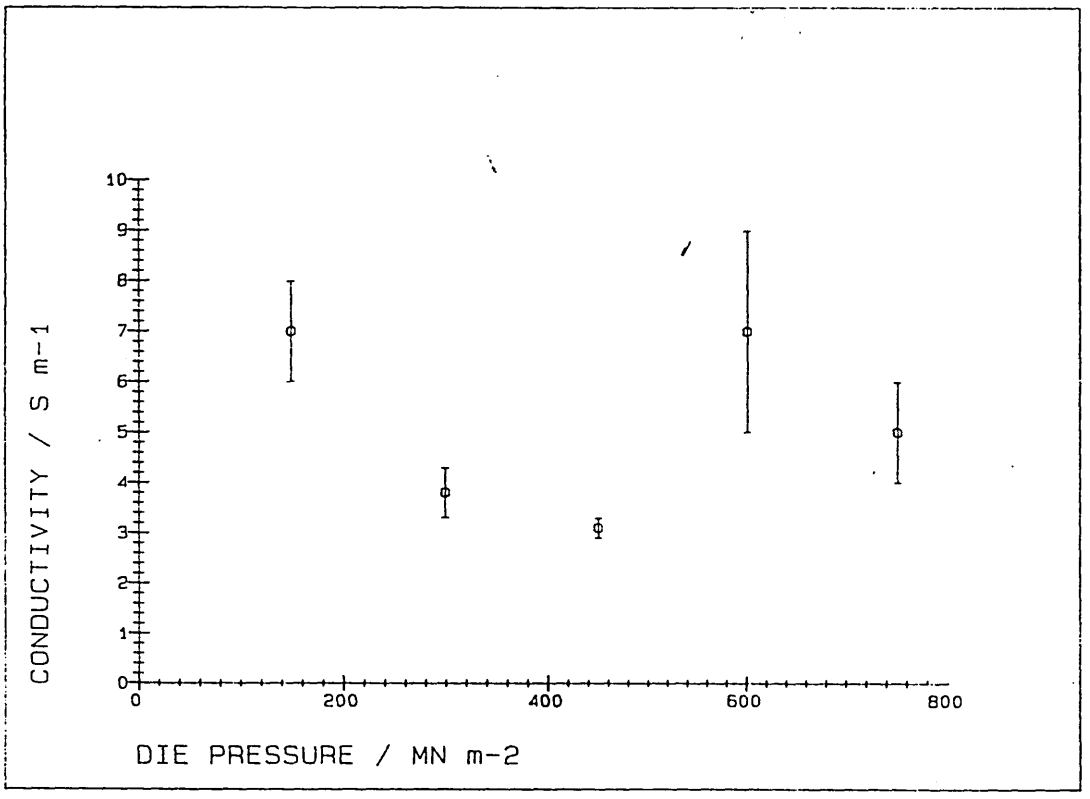

Figure 24.
Conductivity of compacted samples of $DHPE^{2+}(TCNQ)^{-}_{2}(TCNQ)^{o}$ at various compaction pressures.

Peak intensity decreases down the columns.

material/d-spacing (Å)		
TCNQ	Me_3SI	$Me_3S^+(TCNQ.I)^-$
8.25	4.79	13.16
3.49	3.87	6.51
3.28	3.62	4.31
4.82	2.98	4.48
2.74	4.03	4.41
3.00	4.13	5.13

No structure was determined from these results. A full structure could only be determined from single crystal work. Unfortunately, all attempts to produce large crystals by re-crystallisation techniques failed.

7.8 Compaction pressure and conductivity of compressed charge transfer complex samples.

The results are shown graphically in figure 24. The difference in the error bars was due to the differing degrees of precision in the diameter measurements of the silver electrodes.

As shown by figure 24, no general trend in conductivity was observed for the range of compaction pressure chosen. Hence all further compactions were performed in this range.

As an aside to the compaction work, the mass and volume of the discs were measured. Hence, the densities were calculated for the 75 and $752Nm^{-2}$ pressed samples:-

$$d_{75Nm^{-2}} = (1150+/-40)\ kgm^{-3}.$$
$$d_{752Nm^{-2}} = (1410+/-50)\ kgm^{-3}.$$

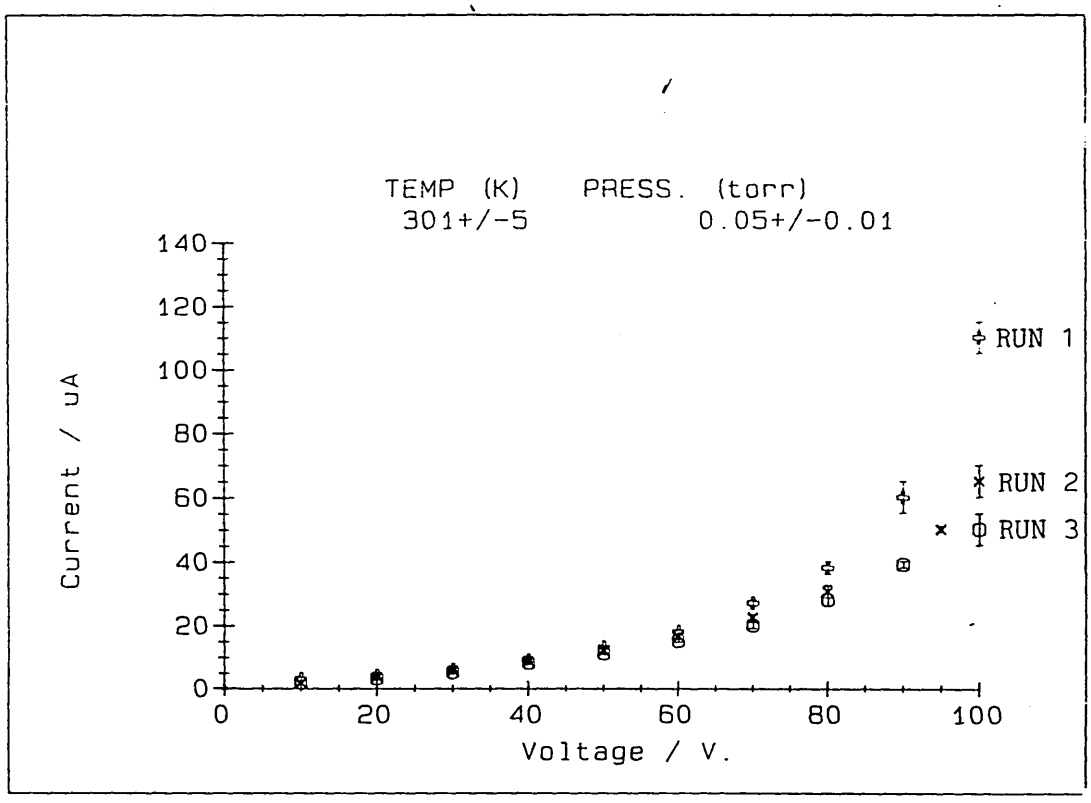

Figure 25.
Current-voltage relationship of $Me_3S^+(TCNQ\text{-}I)^-$ in ellulose acetate.

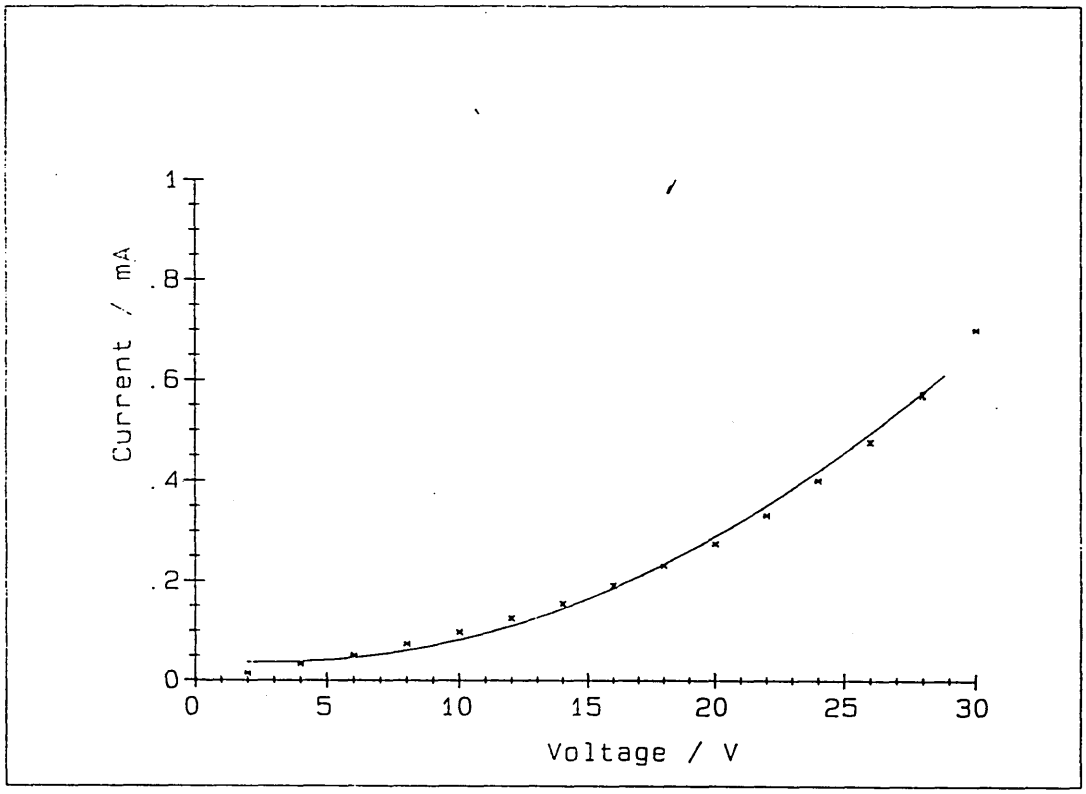

igure 26.
urrent-voltage relationship of $Me_3S^+(TCNQ\text{-}I)^-$ in ellulose acetate with fitted polynomial.

Although the conductivities are in the same range, the density calculations show that the higher compaction pressures produce denser discs, as would be expected.

i). Summary of Electrical Results $DHPE^{+}(TCNQ)^{-}_{2}TCNQ^{o}$.

The conductivity was 0.03-0.07 Scm^{-1} at room temperature, at a sample chamber pressure of (0.05+/-0.01)torr. This conductivity was of the order expected for semi-conductors, however the material was ohmic in character as shown by the linear voltage/current characteristic of the material.

ii). $DPE(TCNQ)_3$, $DPE(TCNQ)_2$ green and orange phase.

The $DPE(TCNQ)_3$ green phase had a measured conductivity of 0.03-0.04 Scm^{-1} at room temperature for a compacted sample. The material was ohmic in behaviour.

The orange phase could not be measured since the resistance reading exceeded the range of the resistance measuring apparatus and therefore we could only conclude that this phase was a good insulator.

iii). $Me_3S^{+}(TCNQ.I)^{-}$ in cellulose acetate.

Figures 25 and 26 show the current and voltage characteristics of a 10wt% $Me_3S^{+}(TCNQ\text{-}I)^{-}$ in cellulose acetate. Note that the plots are not linear as would be expected for an ohmic material. A curved line would be typical of a semiconductor and would be exponential in shape. However, the nearest fit (as shown by the continuous line in figure 26) was a two degree polynomial

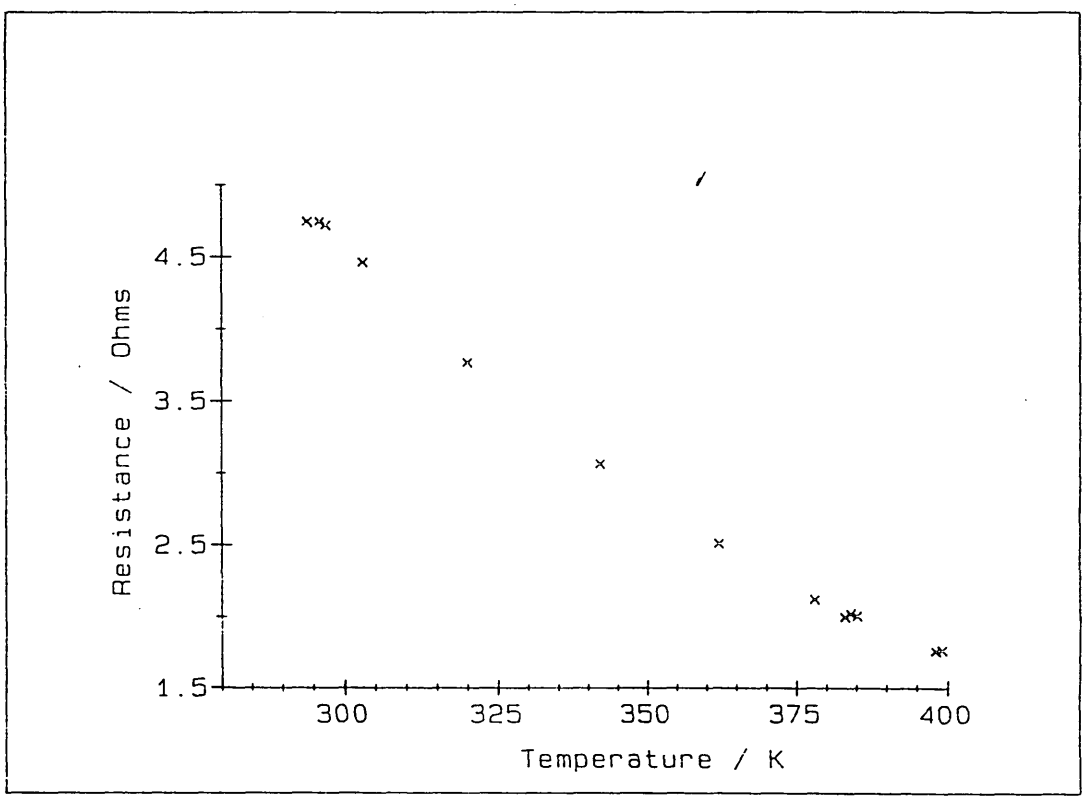

Figure 27.
Resistance-temperature relationship of $Me_3S^+(TCNQ\text{-}I)^-$ in cellulose acetate.

interpolation fit giving an equation of the form:-

$$I = A + BV + CV^2$$

where:

I = current

V = voltage

A = $4.14*10^{-2}$ Amp

B = $-4.47*10^{-3}$S

C = $8.4*10^{-4}$S

coefficient of determination = 0.993771

coefficient of correlation = 0.9968556

standard error = 0.018

The temperature dependence is shown in figure 27.

The addition of a charge transfer complex to an insulating polymer decreases the bulk resistance of the polymer. However, the conductivity was not quantified in this study. Many factors hindered the full conductivity determination of the filled polymers. Time restraints being the greatest, followed by poor sample preparation and the choice of conductivity measurement technique.

8. Solubility Studies/blending of $Me_3S^+(TCNQ.I)^-$ charge transfer complex with polymers and film casting

8.1 $Me_3S^+(TCNQ\text{-}I)^-$ solubility

The trimethylsulphonium TCNQ iodide salt was found to be soluble in a small number of solvents as listed below:

solvent	comment
CH_3CN	readily soluble
DMF	readily soluble
acetone	readily soluble
ethanol	slightly soluble
chloroform	insoluble
toluene	poor solubility
THF	poor solubility

8.2 $Me_3S^+(TCNQ\text{-}I)^-$ solubility in insulating polymers.

The solubility parameter of 23 $(MJm^{-3})^{\frac{1}{2}}$ for the trimethylsulphonium TCNQ iodide salt gave a range of possible polymers with similar solubility parameters suitable for blending. These are listed below:

Polymer	Solubility parameter $(MJm^{-3})^{\frac{1}{2}}$
poly(vinylidene chloride)	20.0-25.0
acetal resin	22.6
cellulose diacetate	23.2
cellulose acetate (CA)	22.2
poly(vinyl chloride) (PVC)	19.4
ethylcellulose	17.3-21
cellulose di(nitrate)	21.6
poly(ethylene terephthalate)	21.8
poly ethersulphone (PES)	25.1
polysulphone (PSul)	21.6-22.2
poly vinyl acetate	19.1
poly methyl methacrylate (PMMA)	19.0

polystyrene (PS)	18.7
poly (ethylene oxide) (PEO)	----

8.3 Polymer/charge transfer complex/solvent blending and casting

The polymers chosen for blending were (poly vinyl) acetate (PVA), poly ether sulphone (PES), poly (ethylene oxide) (PEO), polystyrene (PS), poly (methyl methacrylate) (PMMA) and cellulose acetate (CA). Note that the solubility parameters of PS, PVA and PMMA are outside the required range of 21-25 $(MJm^{-3})^{\frac{1}{2}}$, but they were found to have some degree of solubility in CH_3CN or DMF, solvents that could be used in the synthesis of $Me_3S^+(TCNQ\text{-}I)^-$.

The range of polymers was narrowed down even further to include only PVA and PMMA as they both produced good clear films on casting, unlike PS and PES cast from DMF which produced opaque films. This opacity was attributed to trapped solvent as a bubble morphology was observed under the optical microscope (see micrograph 1).

PEO was rejected when a casting of the film showed that a spherulitic type morphology had formed. It was thought this would interfere with the growth of the charge transfer complexes. CA was found to be soluble in acetone which has a similar solubility parameter to the trimethylsulphonium TCNQ iodide salt, and was also used in blending experiments.

THF, toluene and chloroform did not allow any reaction

between the acceptor and donor moieties of the charge transfer complex of the trimethylsulphonium TCNQ iodide salt and were therefore rejected as possible mutual solvents.

Premixing of the salt with THF and toluene prevented the CA polymer from being taken into solution. Also, the salt tended to dissociate into the TCNQ and trimethylsulphonium-iodide moities when redissolved in these solvents. This was totally unsatisfactory for the purpose of producing doped polymers. It was also noted that prolonged storage of any of the charge transfer complexes in any solvent led to their decomposition. This greatly hindered work as each time blending work was required a new batch of solutions had to be made up. A further restriction resulted from the small amounts of complex salts available (due to low yields of the preparations).

The blend chosen for detailed study was $Me_3S^+(TCNQ\text{-}I)^-$ in celulose acetate cast from CH_3CN. However, the somewhat toxic nature of the CH_3CN solvent was always borne in mind.

8.4 Casting films of $Me_3S^+(TCNQ\text{-}I)^-$/solvent/insulating polymer

Cellulose acetate in acetone was chosen as a promising medium for blending with the charge transfer complex $Me_3S^+(TCNQ.I)^-$, and spin coating trials were carried out with these materials. However, spin coating of an acetone based solution led to an explosion of the acetone vapour on

one occasion, and consequently this method was terminated. However, very good films of even thickness were produced. Unfortunately, no precipitation of charge transfer complex occurred, possibly due to the over rapid an evaporation of the acetone. The charge transfer complex remained dissolved in the celulose acetate. This would seem a reasonable assumption since the polymer and complex were chosen for their mutual solubility parameters.

Work was continued using acetonitrile as solvent. However, due to its toxic nature, the method was limited to the production of films mainly on glass slides. The work was performed in a fume cupboard and involved only 5 to 10ml of solution at any one time. Most of the micrographs presented in the next section show $Me_3S^+(TCNQ\text{-}I)^-$ in various polymers cast from acetonitrile onto glass slides.

The casting of films onto either water or mercury was unsuccessful. The water tended to decompose the complexes, while the mercury formed uneven films of varying thickness. Mercury also tended to become incorporated within the film, a highly unsatisfactory situation. Furthermore, mercury is highly toxic.

9. Charge transfer complex/polymer film morphology

Micrographs 2 to 15 show optical microscope images of $Me_3S^+(TCNQ\text{-}I)^-$ charge transfer complex in polystyrene (PS), poly (methyl methacrylate) (PMMA) and

cellulose acetate (CA). All show the morphologies of the charge transfer complexes as grown from cast solutions of the charge transfer complex/polymer/solvent blends. All micrographs are x20 magnification.

From the series of micrographs, several observations may be made relating to crystal morphology. Dendrites, spherulites, fractals, and long branched crystals are formed in the polymers, sometimes under the same conditions. Also, inoculation of the charge transfer complex crystals occurs from nucleation sites formed by impurities (dust) and unreacted TCNQ crystals within the polymer. Crystal growth was parallel to the solvent evaporation gradient for slow evaporation rates. Faster rates tended to favour spherulite growth.

Micrograph 1 shows how polyethylene oxide cast from DMF produced an opaque film and exhibited the bubble structure responsible for this.

Micrographs 2 and 3 show $Me_3S^+(TCNQ\text{-}I)^-$ in PS cast from DMF. The morphology of the charge transfer complex was spherulitic, being nucleated from impurities or small TCNQ crystals. The spherulites were visible under crossed polaroids.

Micrograph 5 shows the morphology of the $Me_3S^+(TCNQ\text{-}I)^-$ crystals as they are produced from the synthesis described earlier. Note the low aspect ratio of some of the crystals typical of long precipitation times.

Micrographs 4, and 6-13 all show $Me_3S^+(TCNQ\text{-}I)^-$ in CA cast from acetonitrile. The morphologies generally correspond to two similar structures (with the exception of micrograph 3 which shows spherulites). The first type is a branched fractal with all the crystals growing in the same direction(see micrographs 6,8,9,11, and 13), parallel to the solvent evaporation gradient. Nucleation of growth starts at the edge of the film, as exemplified by micrograph 11.

The second type is exemplified in micrographs 10 and 12. They show random orientated crystals of $Me_3S^+(TCNQ\text{-}I)^-$ producing fractals at both ends of the crystal. This type of morphology was thought to be favourable for a reticulate doped polymer without electrical anisotropy and further work was planned to produce more polymers having this morphology.

The observation that charge transfer complex crystals could nucleate at the edge of the film or at impurities in the blends suggested two further experiments. Firstly, the charge transfer complex/polymer/solvent blends could be inoculated with a fourth material. This material would seed the polymer with nucleation sites for the initiation of crystal growth. The inoculation material would have to be conductive as these sites would effectively be the "cross-over" points of conduction from one charge transfer complex crystal to the next. A sensible choice would be carbon black.

The second experiment would use the fact that the crystal grows parallel to the direction of the solvent evaporation gradient as do the zone solidified charge transfer complex/polymer/solvent blends discussed in the literature review. A different method of producing an evaporation gradient was attempted whereby a substrate was drawn from a charge transfer complex/polymer/solvent blend. The crystals nucleate at the film edge and continue to grow away from the edge and perpendicular to it. The preliminary experiments showed that this was possible but long crystals were only produced when the speed of drawing the substrate out of the blend solution was the same as the crystal growth speed; too rapid a substrate speed and the crystals became isolated from each other, too slow and the crystals grew too large.

The final micrographs 14 and 15, show $Me_3S^+(TCNQ.I)^-$ crystal morphology in PMMA. Micrograph 14 shows how the crystals have grown around bubbles present in the cast solution. Again, the morphology of the crystals was a branched fractal.

10. MICROGRAPHS OF POLYMER BLENDS

Micrograph No.	Title
1	Poly(ethylene oxide) cast from DMF at room temperature showing bubble inclusions of solvent.
2,3	$Me_3S^+(TCNQ.I)^-$ in polystyrene cast from DMF showing spherulite of charge transfer complex nucleated from impurities or TCNQ crystals.
4	$Me_3S^+(TCNQ.I)^-$ in cellulose acetate cast from CH_3CN at elevated substrate temperature.
5	$Me_3S^+(TCNQ.I)^-$ crystals as deposited from CH_3CN.
6	$Me_3S^+(TCNQ.I)^-$ in cellulose acetate cast from CH_3CN. Charge transfer complex crystals have a fractal type morphology running in the same direction.
7	$Me_3S^+(TCNQ.I)^-$ in cellulose acetate cast from CH_3CN. Spherulite morphology nucleated at impurities/TCNQ crystals.
8 ,9	$Me_3S^+(TCNQ.I)^-$ in cellulose acetate cast from CH_3CN at room temperature, crystals are running in the same direction.
10	$Me_3S^+(TCNQ.I)^-$ in cellulose acetate cast from CH_3CN at room temperature. Branched fractal morphology, randomly spreading out over film.
11	$Me_3S^+(TCNQ.I)^-$ in cellulose acetate cast from CH_3CN at room temperature. Fractals all running in same direction (zone solidification, parallel to evaporation gradient). Nucleation of crystals is from the edge of the film.
12	$Me_3S^+(TCNQ.I)^-$ in cellulose acetate cast from CH_3CN at room temperature. Random fractal morphology of crystals in a thin film of cellulose acetate.
13	$Me_3S^+(TCNQ.I)^-$ in cellulose acetate cast from CH_3CN at room temperature. Two types of crystal morphology in the same polymer film.
14,15	$Me_3S^+(TCNQ.I)^-$ in PMMA cast from CH_3CN. Limited concentration (<.1wt%) of charge transfer complex gives rise to limited crystal growth within the polymer. The large objects in the polymer are bubbles.

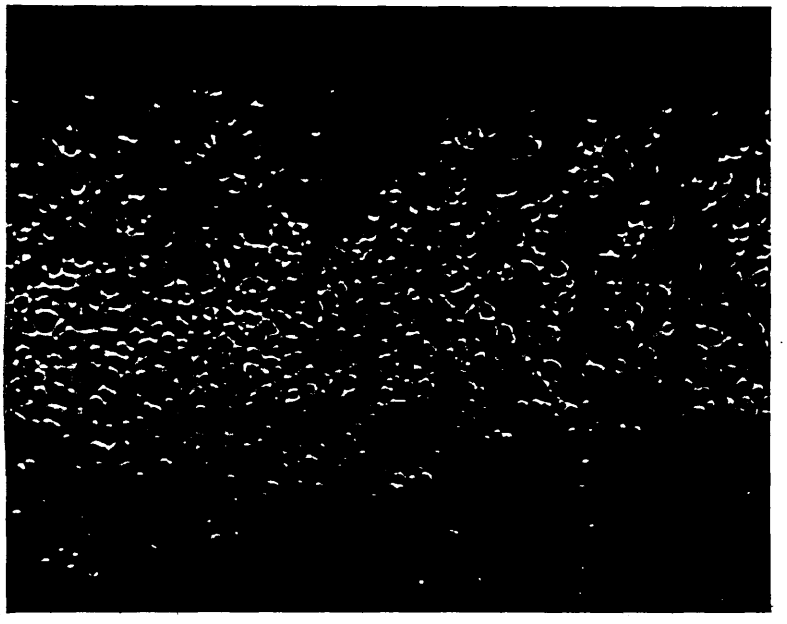

Micrograph No. 1
Poly(ethylene oxide) cast from DMF at room temperature showing bubble inclusions of solvent.

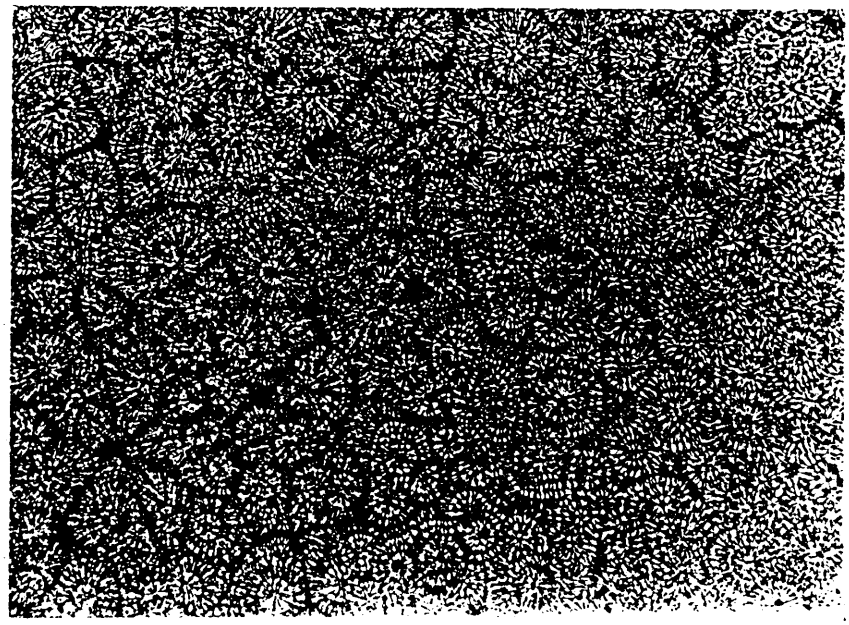

Micrograph No. 2
$Me_3S^+(TCNQ\text{-}I)^-$ in polystyrene cast from DMF showing spherulites of charge transfer complex nucleated from impurities or TCNQ crystals.

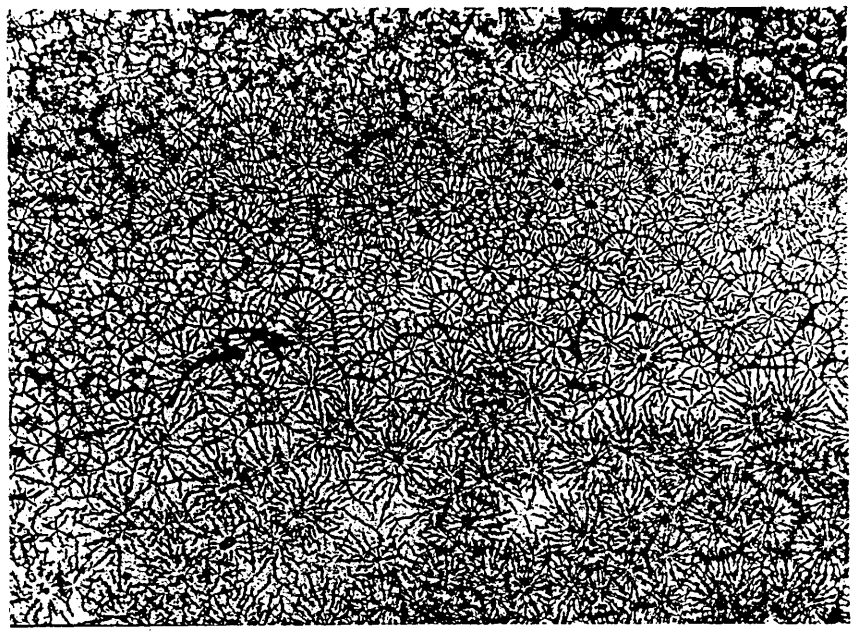

Micrograph No. 3
$Me_3S^+(TCNQ\text{-}I)^-$ in polystyrene cast from DMF showing spherulites of charge transfer complex nucleated from impurities or TCNQ crystals.

Micrograph No. 4
$Me_3S^+(TCNQ\text{-}I)^-$ in cellulose acetate cast from CH_3CN at elevated substrate temperature.

Micrograph No. 5
$Me_3S^+(TCNQ\text{-}I)^-$ crystals as deposited from CH_3CN

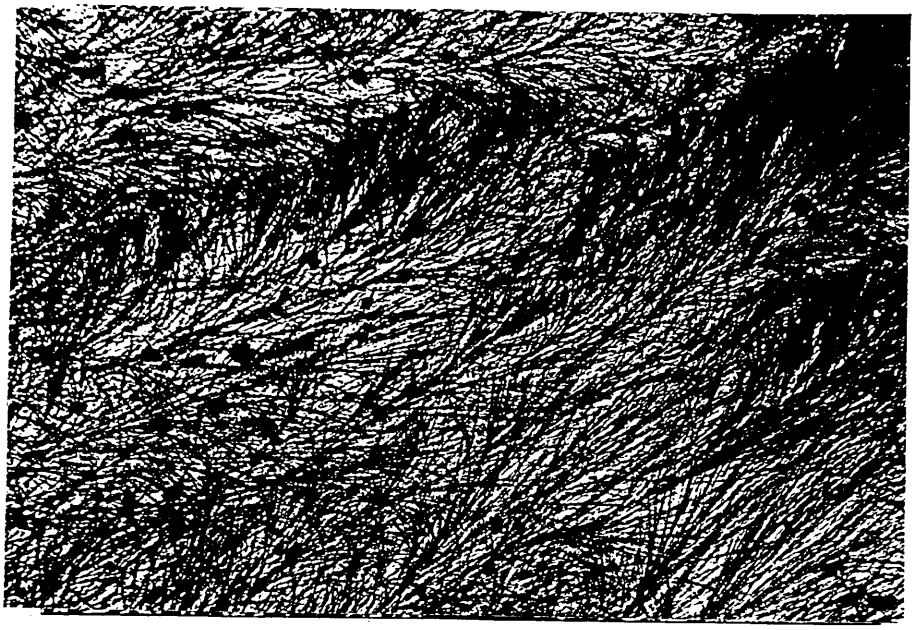

Micrograph No. 6
$Me_3S^+(TCNQ\text{-}I)^-$ in cellulose acetate cast from CH_3CN. Charge transfer complex crystals have a fractal type morphology running in the same direction.

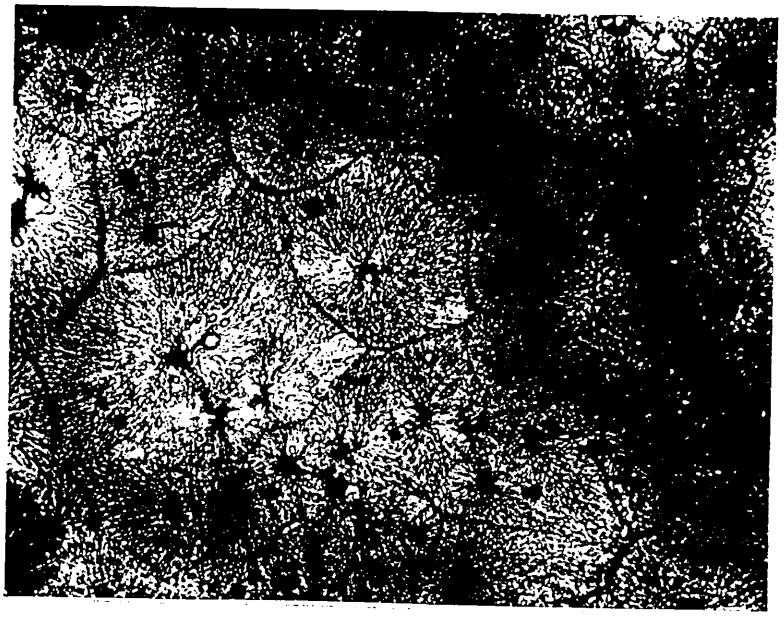

Micrograph No. 7
$Me_3S^+(TCNQ\text{-}I)^-$ in cellulose acetate cast from CH_3CN. Spherulite morphology nucleated at impurities/TCNQ crystals.

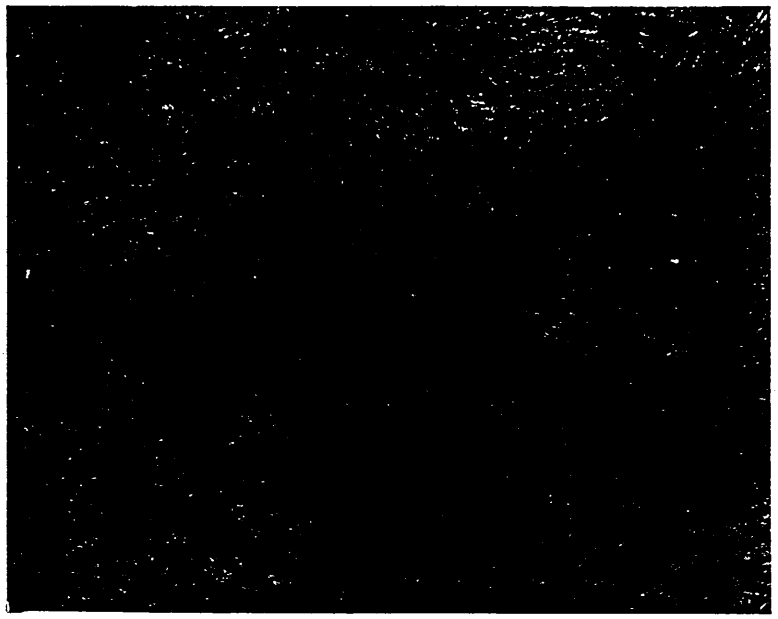

Micrograph No. 8
$Me_3S^+(TCNQ\text{-}I)^-$ in cellulose acetate cast from CH_3CN at room temperature, crystals are running in the same direction.

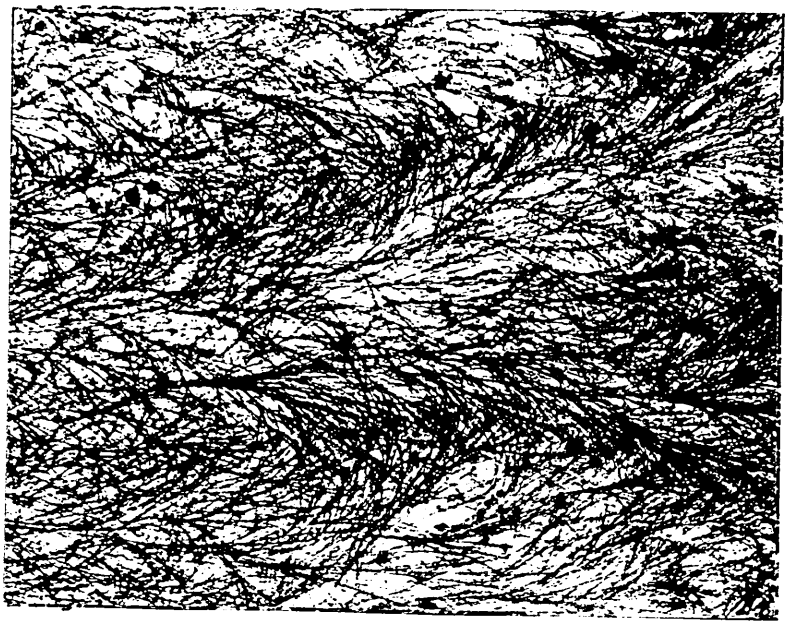

Micrograph No. 9
$Me_3S^+(TCNQ\text{-}I)^-$ in cellulose acetate cast from CH_3CN at room temperature, crystals are running in the same direction.

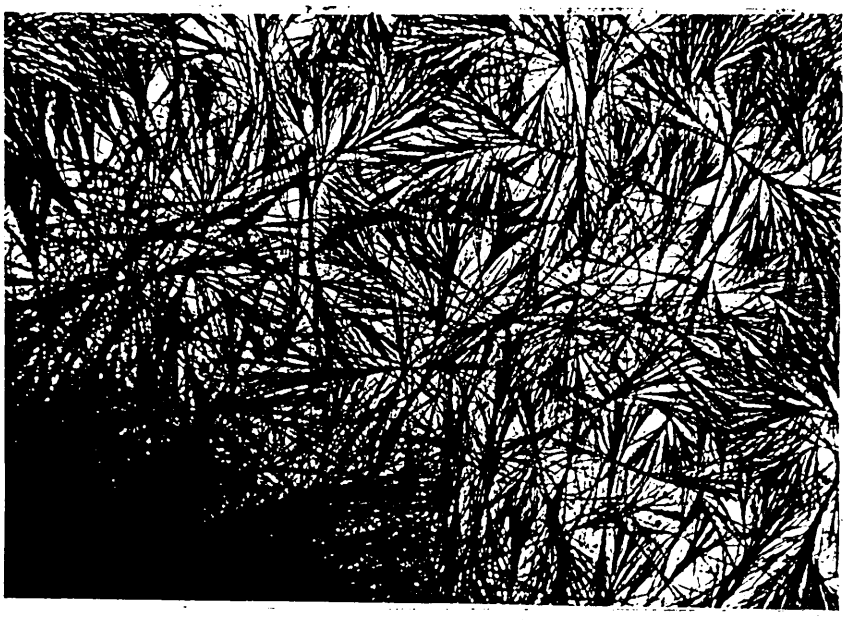

Micrograph No. 10
$Me_3S^+(TCNQ\text{-}I)^-$ in cellulose acetate cast from CH_3CN. at room temperature. Branched fractal morphology, randomly spreading out over film.

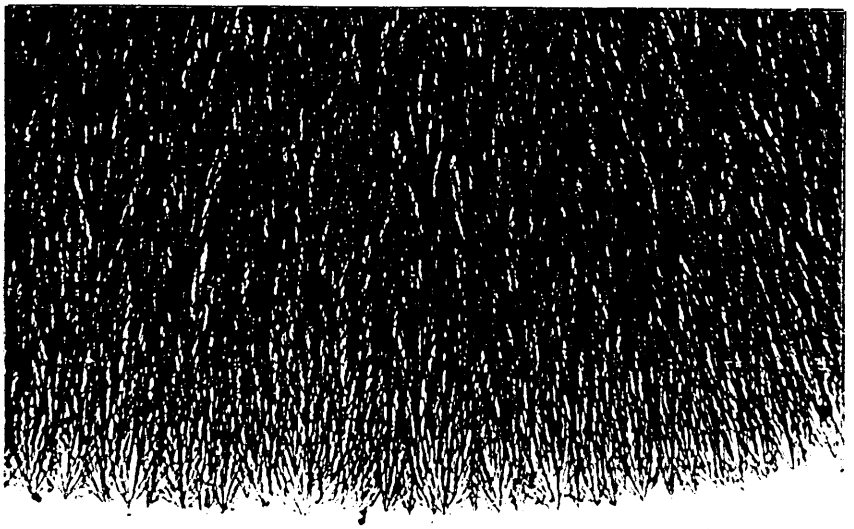

Micrograph No. 11
$Me_3S^+(TCNQ\text{-}I)^-$ in celulose acetate cast from CH_3CN at room temperature. Fractals all running in same direction (zone solidification, parallel to evaporation gradient). Nucleation of crystals is from the edge of the film.

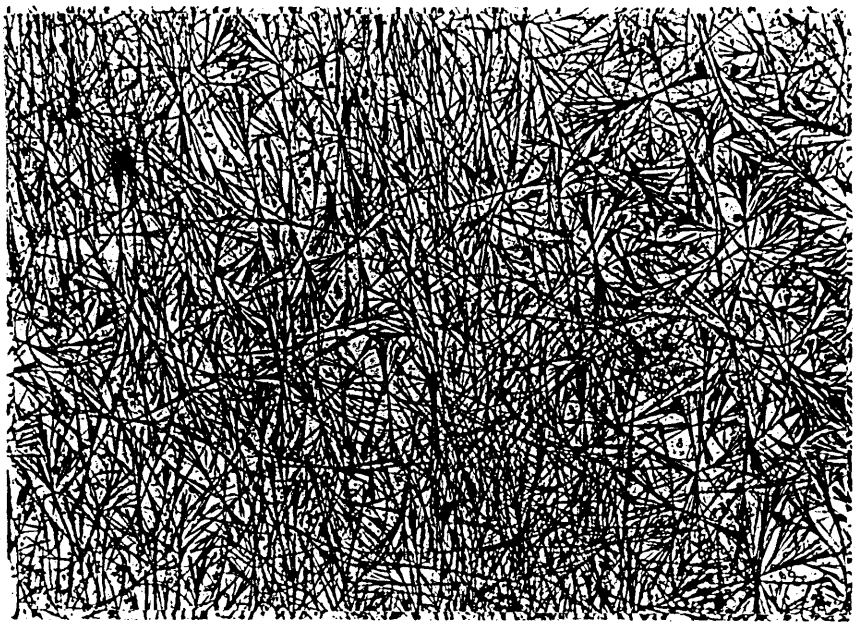

Micrograph No. 12
$Me_3S^+(TCNQ\text{-}I)^-$ in cellulose acetate cast from CH_3CN at room temperature. Random fractal morphology of crystals in a thin film of cellulose acetate.

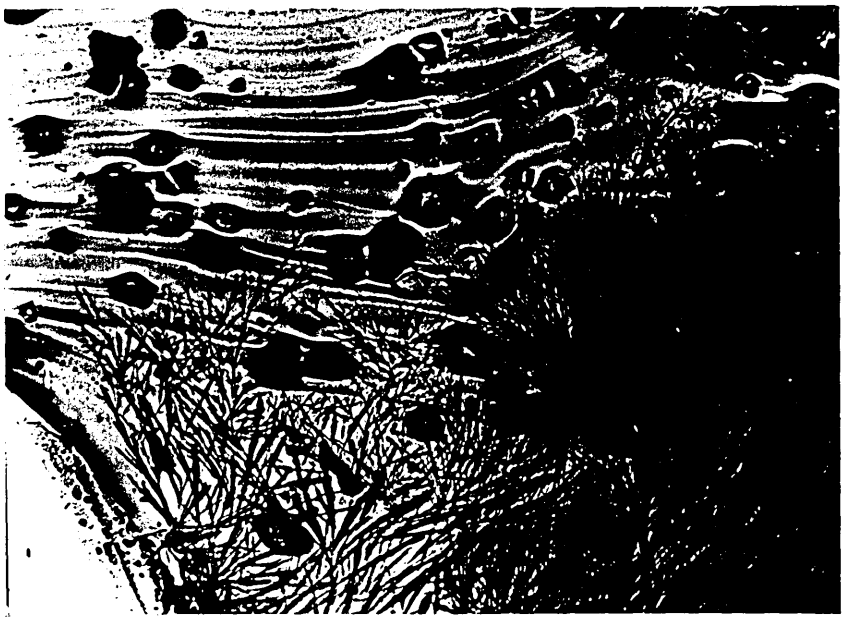

Micrograph No. 13
$Me_3S^+(TCNQ\text{-}I)^-$ in cellulose acetate cast from CH_3CN at room temperature. Two types of crystal morphology in the same polymer film.

Micrograph No. 14
$Me_3S^+(TCNQ\text{-}I)^-$ in PMMA cast from CH_3CN. Limited concentration (<.1wt%) of charge transfer complex gives rise to limited crystal growth within the polymer. The large objects in the polymer are bubbles.

Micrograph No. 15
$Me_3S^+(TCNQ\text{-}I)^-$ in PMMA cast from CH_3CN. Limited concentration (<.1wt%) of charge transfer complex gives rise to limited crystal growth within the polymer. The large objects in the polymer are bubbles.

11. CONCLUSIONS

11.1 General Synthesis and properties of charge transfer complexes

11.1.1 $DHPE^{2+}(TCNQ)^{-}_{2}TCNQ^{o}$

The synthesis of this material gave poor yields (36%) and involved large quantities of the somewhat toxic acetonitrile. The synthesis involved four stages, the final product giving an excellent elemental analysis result. The material was thermally stable to (260±20)°C, subliming at (200±50)°C.

UV/Visible spectrophotometry gave (1.5±0.2) neutral TCNQ molecules per lattice unit.

11.1.2 $DHPE^{2+}(TCNQ)^{-}_{2}$

The synthesis gave low yields (45%) and the final product was shown to have lithium chloride as an impurity. This impurity could not be removed by washing with water as this decomposed the charge transfer complex. The elemental analysis for the product was poor, even when the presence of the lithium chloride was accounted for.

The product was stable to (240±20)°C, and sublimed at (250±50)°C.

Due to the poor elemental analysis it was concluded that this product was not successfully synthesised.

11.1.3 $DPE(TCNQ)_{3}$

The synthesis of this product gave two phases referred to

as green or orange. The synthesis was simple, but gave unreliable results even for differing synthesis solvents. The green phase gave an elemental analysis on the limits of acceptance.

The UV/Visible spectrophotometry results gave inconclusive results. The product was thermally stable up to (260±20)°C and sublimed at (300±50)°C.

11.1.4 $Me_3S^+(TCNQ.I)^-$

The synthesis gave low yields, however it was straightforward giving long needle like crystals.

Good elemental analysis was obtained, and the product was thermally stable up to (150±10)°C.

11.2 Magnetic susceptibility results

11.2.1 $DHPE^{2+}(TCNQ)^-_2TCNQ^o$

This material followed a Curie-Weiss relationship of the form:-

$$\chi = \chi_{cm}/\tau-\theta \quad .$$

where:

χ_{cm} = molar Curie constant
= (0.3≃0.3) $JK^{-2}mol^{-1}$

θ = Curie temperature = -87K

From these results, and assuming that a spin only formula applied, the material was paramagnetic or anti-ferromagnetic with an effective number of bohr magnetons (μ_{eff}) of (1.65±0.07) μb/ion which was in good agreement with the theoretical result of 1.73 μb/ion (a -4% difference) and 1 unpaired electron per lattice unit.

11.2.2 $DPE(TCNQ)_3$

This material gave an initial field dependent susceptibility typical of a ferromagnetic material. The material was not Curie-Weiss in behaviour and contained no ferromagnetic impurities. The magnetic properties of this material were inconclusive.

11.2.3 $\underline{DPE(TCNQ)_3}$

This material was Curie-Weiss in behaviour of the form:-

$$\chi = \chi_{cm}/\tau-\theta$$

where:

χ_{cm} = molar Curie constant
= (8±2) $JK^{-2}mol^{-1}$

θ = Curie temperature = -95K

giving a μ_{eff} value of (2.6±0.2) μb/ion and 2 unpaired electrons per lattice when the spin only model applied.

11.2.4 $Me_3S^+(TCNQ.I)^-$

No predictive magnetic theory applied to this material.

11.3 Magnetic susceptibility calculations

11.3.1 A correction was required to the magnetic susceptibility calculation for the temperature dependence of the calibrant. This may be performed using the Curie-Weiss equation for this material.

11.3.2 The calibrant susceptibility used was in terms of mass susceptibility where molar mass susceptibility would have been better. This drawback arose in earlier work when

setting up the computer calculation of the susceptibility. For future studies, changes should be made so that better consistency, and more valid comparisons are available.

11.4 X-ray powder diffraction measurements

11.4.1 The calibration of the diffractometer was found to be accurate to 0.7 and precise to 0.01 .

11.4.2 The greatest intensity peak was found for a lattice d-spacing at 13.16 for the $Me_3S^+(TCNQ.I)^-$ material.

11.5 Electrical conductivity measurements

11.5.1 Measurement of the compacted discs conductivities by the silver point electrode method had a precision of 3%. This was achieved by measuring dimensions using a calibrated optical microscope. However, it was recommended that this method be abandoned and a true four point probe method be used instead.

11.5.2 The die pressure, in the range of 150-752Nm^{-2}, employed in the production of compacted material discs gave no significant variation in the room temperature measurement of the electrical conductivity of the compacted discs of $DHPE^{2+}(TCNQ)^-_2TCNQ^o$ complex.

11.5.3 $DHPE^{2+}(TCNQ)^-_2TCNQ^o$ was ohmic in character, with a room temperature conductivity of 0.03-0.07 Scm^{-1}.

11.5.4 $DPE(TCNQ)_3$ was ohmic in character with a room temperature conductivity of 0.03-0.04 Scm^{-1}.

11.5.5 $DPE(TCNQ)_2$ was a good insulator, the conductivity could not be determined using the apparatus available.

11.5.6 $Me_3S^+(TCNQ.I)^-$ in cellulose acetate had a current voltage relationship of the form:-

$$I = A + BV + CV^2$$

where:

I = current

V = voltage

A = $4.14*10^{-2}$ Amp

B = $-4.47*10^{-3}$S

C = $8.4*10^{-4}$S

coefficient of determination = 0.993771

coefficient of correlation = 0.9968556

standard error = 0.018

This was a two degree polynomial fit.

The temperature dependence was non-linear with no fittable equation available.

11.6 Solubility studies

11.6.1 The solubility parameter given by the method of heat of vaporisation was $23(MJm^{-3})^{\frac{1}{2}}$ for $Me_3S^+(TCNQ.I)^-$ and the material was found to be soluble in acetonitrile, DMF and acetone.

11.6.2 The solubility parameter given by the method of heat of vaporisation was $23\text{-}6(MJm^{-3})^{\frac{1}{2}}$ for the bis-pyridinium TCNQ salts. Acetonitrile was found to be the best solvent for these materials.

11.6.3 $Me_3S^+(TCNQ.I)^-$ was soluble in a range of polymers, however cellulose acetate was chosen as the best of the candidates on an availability basis.

11.6.4 $Me_3S^+(TCNQ.I)^-$ was blendable with acetone and cellulose acetate.

11.6.5 Prolonged storage of all charge transfer complexes studied resulted in their decomposition.

11.6.6 $Me_3S^+(TCNQ.I)^-$ would remain dissolved in cellulose acetate under certain casting conditions (e.g. spin casting or glass slide casting at elevated temperatures).

11.7 Film casting

11.7.1 The casting of solutions of charge transfer complex/solvent/polymer onto water or mercury was unsatisfactory, producing decomposition of the complexes in the case of water casting and uneven, mercury embedded films for the mercury cast films.

11.7.2 Spin coating gave good even films for $Me_3S^+(TCNQ.I)^-$ /cellulose acetate/acetone cast solutions of reasonable dimensions. However, the complex stayed dissolved in the polymer and no $Me_3S^+(TCNQ.I)^-$ network was observed for this method of film production.

11.7.3 Casting acetonitrile based solutions of complex and polymers onto glass slides gave good films, of small dimensions, with networked charge transfer complex. However, the films tended to be brittle.

11.8 Charge transfer complex morphology in the polymers

11.8.1 Inoculation of charge transfer complexes from sites of impurities was possible.

11.8.2 Poly(ethylene oxide)/$Me_3S^+(TCNQ.I)^-$ cast from DMF gave opaque films with no charge transfer complex crystal

growth.

11.8.3 Polystyrene/$Me_3S^+(TCNQ.I)^-$ cast from DMF gave a spherulitic crystal structure of the polymer. No crystal structure was observed.

11.8.4 Slow evaporation rates tended to favour large crystal growth with high aspect ratios.

11.8.5 Crystal growth parallel to the solvent evaporation gradient for slow evaporation rates was observed.

11.8.6 Crystal growth as sperulites tended to be favoured for fast evaporation rates.

11.8.7 Fractal growth of crystals was observed.

11.8.8 Nucleation of crystals may occur at the edge of the forming polymer film.

12. SCOPE FOR FUTURE STUDY

The main aim of the present investigation was to select and prepare suitable complexes that could be cast into filled polymer films displaying appropriate morphologies.

Clearly one of the main areas or further study is the determination of the conductivities of reticulately filled polymers especially as a function of charge transfer complex mass percent. The aim of this work would be to determine the critical concentration of percolation. Would this be at a level observed by other workers (Jeszka et al 1981, Ulanski et al 1984a, 1985, Sorm et al 1984) using charge transfer complexes as dopants, or would the level be similar to that observed for conventional filled polymers?

The predictive theory outlined in the literature review could be examined in the light of this further study, in particularly that postulated by the Lodz workers (Ulanski et al 1984b).

The tensile properties of reticulately doped insulating polymers and elastomers would be a suitable area of further study. Does doping enhance, depress or have no effect on the parent properties of the pristine insulating polymer? Are there any novel conductivity properties for such polymers and elastomers under the action of an applied stress?

Further work has to be performed in the area of polymer/solvent/charge transfer complex blending and casting to produce suitable reticulately doped polymer

films. Variations in casting temperature would probably have profound effects in terms of solvent evaporation and hence charge transfer complex recrystallisation rates. A study of various casting temperatures should be undertaken for a set solvent/polymer/charge transfer complex blends to determine an optimum casting temperature for that set system.

Other methods of producing doped polymers should be studied. In this work, polymer films with reticulate charge transfer complexes were produced by casting highly loaded polymer/solvent mixes onto glass microscope slides. The resulting films were small and fragile. However, they were conductive in comparison with the parent insulating polymer.

Spin coating did produce good films. They had the disadvantage that no reticulate charge transfer complex formed; the complexes remained dissolved in the polymer. Another proposed method of producing polymer films with a reticulate complex was to force the growth of the complex in a uni-axial direction. It was expected that a suitable substrate would be drawn from a polymer/solvent/complex blend at the same speed as the recrystallisation rate of the complex. Thus crystals would grow parallel to the evaporation gradient perpendicular to the solution surface.

An experimental improvement in the measurement of the conductivity is required. The technique employed for this study was slow and inadequate. Progress in this area was

achieved by the development of a four point probe technique by another worker in a related field of study. That work considered the attachment of TCNQ acceptor and suitable donor materials onto the backbone of a polymer.This work developed into the next major tranch of further study (Batty S V, PhD Thesis "The investigation of novel charge transfer systems", Sheffield City Polytechnic, March 1991).

13. STATEMENT OF POSTGRADUATE COUSES AND RESEARCH PRESENTATIONS

13.1 Postgraduate Courses

a). Analytical scanning electron microscopy for scientists and engineers 1989.

b). CRAC course; The Careers Research and Advisory Centre, 23-28 July, 1987.

c). Polymer processing lecture course, Sheffield City Polytechnic, March, 1988.

d). SEESCAN. Image analysis course, 2nd/3rd June, 1988.

e). Conducting organic polymers, research colloquium M Kryswenski, 4 Feburary, 1986.

f). IBM postgraduate seminars in polymer science and technology, Department of Mechanical Engineering, Imperial Colledge, London; 26 May, 1988; 4 April, 1989; 18 September, 1989.

13.2 Presentations of research studies

a). Polymer Group seminars, Sheffield City Polytechnic, 23 Feburary, 1988.

b). Department of Metals and Materials Engineering, Sheffield City Polytechnic, 27 April, 1988.

c). Department of Metals and Materials, Nottingham University, 8 June, 1988.

14. REFERENCES

Agari, Y., Uno, T. (1986) J. Appl. Polym. Sci. 32, 5705-5712.

Aharoni, S.M. (1972) J. Appl. Phys. 43(5), 2463-2465.

Ashwell, G.J., Allen, G., Cross, G., Nowell I. (1983b) Phys. Stat. Sol. (A) 79, 455.

Ashwell, G.J. (1984b) Phys. Stat. Sol. (A), 81, 361.

Ashwell, G.J., Kennedy, D.A., Nowell, I.W. (1983b) Acta Cryst. Allogr. Sect. C39, 733-734.

Benguigui, L., Yacubowicz, J., Narkis, M. (1987) J. Polym. Sci., Part B: Polym. Phys. 25, 127-135.

Bigg, D.M. (1977) Polym. Eng. and Sci. 17 No. 12, 842-7.

Bigg, D.M. (1983) Polym. Composites 4(1), 40-46.

Bigg, D.M., Bhattachatya, S.K. (Ed) (1986) Metal Fill. Poly: Prop & Appl., Dekker, 165.

Bigg, D.M., Bradbury, E.J., R.B. Seymour (Ed) (1981) Conductive Polymers, 23-28.

Bloor, D, (1983) Chem. in Britain 19(9), 725-728.

Blythe, A.R. (1979) Electrical Prop. of Polymers, Cambridge Univ. Press.

Bolt, T.D. (1960) Rubb. Plast. Age 41(12), 1520-1526.

Bradish, F.W. Jr. (1976) Reinforced Plast. Compo. Inst. Sect. 7D, 1.

Bryce, M.R., Murphy, L.C. (1984) Nature (London) 309, 119-126.

Bryce, M.R. (1985) R.S.C. Ann. Report 85 Sect. B, 377-394.

Brydson, J.A. Plastic Materials, 70-99.

Bueche, F. (1973) J. Appl. Phys. 44(1), 532-533.

Bulgin, D. (1953) Brit. J. Appl. Phys. No. 2, 883-7.

Burda, L., Tracz, A., Pakula, T., Ulanski, J., Kryszewski, M. (1983) J. Phys. D: Appli. Phys. 16, 1737.

Chung, K.K.T., Leung, L.M. (1987) ITEM, 180-194.

Clarke, P.S., Orton, J.W., Guest, A.J. (1978) Phys. Rev. B 18(4), 1813-1817.

Crangle J. (1977), The Magnetic Properties of Solids, Arnold.
Davenport, D.E, Seymour, R.B. (Ed) (1981) Conductive Polymers, 39-47.

Duke, C.B., Gibson, H.W. (1982) Encyclopedia of Chemical. Technology, ed. Kirk-Othmer, Wiley,N.Y., Vol 18, p755-793.

Ellis, J.R., Skotheim, T.A. (Ed) (1986) Handbook of Conducting Polymers, 489-505.

Epstein, A.J., Etemad, S., Garito, A.F., Heeger, A.J., (1971) Solid State Comm 9, 1803-1808.

Ferraris, J.P., Skiles G.D. (1987) Polymer 28, 179-182.

Ferraro, J.R., Williams J.M., (1987) Introduction to

Synthetic Electrical Conductors, Chap 2, Academic Press, San Diego.

Figgis, B.N., Nyholm, R.S. (1958) J. Chem. Soc., 4190-4191.

Forster, E.O. (1971), IEEE Trans. Power Appar. Syst. Pas-90, 913-916.

Frish, H.L., Hammersley, J.M., Welsh, D.J.A. (1962) Phys. Rev. 126, 949-951.

Gerbig, S.D. (1985), Evaluation Engineering.

Gersteisen, S.R., Nangrani, K.J. (1986) Wilson-Fiberfil International, PO Box 3333, Evansville, IN 47732.

Gersteisen, S.R. (1985) Proceedings of Northcon/85, 22-24 October

Gersteisen, S.R. Plastics 85 Proceedings of the SPE 43rd Annual Technical Conference and Exhibition.

Gilg, R.G. (1986) Elektrish Leitende Kunstoffe, Carl Hauser, Munchen, Wien.

Gilles, J.M., Tompa H (1971) Nature Phys. Sci 299.

Gul, V.Y.E. (1978) Polym. Sci. USSR (Engl. Transl.), 2427-2441.

Gurland, J. (1962), . Proceedings of the Plansee Seminar p507-518.

Gurland, J. (1966), Trans. of the Metallurgical Soc. of AIME 236, 642-645.

Hansen, D., Tomkiewicz, R. (1975) Polym. Eng. 15(5), 353-56.

Heinze, R.E., Ritter, J.R. (1976) 32nd Ann. Tech. Conf. Reinforced Plat./Compo. Inst., Sect. 8A, 1.
Herman, A.M., Frisch, K.C. (Ed) (1972) Electrical Properties of Polymers.

Herman, A.M., Wilhite, L.G. (1968) Proc. Louisiana Academy of Sciences 32, 162.

Hewlett-Packard Company, (1970) Floating Measurement and Guarding, Hewlett-Packard Company.

Ikeno, S., Matsumoto, K., Yokoyama, M., Mikawa, H. (1977) Polym. Journal 9(3), 261-273.

Ikeno, S., Yokoyama, M., Mikawa, H. (1979) Polym. Journal 11(5), 371-375.

Ikeno, S., Yokoyama, M., Mikawa, H. (1978) Polym. Journal 10(2), 231-234.

Ikeno, S., Yokoyama, M., Mikawa, H. (1978) J. Polym. Sci., Polym. Phys. Ed. 16, 717-723.

Jachym, B.J., Sichel, K. (Ed) (1982) Carbon Black Polymer Composites, Dekker, N.Y.

Janeczek, D.A., Diriscoll, S.B. (1985) Procs. Antec. Procs. 43 Ann. Tech. Conf..

Janzen, J. (1975) J. App. Phys. 46(2), 966-969.

Jeszka, J., Ulanski, J., Kryszewski, M. (1981) Nature (London) 289.

Jeszka, J.K., Ulanski, J., Tracz, A., Kryszewski, M. (1984) Materials Sci. 10(1-2), 117-120.

Kirkpatrick, S. (1973) Rev. of Modern Physics 45(4), 574-588.

Kommandeur, J., Hall, F.R. (1960) J. Chem. Phys. 34/291.

Kryszewski, M., Jeszka, J., Ulanski, J., Tracz, A. (1984) European Patent Application, Publ. No. EP 0 134 026 A1.

Kryszewki, M. (1984) Pure Appl. Chem. 56, 355.

Kusy, R.P., Corneliussen, R.D. (1975) Polym. Eng. and Sci. 15(2).

Lagues, M., Sauterey, C., (1980) J. Phys. Chem. 84, 3503-3508.

Lequan, M., Lequan, R.M., Delheas, P., Hauw, C. (1985) Mol.

Cryst. Liq. Cryst. 120, 353-356.

Luxton, B.A. (1986) 41st Ann. Conf. Reinforced Plast./Composites, Session D-8, 1-4.

Lynn, P.A. (1972) Analysis and Processing of Signal, Macmillan Press Ltd.

Malliaris, A., Turner, D.T. (1971) J. Appl. Phys. 42(2), 614-618.

Medalia, A.I., Sichel, K. (Ed) (1982) Carbon Black Polymer Composites, Dekker, N.Y.

Miyasaka, R., Watanabe, K., Jojima, E., Aida, H., Sumita,

M.M. (1982) J. Material Sci. 17, 1610-1616.

Munstedt, H., Naarmann, G., Kohler, G. (1985), Mol. Cryst. Liq. Cryst. 118, 129-136.

Munstedt, H. (1985) Electronic Prop. of Polymers & Related Compounds.

Munstedt, H. (1988), Polymer 29, 296-302.

Nakatani, K., Sakata, T., Tsubomura, H. (1975b) Bull. Chem. Soc. Jap. 7, 2205-2206.

Nakatani, K., Sakata, T., Tsubomura, H. (1975a), Bull. Chem. Soc. Jap. 48(2), 657-660.

Nielsen, L.E. (1974) Ind. Eng. Chem., Fundam. 13(1), 17-20.

Norman, R.H. (1970) Conductive Rubbers and Plastics, App. Sci. Pub. Ltd.

Openshaw, H.T. (1968) A Laboratory Manual of Quantitative Organic Analysis, 3rd Edition, Cambridge University Press.

Ohima, R., Kumanotani, J. (1987) J. Polym. Sci: Polym. Chem. 25, 2343-2350.

Peierls, R. (1955) Quantum Theory of Solids.

Probst, N. (1984), European Rubber Journal, 25-28.

Rembaum, A., Hermann, A.M., Stewart, F.E., Gutmann F. (1969) J. Phys, Chem. 73, 513.

Sichel, E.K., Gittleman, J.I., Sheng, P., Sichel, K. (Ed), (1982) Carbon Black Polymer Composites, Dekker, N.Y.

Smoluk, G. (1982) Modern Plastics International, 46-49.

Sommers, D. Technical Report S-39, Cabot Corp., Massachusetts, USA.

Sorm, M., Nespurek, S., Kucer, I. (1984) Materials Sci 10(1-2).

Stephen, M.J. (1978) Phys. Rev. B 17(11), 4444-4453.
Sykes, M.F., Esam, J.W. (1964) Phys. Rev. 133, A310-15.

Techtrends (1987) Techtrends International Reports on Emerging Technologies.

Tracz, A., Pakula, T., Ulanski, J., Kryszewski, M., Kryszewski M. et al (Ed) (1984) Polymer Blends, 173-178.

Tracz, A., Ulanski, J., Kryzewski, M. (1983) Polym. Journal 15(9), 635-639.

Ulanski, J., Jeszka, J.K., Kryszewski, M. (1981) Polym. Plastics Technol. Eng. 17(2), 139-191.

Ulanski, J., Jeszka, J.K., Kryszewski, M., Kryszewski, M., (Ed) (1984) Polymer Blends 2, 165-172.

Ulanski, J., Tracz, A., Jeszka, J., Kryszewski, M. (1985) Mol. Cryst. Liq. Cryst. 118, 443-446.

Ulanski, J., Jeszka, J.K., Tracz, A., Kryszewski, M. (1984) Materials Sci. 10(1-2).

Ulanski, J., Tracz, A., Kryszewski, M. (1985) J. Phys. D: Appl. Phys. 18, 451-459.

Ulanski, J. Steffan, G. Bio, Seytre, G., Tracz, A., Jeska, J., Vallet (1985) J. Phys. D: Appl. Phys. 18(L5-L7).

Van Beek, L.K.H., Van Pul, B.I.C.F. (1962) J. Appl. Polym. Sci. VI(24), 651-655.

Voet, Whitten, Cook (1965) Kolloid 201, 39.

Waclawek, W., Zabrowska-Waclawek, M. (1987) J. Materials Sci. 6, 784-786.

Wegner, G. (1986) Angew. Makromol. Chem. 145/146, 181-189.

Williams, D.H., Flemming, I. (1980) Spectroscopic Methods in Organic Chemistry, 3rd Edition, McGraw-Hill.

Wnek, G.E., Skotheim, T.A. (Ed) (1986) Handbook of Conducting Polymers, 205-212.

Wojchiechowski P., Kryszewski, M. (1981) Acta Phys. Polonica A59(1), 57-66.

Wu, M.K. et al (1987) Phys. Rev. Lett. 58(9), 908-910.

Young, R.J. (1984) Plast. and Rubber International 9(1).